

UNIVERSIDADE FEDERAL DO PARANÁ

JUAN MARCELO CARPIO ARÉVALO

EFEITOS PRÓ-OXIDANTES E CITOTÓXICOS DE NITROCHALCONAS  
SINTÉTICAS LIVRES OU ENCAPSULADAS EM NANOPARTÍCULAS DE POLI  
METACRILATO DE METILA SOBRE CÉLULAS HeLa

CURITIBA

2018

JUAN MARCELO CARPIO ARÉVALO

EFEITOS PRÓ-OXIDANTES E CITOTÓXICOS DE NITROCHALCONAS  
SINTÉTICAS LIVRES OU ENCAPSULADAS EM NANOPARTÍCULAS DE POLI  
METACRILATO DE METILA SOBRE CÉLULAS HeLa

Tese apresentada ao Programa de Pós-graduação em Ciências (Bioquímica), setor de Ciências Biológicas da Universidade Federal do Paraná-PR, como parte dos requisitos para obtenção do título de doutor em Ciências (Bioquímica).

Orientadora: Dra. Maria Eliane Merlin Rocha

Co-orientadoras: Dra. Glaucia Regina Martinez e  
Dra. Guilhermina Rodrigues Noleto.

CURITIBA

2018

Universidade Federal do Paraná. Sistema de Bibliotecas.  
Biblioteca de Ciências Biológicas.  
(Rosilei Vilas Boas – CRB/9-939).

Carpio Arévalo, Juan Marcelo

Efeitos pró-oxidantes e citotóxicos de nitrochalconas sintéticas livres ou encapsuladas em nanopartículas de polimetacrilato de metila sobre células HeLa. / Juan Marcelo Carpio Arévalo. – Curitiba, 2018.

136 f. : il. ; 30cm.

Orientadora: Maria Eliane Merlin Rocha

Coorientadores: Glaucia Regina Martinez e Guilhermina Rodrigues Noleto  
Tese (Doutorado) – Universidade Federal do Paraná, Setor de Ciências Biológicas. Programa de Pós-Graduação em Ciências – Bioquímica.

1. Células HeLa. 2. Oxigênio. 3. Glutathione. 4. Nanopartículas. 5. Ácido Fólico. I. Título. II. Rocha, Maria Eliane Merlin. III. Martinez, Glaucia Regina. IV. Noleto, Guilhermina Rodrigues. V. Universidade Federal do Paraná. Setor de Ciências Biológicas. Programa de Pós-Graduação em Ciências – Bioquímica.

CDD (20. ed.) 611.0181

# TERMO DE APROVAÇÃO



MINISTÉRIO DA EDUCAÇÃO  
SETOR CIÊNCIAS BIOLÓGICAS  
UNIVERSIDADE FEDERAL DO PARANÁ  
PRÓ-REITORIA DE PESQUISA E PÓS-GRADUAÇÃO  
PROGRAMA DE PÓS-GRADUAÇÃO CIÊNCIAS  
(BIOQUÍMICA)

## TERMO DE APROVAÇÃO

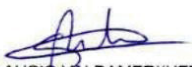
Os membros da Banca Examinadora designada pelo Colegiado do Programa de Pós-Graduação em CIÊNCIAS (BIOQUÍMICA) da Universidade Federal do Paraná foram convocados para realizar a arguição da Tese de Doutorado de **JUAN MARCELO CARPIO AREVALO**, intitulada: **EFEITOS PRÓ-OXIDANTES E CITOTÓXICOS DE NITROCHALCONAS SINTÉTICAS LIVRES OU ENCAPSULADAS EM NANOPARTÍCULAS DE POLIMETACRILATO DE METILA SOBRE CÉLULAS HELA**, após terem inquirido a aluna e realizado a avaliação do trabalho, são de parecer pela sua Aprovação no rito de defesa. A outorga do título de Doutor está sujeita à homologação pelo colegiado, ao atendimento de todas as indicações e correções solicitadas pela banca e ao pleno atendimento das demandas regimentais do Programa de Pós-Graduação.

Curitiba, 21 de Fevereiro de 2018.

  
MARIA ELIANE MERLIN ROCHA(UFPR)  
(Presidente da Banca Examinadora)

  
PEDRO HENRIQUE HERMES DE ARAUJO(UFSC)

  
SÍLVIA MARIA SUTER CORREIA CADENA(UFPR)

  
GLAUCIO VALDAMERI(UFPR)

  
ALEXANDRA ACCO(UFPR)

## **AGRADECIMENTOS**

Agradeço à professora Maria Eliane por ter me aceitado para o doutorado e ter compartilhado comigo seu tempo e conhecimento, além da paciência e toda dedicação.

Agradeço às professoras Guilhermina e Glaucia pela coorientação e pelo acompanhamento da tese. Agradeço também a professora Sheila pelo esclarecimento em muitas dúvidas ao longo do doutorado.

Agradeço às professoras Alexandra e Silvia pelo acompanhamento interno da tese, com paciência e dedicação todos esses anos, com muitas dicas e conselhos experimentais.

Agradeço ao professor Alfredo R. M. de Oliveira do Departamento de Química da Universidade Federal do Paraná (UFPR), por ceder gentilmente as chalconas utilizadas nos estudos.

Agradeço ao professor Pedro H. Hermes de Araújo e ao Dr. Paulo Emílio Feuser do Departamento de Engenharia Química e Engenharia de Alimentos da Universidade Federal de Santa Catarina (UFSC) pela colaboração nos experimentos com nanopartículas.

Agradeço aos professores Glaucio Valdameri e Fabiana Gomes de Moraes Rego e ao aluno Diogo Henrique Kita do Departamento de Análises Clínicas da UFPR pela colaboração nos experimentos com células BHK21.

Agradeço ao professor Edvaldo S. Trindade e ao doutorando Gustavo Rodrigues Rossi pela colaboração nos experimentos de microscopia confocal.

Agradeço ao professor Lauro M. de Souza do Instituto Pelé Pequeno Príncipe pela colaboração nos experimentos de espectrometria de massas.

Agradeço ao professor Emanuel Maltempi de Souza por facilitar o uso do citômetro de fluxo e ao professor Marcelo Müller pelo uso do espectrômetro de massas.

Agradeço a todos os amigos dos laboratórios, e em especial gostaria de agradecer à Carolina, Huliana, Juliana, Otávio e Rafaela pela ajuda nos experimentos. Também gostaria de agradecer à Anna, Diego e Elaine por todo companheirismo e paciência na minha adaptação aqui no Brasil.

Agradeço aos doutores Arquimedes Paixão e ao Carlos Alves de Souza por serem sempre presentes e dispostos a ajudar.

Agradeço às técnicas do laboratório de Cultivo Celular, por toda dedicação e organização do laboratório.

Agradeço à Pós-Graduação em Ciências-Bioquímica representada pelos professores Glaucia e Guilherme e pelo secretário Thiago, pessoas sempre dispostas a nos dar suporte.

Agradeço a Capes, Organização dos Estados Americanos e Grupo Guarulhos de Universidades Brasileiras pela bolsa de estudos de quatro anos, assim como também ao Redoxoma e ao CNPQ pelo suporte financeiro.

Agradeço também a Universidade Católica de Cuenca pelo apoio para a realização do doutorado.

Agradeço aos meus pais, irmãos e a Juliana pelo amor e suporte emocional para conseguir realizar o doutorado.



## RESUMO

Novos antitumorais mais efetivos e com menos efeitos adversos são necessários para o tratamento do câncer. As chalconas são um grupo de polifenóis de origem natural que tem mostrado ampla variedade de ações biológicas incluindo a ação antitumoral. Modificações na estrutura química das chalconas têm sido realizadas com o intuito de melhorar suas atividades biológicas. Neste trabalho foi realizada, de forma comparativa, análise das atividades citotóxicas da chalcona (CH), 2'-hidroxichalcona (2HC), da 3-nitrochalcona (3NC) e da 2'-hidroxi-3-nitrochalcona (HNC) sobre células HeLa, com o objetivo de verificar a importância dos grupamentos nitro e hidroxil para a potencial atividade antitumoral destes compostos. Observou-se que as chalconas nitradas (3NC e HNC) foram as que tiveram maior efeito citotóxico. A HNC foi a nitrochalcona escolhida para a continuação do estudo de suas propriedades pró-oxidantes e o IC<sub>50</sub> observado foi de 24 µM. A HNC (20 e 30 µM) aumentou a porcentagem de células hipodiplóides e com dupla marcação (anexina V/PI). HNC (30 µM) demonstrou a capacidade de formar aduto com GSH no interior da célula, reduzir os níveis de GSH e aumentar os níveis de espécies reativas de oxigênio (EROs). O efeito citotóxico de HNC não foi revertido com a adição de NAC (10 mM), mas a pré-incubação com BSO (100 µM) fez com que as células ficassem mais sensíveis aos efeitos da HNC (10 e 20 µM). Assim, pode-se sugerir que a HNC promove a morte de células HeLa, possivelmente por apoptose, e que seus efeitos pró-oxidantes podem, pelo menos em parte, colaborar para a indução da morte celular. Neste trabalho também foram analisados os efeitos sobre células HeLa da 4-nitrochalcona (4NC) livre e encapsulada em nanopartículas de polimetacrilato de metila com funcionalização (4NC-PMMA-AF) ou sem funcionalização com ácido fólico (4NC-PMMA). Os objetivos desta parte do trabalho foram verificar os efeitos citotóxicos da 4NC e da 4NC-PMMA-AF em comparação com a 4NC-PMMA em células HeLa que super-expressam receptor para ácido fólico (RAF). A 4NC (15 - 45 µM) promove efeitos citotóxicos de forma dependente da concentração com IC<sub>50</sub> de 32.9 µM, sem alterar o ciclo celular nas concentrações testadas (20 e 30 µM). 4NC aumentou rapidamente os níveis de EROs e os efeitos sobre a viabilidade foram reduzidos com a pré-incubação com NAC. A pré-incubação com BSO deixou as células HeLa mais sensíveis aos efeitos da 4NC. A 4NC (30 µM) forma aduto com GSH em sistema

livre de células. A depleção de GSH pode ser consequência do aumento de EROS. Nanopartículas com 4NC-PMMA-AF foram internalizadas, possivelmente por endocitose envolvendo o RAF. Essa entrada promoveu efeitos citotóxicos em media 25% superiores aos da 4NC livre (15 e 30  $\mu$ M), sugerindo que esta pode ser uma maneira eficiente de entrega da 4NC para gerar seus efeitos em células HeLa. Desta forma, pode-se concluir que as chalconas nitradas promovem efeitos citotóxicos e pró-oxidantes sobre as células HeLa e que a utilização de nanopartículas funcionalizadas de PMMA-AF podem ser uma forma promissora de entrega deste tipo de compostos a este tipo de células.

**Palavras chave:** Nitrochalconas. HeLa. Espécies reativas de oxigênio. Glutathione. Nanopartícula. Ácido fólico.



## ABSTRACT

Novel and more effective antitumor drugs with less adverse side effects are necessary to cancer treatment. Chalcones are polyphenols of natural origin that have shown a wide variety of biological effects including the antitumoral action. Modifications in the chemical structure of chalcones have been conducted in order to improve their biological activities. In this study, we conducted a comparative analysis of the cytotoxic activities of the chalcone (CH), 2'-hydroxychalcone (HC), 3-nitrochalcone (3NC) and 2'-hydroxy-3-nitrochalcone (HNC) on HeLa cells. The objective of the study was to verify the importance of the nitro and the hydroxyl groups in order to test the potential antitumor activity of these compounds. We founded that the nitrated chalcones (3NC and HNC) were those that had the highest cytotoxic effect. We chose HNC to continue the study of its mechanism of action and pro-oxidant properties, and the  $IC_{50}$  observed for it was 24  $\mu$ M. The HNC (20 and 30  $\mu$ M) was able to increase the percentage of hypodiploid and double-labeled cells (annexin V/PI). HNC demonstrate the capacity to form an adduct with GSH inside the cell, reduced GSH levels and increase the levels of reactive oxygen species (ROS). The cytotoxic effect of HNC was not reversed with the addition of NAC (10mM); however, pre-incubation with BSO (100  $\mu$ M) made the HeLa cells more sensitive to the effects of HNC (10 and 20  $\mu$ M). Thus, it may be suggested that HNC promotes tumor cell death, possibly by apoptosis, and that its pro-oxidant effects may, at least in part, induce cell death. In this study, were also analyzed the effects of 4-nitrochalcone (4NC) free and encapsulated on polymethyl methacrylate nanoparticles functionalized (4NC-PMMA-FA) or not with folic acid (FA) on HeLa cells. For this part of the study the objectives were to assess the cytotoxic and pro-oxidant effects of 4NC and to verify if using PMMA-AF compared to PMMA would collaborate with the delivery of 4NC to HeLa cells that overexpress the folate receptor (RFA). The 4NC (15 - 45  $\mu$ M) promotes cytotoxic effects in a concentration-dependent manner with an  $IC_{50}$  of 32.9  $\mu$ M, without affecting the cell cycle at the tested concentrations (20 e 30  $\mu$ M). 4NC rapidly increases the levels of ROS and the effects on cell viability were reduced by pre-incubation with NAC. Pre-incubation with BSO turn the cells more sensitive to the effects of 4NC. 4NC (30  $\mu$ M) formed an adduct with GSH in a cell-free system. GSH depletion may be a consequence of increased ROS. Nanoparticles with 4NC encapsulated in PMMA-AF were

internalized, possibly through an endocytic mechanism involving RFA. This entry promoted 25% higher cytotoxic effects than free 4NC (15 and 30  $\mu$ M), suggesting that this could be an efficient way to deliver 4NC in order to generate its effect in HeLa cells. Thus, we conclude that nitrated chalcones promote cytotoxic and pro-oxidant effects on HeLa cells and that the use of PMMA-AF functionalized nanoparticles containing 4NC may be a promising strategy to the delivery of these types of compounds at these cells.

**Keywords:** Nitrochalcones. HeLa. Reactive oxygen species. Glutathione. Nanoparticles. Folic acid.

## LISTA DE ABREVIATURAS

2HC	2'-hidroxichalcona
3NC	3-nitrochalcona
4NC	4-nitrochalcona
AF	Ácido fólico
ARE	<i>Antioxidant response element</i>
ATP	Adenosina trifosfato
CAT	Catalase
CCU	Câncer cérvico uterino
CH	Chalcona
DCFDA	2'-7'-Dichlorodihidrofluorescina diacetato
DMSO	Dimetilsulfoxido
EROs	Espécies reativas de oxigênio
FDA	<i>Food and Drug Administration</i>
GSH	Glutathiona reduzida
GSSG	Glutathiona oxidada
GST	Glutathiona-S transferase
H <sub>2</sub> O <sub>2</sub>	Peróxido de hidrogênio
HIV	<i>Human immunodeficiency virus</i>
HNC	2'-hidroxi-3-nitrochalcona
HPV	<i>Human papillomavirus</i>
INCA	Instituto Nacional do Câncer
KEAP-1	<i>Kelch like ECH associated protein 1</i>
$K_m$	Constante de Michaelis
$K_{mapp}$	Constante de Michaelis aparente
mBCI	Monoclorobimano
MTT	Brometo de 3-(4,5-dimetiltiazol-2-il)-2,5-difeniltetrazólio
NAC	N-acetilcisteína
NCI	<i>National Cancer Institute</i>
NF- $\kappa$ B	<i>Nuclear factor-kappa B</i>
NNPs	Nanopartículas
Nrf2	<i>Nuclear factor erythroid 2-related factor 2</i>
PBS	Solução salina tamponada

PMMA	Polimetacrilato de metila
pRb	Proteína do retinoblastoma
SOD	Superóxido dismutase
WHO	<i>World Health Organization</i>

## SUMÁRIO

Capítulo 1: INTRODUÇÃO .....	17
Capítulo 2. REVISÃO BIBLIOGRÁFICA .....	20
2.1. Aspectos gerais do câncer cérvico uterino .....	20
2.2 Mecanismos de ação antitumoral.....	22
2.2.1. Regulação do ciclo celular .....	22
2.2.2. Indução de morte celular .....	23
2.2.2.1. Apoptose.....	23
2.2.2.2. Necrose.....	24
2.3. Papel de espécies reativas de oxigênio e indução de morte celular .....	26
2.4. Envolvimento da glutathiona no controle redox e na detoxificação de xenobióticos.....	27
2.5. Transportador MRP1 .....	29
2.6 Chalconas como potenciais fármacos antitumorais.....	30
2.6.1 Atividade antitumoral de chalconas hidroxiladas .....	31
2.6.2 Chalconas nitradas .....	32
2.6 Nanopartículas como sistema de entrega de fármacos.....	33
2.7 Justificativa.....	34
Capítulo 3. OBJETIVOS .....	36
3.1 OBJETIVO GERAL .....	36
3.2 OBJETIVOS ESPECÍFICOS .....	36
Capítulo 4: : Prooxidant and cytotoxic effect of 4–nitrochalcone on HeLa cells .....	38
Abstract .....	39
4.1. Introduction .....	40
4.2 . Material and Methods.....	41
4.2.1 Material .....	41
4.2.2 Biological assays.....	41
4.2.3 <i>In vitro</i> cytotoxicity assay .....	42
4.2.4 Fluorescence microscopy analysis .....	42
4.2.5 Morphological analysis of cells stained with hematoxylin and eosin (H&E).....	43
4.2.6 Assessment of the effect of 4NC on the cell cycle .....	43
4.2.7 Assessment of reactive oxygen species .....	43
4.2.8 Assessment of reduced glutathione levels .....	44
4.2.9 Characterization of the adduct 4NC-GS by RP- HPLC and Mass Spectrometry .....	44
4.2.10 Statistical analysis .....	45
4.3 Results.....	45
4.3.1 <i>In vitro</i> cytotoxic effect of 4NC in HeLa cells .....	45

4.3.2 Evaluation of 4NC effect in the HeLa cell cycle .....	47
4.3.3 Effect of 4NC on the cellular levels of reactive oxygen species .....	48
4.3.4 Effect of 4NC on the cellular glutathione levels .....	49
4.3.5 Cytotoxicity assay using cells overexpressing MRP1 transporter.....	52
4.4 Discussion .....	53
4.5 Conclusion.....	56
4.6 References .....	56
Capítulo 5: Synthesis and evaluation of a formulation of 4–nitrochalcone loaded in poly(methyl methacrylate) nanoparticles functionalized with folic acid against HeLa cells .....	65
Abstract....	66
5.1 Introduction.....	67
5.2 Material and Methods.....	69
5.2.1 Material.....	69
5.2.2 Methods.....	69
5.2.2.1. Synthesis of 4NC loaded in folic acid – PMMA nanoparticles.....	69
5.2.2.2. Synthesis of 4NC loaded in folic acid - PMMA nanoparticles labeled with 6-coumarin.....	70
5.2.3 Characterization .....	70
5.2.3.1. Entrapment efficiency (EE %) of 4NC .....	70
5.2.3.2. Controlled and kinetic release .....	71
5.2.4. Biological assays .....	72
5.2.4.1. <i>In vitro</i> cytotoxicity assay.....	72
5.2.4.2. Cellular uptake assay by laser scanning confocal microscopy....	72
5.2.4.3. Statistical analysis .....	73
5.3 Results and discussion.....	73
5.3.1. Physicochemical proprieties analyses of nanoparticles .....	73
5.3.2. Kinetic release studies of 4NC.....	75
5.3.3. Evaluation of the effect on the cell viability of 4NC encapsulated in folic acid-PMMA nanoparticles .....	76
5.3.4. Cellular uptake of folic acid-PMMA nanoparticles .....	78
5.4 Conclusion.....	80
5.5 References.....	81
Capítulo 6: Prooxidant and cytotoxic effects of nitrochalcones on HeLa cells.....	93
Abstract.....	94
6.1 Introduction.....	95
6.2 Material and Methods.....	96



6.2.1 Materials.....	96
6.2.2 Cell cultures .....	97
6.2.3 Methods .....	97
6.2.3.1 Cell viability assays .....	97
6.2.3.2 Morphological analysis of HeLa cells treated with HNC.....	98
6.2.3.3 Cell cycle analysis.....	98
6.2.3.4 Annexin V-FITC/Propidium iodide double labeling assay .....	98
6.2.3.5 Measurement of intracellular ROS generation .....	99
6.2.3.6 Fluorescence microscopy analysis.....	99
6.2.3.7 Characterization of the adduct by RP- HPLC and mass spectrometry.....	100
6.2.3.8 Statistical analysis .....	100
6.3 Results.....	101
6.3.1 Effects of chalcones on the viability of HeLa cells.....	101
6.3.2 Effects of HNC on cell cycle .....	103
6.3.3 Annexin V-FITC/Propidium iodide double labeling assay .....	104
6.3.4 Effect of HNC on the ROS levels .....	105
6.3.5 Effect of HNC on the reduced GSH levels.....	107
6.3.6 Formation of adduct between HNC and GSH.....	107
6.3.7 Influence of the overexpression of MRP1 transporters in the HNC effect .....	109
6.4. Discussion.....	110
6.5. Conclusion.....	113
6.6. References.....	114
Capítulo 7. CONSIDERAÇÕES FINAIS.....	121
Capítulo 8: CONCLUSÕES .....	126
REFERÊNCIAS .....	128

# Capítulo 1: Introdução

## Capítulo 1: INTRODUÇÃO

O câncer cérvico uterino é um dos tumores mais frequentes em mulheres e especialmente incidente em países não desenvolvidos (WHO, 2017). O prognóstico para as pacientes piora com a progressão da doença e vários quimioterápicos se tornam menos eficazes ao longo do tempo. Diante das condições atuais de tratamento, há necessidade de desenvolvimento de novos fármacos, que sejam potencialmente mais efetivos e menos tóxicos. Nesse contexto, destacam-se as chalconas, um grupo de flavonóides que apresenta importantes atividades citotóxicas e antiproliferativas sobre algumas linhagens de células tumorais (LEE et al., 2016a; ZHANG et al., 2015a). As chalconas são moléculas constituídas por dois anéis aromáticos de seis carbonos identificados como anéis A e B, os quais são conectados por um sistema ceto-enona de três carbonos. Várias chalconas com grupo hidroxila, especialmente quando localizado na posição 2 do anel A (2'), possuem atividade pró-oxidante (GALATI et al., 2002; JIN et al., 2008), assim como maior reatividade com grupos tióis presentes em alguns dos seus alvos celulares (AMSLINGER et al., 2012a).

O grupo funcional nitro é menos frequente em moléculas naturais, porém é encontrado em vários fármacos usados para tratar diferentes doenças (CHIN CHUNG; LONGHIN BOSQUESI; LEANDRO DOS SANTOS, 2011). No entanto, vários efeitos adversos dessas drogas se relacionam com o potencial deste grupo para gerar espécies reativas de oxigênio (EROs) e metabólitos tóxicos (BOELSTERLI et al., 2006).

Neste estudo foram analisados os efeitos de chalconas nitradas nas posições 3 (3NC) e 4 (4NC), cujos efeitos citotóxicos sobre células tumorais são pouco conhecidos e também da HNC (2'hidroxi-3-nitrochalcona), cujos efeitos sobre células HeLa não foram relatados na literatura. O objetivo principal foi verificar a importância destes grupamentos para os efeitos pró-oxidantes e citotóxicos destas nitrochalconas sobre as células HeLa.

Uma estratégia para reduzir a toxicidade de fármacos e conseguir maior seletividade para eliminar células tumorais é usar nanopartículas (NNPs) para seu encapsulamento. Estas NNPs podem ser funcionalizadas com diversos ligantes como ácido fólico (AF), o qual favorece a sua internalização em células com altos níveis de expressão do seu receptor, como células HeLa. No presente

trabalho foram verificados a internalização e os efeitos citotóxicos sobre células HeLa da 4NC carregada em NNPs de polimetacrilato de metila funcionalizadas ou não com AF e comparados com os da 4NC livre para verificar a efetividade da formulação.

Empregando a chalcona (núcleo básico), 3NC, 2'-hidroxichalcona (2HC) e HNC foram analisadas as contribuições dos grupos hidroxila e nitro para os seus efeitos na viabilidade de células HeLa. As chalconas que induziram as maiores reduções da viabilidade formam a 3NC e a HNC. Por ser mais hidrossolúvel e ter os maiores efeitos citotóxicos a HNC foi escolhida para avaliar o mecanismo de indução de morte e os possíveis efeitos sobre níveis de EROs e GSH.

Estes estudos foram realizados com a finalidade de verificar se chalconas nitradas seriam compostos promissores e com potencial antitumoral para o tratamento do câncer cérvico uterino utilizando como modelo as células HeLa.

## Capítulo 2: Revisão Bibliográfica

## Capítulo 2. REVISÃO BIBLIOGRÁFICA

### 2.1. Aspectos gerais do câncer cérvico uterino

O câncer cérvico uterino (CCU) é um dos tipos de câncer mais prevalentes no mundo, com aproximadamente 528.000 novos casos por ano, e a quarta causa mais comum de óbitos em mulheres (WHO, 2017). Os países africanos concentram as maiores taxas de incidência e de mortalidade, sendo confirmadas mais de 260.000 mortes anuais (WHO, 2017). No Brasil, as estimativas anuais são de mais de 16.300 novos casos, com 5.400 óbitos e ainda a permanência como terceiro tipo de tumor mais frequente em mulheres, atrás somente de câncer de mama e colorretal (INCA, 2017).

A maior parte dos casos de CCU é resultado da infecção pelo vírus do papiloma humano (*human papillomavirus*, HPV). Essa infecção, na maior parte das vezes, pode ser transiente e melhorar espontaneamente (condição mais comum em mulheres jovens, com menos de 30 anos), ou desenvolver-se uma condição pré-maligna de neoplasia intra-epitelial cervical ou ainda, o adenocarcinoma *in situ* (mais frequente em mulheres com mais de 30 anos de idade). Alguns fatores que contribuem para a malignização são o fumo, o uso prolongado de contraceptivos orais, e a co-infecção com os vírus do herpes tipo dois e também com vírus da imunodeficiência humana (*human immunodeficiency virus*, HIV) (NCI, 2017).

O genoma do HPV é dividido em três regiões com genes responsáveis pela codificação de proteínas regulatórias denominadas E (*early*, as quais são expressas primeiramente pelo vírus durante a infecção), as proteínas estruturais de capsídeo denominadas L (*late*, as quais são expressas tardiamente pelo vírus durante a infecção) e o segmento LCR (*long control region*, que serve como ponto inicial de replicação e de ligação de fatores de transcrição) (ZHENG; BAKER, 2006). A oncoproteína viral E6 afeta a função da proteína supressora tumoral p53 induzindo sua degradação, enquanto que a oncoproteína E7 interfere com as funções da proteína do retinoblastoma (pRb) resultando em perda de controle do ciclo celular, que é determinante para o início e a progressão de CCU (BRAUN et al., 2004; THOMAS; PIM; BANKS, 1999).

A primeira vacina desenvolvida para HPV foi o Gardasil aprovada pela FDA (*Food and Drug Administration*) em 2006 (HAJJ HUSSEIN et al., 2015).



Atualmente estão disponíveis as versões denominadas Gardasil (Merck, Sharpe e Dohme) e Cervarix (Glaxo, Smith e Kline), as duas são baseadas no desenvolvimento da proteína recombinante de capsídeo L1. Gardasil é efetiva contra os sorotipos HPV 16 e 18, enquanto Cervarix é mais específica contra os sorotipos 6, 11, 16 e 18 (SZAREWSKI, 2012).

As estratégias terapêuticas utilizadas no tratamento de pacientes acometidos com CCU variam de acordo com o estágio da doença. Nas etapas iniciais (denominada carcinoma *in situ*), a ressecção cirúrgica, radioterapia, assim como a histerectomia são opções que resultam em altas taxas de sobrevivência. Nos estágios mais avançados é frequente a combinação de radioterapia com quimioterápicos como cisplatina, usada como único agente ou em associação a paclitaxel, 5-fluorouracil, ou topotecam (NCI, 2017). Mais recentemente, o desenvolvimento do anticorpo monoclonal com atividade antiangiogênica Bevacizumab tem mostrado interessante potencial para melhorar o prognóstico de pacientes com câncer cervical em estágio avançado (TEWARI et al., 2017).

Apesar dos avanços na prevenção, diagnóstico e tratamento do CCU, ainda são necessárias novas alternativas terapêuticas que sejam mais eficazes e que causem menos efeitos adversos. Tradicionalmente moléculas isoladas de fontes naturais têm servido para o desenvolvimento de vários agentes antitumorais (LI; WENG, 2017). Os flavonóides são um grupo de polifenóis de origem vegetal que podem ser classificadas em flavonas, flavanonas, flavonóis, antocianidinas e isoflavonóis (FALCONE FERREYRA; RIUS; CASATI, 2012). Vários flavonóides têm mostrado capacidade de sensibilizar células tumorais para a efetiva ação dos quimioterápicos tradicionais (SAHIN et al., 2012). No entanto, também apresentam efeitos citotóxicos e anti-proliferativos sobre vários tipos de células tumorais como pulmão, mama, rim e incluindo linhagens derivadas de câncer cérvico uterino como HeLa (BATRA; SHARMA, 2013; KIM et al., 2009; LAZZE et al., 2004; SRIVASTAVA et al., 2016; WANG et al., 2015).

As chalconas, objetos de estudo desta tese, são intermediários na biossíntese dos flavonóides, porém são frequentemente incluídos neste grupo e compartilham várias dos seus efeitos biológicos como antioxidantes, antiinflamatórios, antibacterianos e potenciais efeitos antitumorais (CASTRO-VAZQUEZ et al., 2016; FANG et al., 2016; PÉREZ-CANO; CASTELL, 2016).

## **2.2 Mecanismos de ação antitumoral**

Em geral, fármacos usados em quimioterapia podem atuar através de mecanismos capazes de diminuir a capacidade de proliferação tumoral (citostáticos) ou induzindo a morte celular (citotóxicos) (RIXE; FOJO, 2007).

A seguir, serão descritas brevemente algumas das vias que participam nestas respostas celulares.

### **2.2.1. Regulação do ciclo celular**

De forma abrangente as células passam por um ciclo para sua replicação que se organiza em cinco fases principais: 1) fase mitótica, denominada M, 2) fase G1 (*gap 1*), onde a célula responde ao controle positivo ou negativo de fatores de crescimento e etapa onde proteínas responsáveis pela duplicação do DNA são expressas; 3) fase G0, etapa reversível onde alguns tipos celulares entram em estado quiescente; 4) fase S, etapa onde todo DNA celular é duplicado para poder ser distribuído entre duas células; 5) fase G2, responsável pela síntese de moléculas que atuam na fase de mitose (HARTWELL; KASTAN, 1994).

A passagem pelas etapas do ciclo celular é regulada por fosfatases e quinases do tipo CDK (*cyclin dependent kinase*), cuja atividade é controlada em grande medida pela sua associação às correspondentes ciclinas. Alguns dos membros CDK e ciclinas expressos em mamíferos são: Cdk2, Cdk4 e Cdk1 e ciclinas A, B, D e E (FOSTER, 2008).

O câncer se estabelece quando as taxas de proliferação são superiores comparadas à morte celular. Essa condição é produto de alterações nos mecanismos que controlam cada etapa do ciclo celular. Frequentemente estas falhas no controle podem se associar com mutações em proto-oncogenes e/ou genes supressores de tumor. Exemplos de oncogenes envolvidos com a progressão do ciclo celular são: Her2/ neu, Ras e c-Myc, enquanto que genes supressores tumorais têm como alguns dos principais membros pRb e p53 (FOSTER, 2008).

O supressor tumoral pRb é chave para o controle da transição G1-S em resposta a sinais mitogênicos (BRAUN et al., 2004). p53 é um supressor tumoral

que em mais da metade dos tipos de câncer apresenta mutações que levam à perda ou ganho de função com potencial oncogênico (KHOO et al., 2014; OREN; ROTTER, 2010). Entre a ampla variedade de atividades se destaca seu envolvimento na regulação da transcrição de varias proteínas encargadas de mecanismos de reparo do DNA (WILLIAMS; SCHUMACHER, 2016). Alguns desses genes codificam para inibidores de quinases dependentes de ciclinas. Esses inibidores agem como supressores tumorais que se ligam diretamente aos pares CDK/ciclina e com isso regulam negativamente a progressão do ciclo celular (MURRAY-ZMIJEWSKI; SLEE; LU, 2008; PAEK et al., 2016).

### ***2.2.2. Indução de morte celular***

Vários mecanismos de morte celular têm sido descritos recentemente na literatura os quais se baseiam principalmente em parâmetros bioquímicos e incluem: apoptose, necrose, necroptose, ferroptose, autofagia entre outros (GALLUZZI et al., 2018). A seguir serão enfatizados somente os principais tipos de indução de morte celular que foram investigados nesta tese: apoptose e necrose.

#### ***2.2.2.1. Apoptose***

A apoptose é definida como um tipo de morte celular regulada (MCR) que está envolvida em importantes funções homeostáticas, porém esta via também pode ser ativada farmacologicamente para induzir a eliminação de células tumorais. Algumas características frequentes em células apoptóticas são: a redução do volume celular, externalização de fosfatidilserina (FS), condensação nuclear, fragmentação de cromatina, entre outras (JIANG et al., 2016). Este tipo de MCR é dependente da ativação das caspases executoras 3 e 7 (TAYLOR; CULLEN; MARTIN, 2008), que são proteases encarregadas de desenvolver todos os processos que culminam na morte celular. A ativação destas caspases pode ser induzida por duas vias denominadas intrínseca e extrínseca.

A via intrínseca ou mitocondrial pode ser ativada por vários estímulos endógenos como estresse oxidativo, falta de nutrientes, ou por estímulos exógenos como os gerados por alguns quimioterápicos. Exemplos desses efeitos são os produzidos por fármacos como a cisplatina que gera danos ao

DNA por alquilação (TANIDA et al., 2012), enquanto outros como o paclitaxel modificam a dinâmica da polimerização de microtúbulos (JORDAN et al., 1996) e em ambos são ativadores da via intrínseca. Em resposta a estas alterações as proteínas pró-apoptóticas da família Bcl-2 (membros Bax e Bak) se dissociam das proteínas anti-apoptóticas da família Bcl-2 (Bcl-2, Mcl-1 e Bcl-w) e formam dímeros que permeabilizam a membrana mitocondrial externa liberando fatores apoptogênicos como citocromo *c*, entre outros (CHEN et al., 2005; LIU et al., 2008). Uma vez no citoplasma o citocromo *c* se liga aos monômeros de Apaf-1 (*apoptotic protease activating factor-1*) para formar um apoptossomo heptamérico que incorpora monômeros de pro-caspase-9, gerando a caspase 9 ativa, que por sua vez ativa as pró-caspases executoras 3 e 7 (LI et al., 1997; YUAN et al., 2011).

A via extrínseca é mediada pela ativação de receptores de superfície denominados de receptores de morte. Essa via inclui mais de 20 proteínas, sendo o grupo CD95 (APO-1/Fas), TNFR1 (*tumor necrosis fator receptor 1*), TRAIL-R1 (*TNF-related apoptosis-inducing ligand-receptor 1*) e TRAIL-R2 os mais caracterizados em mamíferos (FULDA; DEBATIN, 2006). No caso dos receptores CD95 e TRAIL-R1 e TRAIL-R2, após a ligação aos seus respectivos ligantes (FasL e TRAIL) é gerada a trimerização dos receptores, o que permite a interação entre seus domínios de morte citoplasmáticos. No caso do receptor CD95 este processo leva à associação de moléculas adaptadoras FADD (*Fas-associated death domain*) que recruta as caspases 8/10 ao receptor CD95 formando o complexo chamado de DISC (*CD95 death-inducing signaling complex*). A formação deste complexo favorece a oligomerização e consequente autoclivagem e ativação de caspase-8, que por sua vez pode ativar as caspases executoras 3 e 7 (FULDA; DEBATIN, 2006). Algumas células precisam da ativação conjunta da via extrínseca e da intrínseca para o desencadeamento da apoptose (ALGECIRAS-SCHIMNICH et al., 2002). Esta amplificação é gerada pela clivagem dependente das caspases 8/10 de outro membro pró-apoptótico da família Bcl-2, denominado Bid. Esse fragmento truncado (tBid) é capaz de induzir a saída dos fatores pró-apoptóticos das mitocondrias, conectando assim a via extrínseca com a intrínseca (PREMKUMAR et al., 2012).

#### **2.2.2.2. Necrose**

A necrose é tradicionalmente definida como um tipo de morte celular acidental e considerada como um processo passivo (SYNTICHAKI; TAVERNARAKIS, 2002). Morfologicamente este tipo de morte se caracteriza pelo aumento do volume celular, pela perda da permeabilidade seletiva da membrana, ausência de condensação da cromatina e da fragmentação do núcleo (VANDEN BERGHE et al., 2013). Como consequência do rompimento da membrana celular se produz a saída de componentes intracelulares conhecidos coletivamente como DAMPs (*Damage-associated Molecular Patterns*) que incluem HMGB-1, IL-1 $\alpha$ , ATP e calreticulina (KRYSKO et al., 2017).

Os DAMPS são reconhecidos por pelo menos cinco classes de receptores de membrana (SCHAEFER, 2014) provocando respostas imunogênica e inflamatória, as quais são características da necrose *in vivo* (ROSIN; OKUSA, 2011). Apesar de ser um mecanismo com potencial pro-inflamatório e com capacidade para desenvolver dano tecidual, alguns trabalhos sugerem que a indução seletiva deste tipo de morte em tumores poderia ser uma forma de eliminar células que contornam outros mecanismos de morte como apoptose (DINNEN et al., 2007; WONG; LIM; ANG, 2015).

A necroptose é um mecanismo de morte celular que mantém algumas características da necrose. No entanto, uma significativa diferença entre os dois mecanismos de morte é o fato de que a necroptose pode ser regulada pela maquinaria celular, porém é independente da ativação das caspases. Um dos modelos melhor caracterizados de necroptose é o induzido pelo fator de necrose tumoral (TNF) (MORENO-GONZALEZ; VANDENABEELE; KRYSKO, 2016). Após a ligação do TNF a receptor TNFR1 acontece o recrutamento de proteínas como TRADD (*TNFR1-associated death domain protein*), RIP1 (*receptor-interacting protein 1*) e TRAF2, formando o complexo 1 que ativa RIPK3 (*receptor-interacting protein 3*), seguido da fosforilação de MLKL (*mixed lineage kinase domain-like*). Após ativação, MLKL se transloca para a membrana plasmática e se oligomeriza levando à formação de poros que produzem a saída de íons cálcio e que representam um dos eventos iniciais deste mecanismo de morte (CAI et al., 2014). Contudo, existem evidências de que algumas células como HeLa, não expressam RIPK3 e são resistentes a indutores de necroptose (WANG et al., 2012). Por este motivo estratégias adicionais para restabelecer a maquinaria necroptótica poderiam ser necessárias nestes casos (KOO et al.,

2015). Adicionalmente, este mecanismo poderia também ter potencial pro-inflamatório e ainda, em determinados contextos, favorecer a proliferação e metástase. Assim, mais estudos são necessários para estabelecer se indutores desta via poderiam ser uma alternativa em quimioterapia (WANG et al., 2017).

### **2.3. Papel de espécies reativas de oxigênio e indução de morte celular**

As espécies reativas de oxigênio (EROs) são subprodutos do metabolismo celular aeróbico e incluem moléculas com um ou mais elétrons desemparelhados conhecidas como radicais livres de oxigênio, assim como moléculas não radicalares como o peróxido de oxigênio (MENON; GOSWAMI, 2007). Devido a seu potencial tóxico para as células quando atingem certo nível, as suas concentrações são estritamente controladas por vários sistemas antioxidantes (NORDBERG; ARNÉR, 2001). Em geral, células tumorais possuem maiores níveis de EROs, quando comparadas com as células normais, o que faz que as células tumorais sejam mais sensíveis ao aumento de EROs (GALADARI et al., 2017).

Organelas como mitocôndrias, retículo endoplasmático e peroxissomos (GORRINI; HARRIS; MAK, 2013), assim como as enzimas NADPH oxidases, xantina oxidase e ciclooxigenases (VALKO et al., 2007) produzem EROs como consequência das funções fisiológicas que desenvolvem.

O radical superóxido ( $O_2^{\cdot-}$ ), peróxido de oxigênio ( $H_2O_2$ ), radical hidroxila ( $\cdot OH$ ) e oxigênio singlete são as EROs com maior importância biológica. Uma das principais fontes do  $O_2^{\cdot-}$  é a mitocôndria, sendo considerado que, sob condições fisiológicas, aproximadamente 1 a 2% do oxigênio consumido é transformado em  $O_2^{\cdot-}$  (HANDY; LOSCALZO, 2012). Apesar de ser uma das EROs com menor toxicidade devido a sua baixa reatividade, a sua maior importância é a capacidade de originar  $H_2O_2$  como produto da sua dismutação espontânea ou catalisada pela enzima superóxido dismutase (SOD) (SHENG et al., 2014). Adicionalmente, o  $O_2^{\cdot-}$  pode reagir com óxido nítrico e gerar outra espécie muito mais tóxica para a célula, como o peroxinitrito (PACHER; BECKMAN; LIAUDET, 2007).

O  $H_2O_2$  apesar de sua maior estabilidade e de ser um forte oxidante possui uma cinética de reação lenta, o que faz desta molécula pouco reativa



quando comparada com outras espécies como, por exemplo, o radical hidroxila (DOSKEY et al., 2016). As enzimas catalase (CAT), glutathione peroxidase e as peroxiredoxinas estão envolvidas no catabolismo de  $H_2O_2$  controlando os seus níveis intracelulares.

Uma das reações de importância biológica nas quais está envolvido o  $H_2O_2$  é a reação de Fenton que leva a formação de  $\cdot OH$ , o qual é altamente reativo (CADET et al., 1999). O radical  $\cdot OH$  possui um tempo de vida curto e, de forma diferente a outros EROs, não pode ser eliminada enzimaticamente, o que somado a sua alta reatividade frente a moléculas como o DNA, faz deste radical uma das que possui maior potencial citotóxico (KONG; LIN, 2010; NIMSE; PAL, 2015).

Um componente chave nos mecanismos de regulação redox celular é o fator de transcrição Nrf2 (*nuclear factor E2-related factor*) (YANG et al., 2015). Em células não estressadas Nrf2 é ubiquitinado pela proteína Keap1 (*Kelch-like ECH-associated protein 1*) e marcado para degradação no proteassomo (ZHANG et al., 2004). No entanto, o aumento de EROs produz a oxidação de grupos tióis em Keap1, permitindo a dissociação de Nrf2 e sua translocação nuclear para promover a transcrição de enzimas como a SOD, CAT, assim como de algumas enzimas envolvidas na síntese de GSH (DONG; SULIK; CHEN, 2008; LU, 2014).

#### **2.4. Envolvimento da glutathione no controle redox e na detoxificação de xenobióticos**

A glutathione (GSH) é o tiol não protéico mais abundante nas células, encontrada em concentrações entre 1 - 10 mM no citoplasma. Essa molécula é constituída pelos aminoácidos cisteína, glutamato e glicina. A síntese ocorre exclusivamente no citoplasma e na dependência de ATP. As enzimas envolvidas na síntese de GSH são a glutamato-cisteína ligase (GCL) cuja transcrição é controlada por Nrf2 (LU, 2014) e a glutathione sintetase (GS) que incorpora a glicina na molécula da glutamylcisteína na reação final de síntese de GSH (MARÍ et al., 2009b).

A GSH possui um papel chave nos mecanismos de controle redox celular. Em condições de ausência de estresse oxidativo a razão molar entre glutathione reduzida e a forma oxidada (GSSG) é de 100:1 (ZITKA et al., 2012). Uma vez

oxidada, a GSSG é reduzida novamente pela enzima glutathione redutase (GR) numa reação dependente de NADPH. A GSH pode neutralizar diretamente algumas EROs, porém também é co-substrato de várias enzimas antioxidantes, como as glutathione peroxidases (GPx1–GPx8), responsáveis pela redução de  $H_2O_2$  (BRIGELIUS-FLOHÉ; MAIORINO, 2013).

Além da GSH encontrada no citosol, esta molécula também está compartimentalizada em algumas organelas celulares. A mitocôndria possui uma concentração de GSH semelhante à citoplasmática (MARÍ et al., 2009a). No retículo endoplasmático a razão glutathione oxidada e reduzida é maior do que no citoplasma, e com isso favorece a formação de pontes dissulfeto nas proteínas que são processadas neste compartimento (HWANG; SINSKEY; LODISH, 1992). No núcleo existem oscilações no estado de oxidação de glutathione durante o ciclo celular, o que constitui um mecanismo adicional de regulação da transcrição (DIAZ VIVANCOS et al., 2010). Adicionalmente, a GSH está envolvida em vias de detoxificação de vários xenobióticos por mecanismos como a inativação por conjugação ou mediante o seu efluxo por co-transporte (BALLATORI et al., 2009). A conjugação entre a GSH (pelo tiolato da cisteína) e moléculas eletrófilas pode acontecer de forma espontânea, devido ao caráter nucleofílico da GSH. Porém, nas células esta reação é catalisada por várias enzimas da família das glutathione-S transferases (GSTs) e é um dos processos críticos para a detoxificação de eletrófilos (DI PIETRO; MAGNO; RIOS-SANTOS, 2010; HAMADA et al., 1994).

As GSTs são divididas em várias subfamílias como alfa ( $\alpha$ )/ GST A, Kappa ( $\kappa$ )/ GST K, mu ( $\mu$ )/ GST M, ômega ( $\omega$ )/ GST O, pi ( $\pi$ )/ GST P, sigma ( $\sigma$ )/ GST S, theta ( $\theta$ )/ GST T e zeta ( $\zeta$ )/ GST Z (MOHANA; ACHARY, 2017). Altos níveis de expressão de GSTP1 são frequentes em várias linhagens tumorais que apresentam fenótipo de resistência a quimioterápicos como clorambucil (PAUMI et al., 2001), cisplatina (CHEN et al., 2013b), entre outros. Além do seu papel na detoxificação, essas enzimas estão envolvidas em sinalização celular modificando pos-traducionalmente proteínas por S-glutathionilação (GREK et al., 2013). Ainda, a enzima GST P está envolvida na regulação negativa da MAP quinase JNK (c-Jun N-terminal kinase); formando um hetero-complexo GST P - JNK (ADLER; PINCUS, 2004) e impedindo sua função pró-apoptótica (TURELLA et al., 2005).

## 2.5. Transportador MRP1

As proteínas da superfamília de transportadores ABC (do inglês *ATP-binding cassette*) são classificadas nas subfamílias A, B, C, D, E, F e G com base no arranjo de componentes estruturais moleculares como os domínios de união a nucleotídeos ou a topologia dos domínios transmembrana (TOYODA et al., 2008). Sua função no transporte de moléculas está acoplada à hidrólise de ATP e são responsáveis pelo transporte de uma ampla diversidade de substratos endógenos e exógenos (ZHANG et al., 2015c).

Após a reação de uma molécula com GSH, o efluxo do conjugado é efetuado por alguns transportadores da família MRP (BALLATORI et al., 2009; SMITHERMAN, 2003). Destes transportadores um dos mais estudados pela capacidade de eliminar uma ampla variedade de conjugados é o MRP1 (COLE, 2014).

O transportador MRP1 (também denominado ABCC1) é um dos membros da subfamília ABCC, a qual é composta de doze proteínas, das quais pelo menos nove realizam o transporte de moléculas de forma dependente de ATP (COLE, 2014). Além da sua localização na membrana plasmática, esses transportadores também têm sido identificados no núcleo (GORDILLO et al., 2016) e em organelas como lisossomos e mitocôndrias (ROUNDHILL; BURCHILL, 2012).

Os substratos de MRP1 incluem fármacos co-transportados ou conjugados com GSH, assim como conjugados com ácido glicurônico e sulfato (BALLATORI et al., 2009). Adicionalmente, tem sido demonstrado que tanto a GSH reduzida quanto a oxidada podem ser transportadas por esta via, o que representa um mecanismo alternativo de controle redox (BALLATORI et al., 2009). Apesar da baixa afinidade de MRP1 por GSH reduzida ( $K_{\text{mapp}} \sim 10 \text{ mM}$ ), comparada à afinidade pela oxidada ( $K_{\text{mapp}} \sim 70 \text{ }\mu\text{M}$ ), o transporte ainda é suficiente para gerar diferenças no conteúdo de GSH reduzida entre células com níveis basais e as que superexpressam o transportador (COLE, 2014). O transporte de GSSG é especialmente importante em condições de estresse oxidativo nas quais MRP1 promove a diminuição dos níveis intracelulares de GSSG, a qual possui potencial tóxico devido a seu caráter oxidante (PARK et al., 2009a).

Estudos têm mostrado que fármacos, como o bloqueador de canais de cálcio verapamil, (LOE; DEELEY; COLE, 2000), assim como alguns flavonóides como as chalconas (KACHADOURIAN, 2006; NGUYEN; ZHANG; MORRIS, 2003) são capazes de promover o efluxo de GSH através do transportador MRP1 e induzir depleção de GSH. Com isso, estas moléculas podem restaurar a sensibilidade de células tumorais a quimioterápicos que são co-transportados, ou inativados por GSH (BRECHBUHL et al., 2012; RAPP et al., 1997) e ainda são capazes de induzir morte celular pelo produto de depleção de GSH em um processo chamado de sensibilidade colateral.

## 2.6 Chalconas como potenciais fármacos antitumorais

As chalconas são moléculas constituídas por dois anéis aromáticos (A e B) ligados por um sistema carbonila  $\alpha$ ,  $\beta$ -insaturado de três carbonos (AMSLINGER et al., 2012a). Porém, existem vários exemplos na literatura de chalconas nas quais um ou os dois anéis sofrem substituição com diferentes grupos funcionais (MARTEL-FRACHET et al., 2015). Vários efeitos biológicos das chalconas são atribuídos à reatividade da região  $\alpha$ ,  $\beta$ -insaturada com alvos celulares que possuem grupos tióis (-SH) (GAN et al., 2013; PERJÉSI et al., 2012). Relatos da literatura mostram que a reatividade das chalconas é influenciada pela inclusão de grupos funcionais, como hidroxila, metila, nitro, entre outros, os quais conferem mudanças significativas na resposta biológica (MAYDT, DE SPIRT, MUSCHELKNAUTZ, STAHL, & MÜLLER, 2013). Na Figura 1 estão as estruturas químicas das chalconas que foram utilizadas neste trabalho.

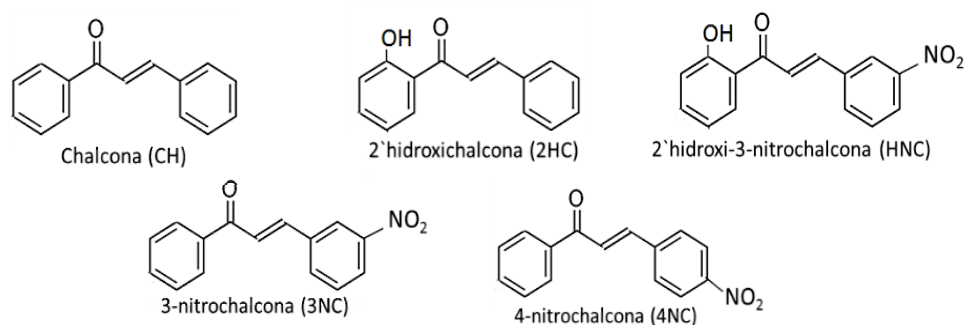


Figura 1. Estrutura de chalconas usadas no presente estudo.

### **2.6.1 Atividade antitumoral de chalconas hidroxiladas**

Chalconas substituídas com grupo funcional hidroxila (-OH) são um dos grupos mais abundantes em fontes naturais e também um dos mais reportados na literatura (SISA et al., 2010). A presença da hidroxila na posição 2 do anel A tem importante influência sobre a reatividade das chalconas. Esta substituição permite a formação de ponte de hidrogênio intramolecular com o grupo carbonila e torna o composto mais eletrófilo, aumentando a sua reatividade química (AMSLINGER et al., 2012a).

Algumas chalconas hidroxiladas induzem citotoxicidade que poderia ser associada aos seus efeitos pró-oxidantes. Como exemplo tem-se a 2'-hidroxi-2,3,5'-trimetoxichalcona, que foi capaz de induzir estresse no retículo endoplasmático de células tumorais de mama (MDA-MB-231) produto do aumento de EROs, porém não gerou efeitos citotóxicos em células epiteliais de mama não tumorais (MCF10A) (LEE et al., 2016). Outro trabalho demonstrou que a 2'-hidroxi-4',5'-dimetoxichalcona promoveu, em células de câncer de pulmão H460, aumento dos níveis de EROs assim como aumento de expressão dos receptores DR5 levando a apoptose pela ativação da via extrínseca (YANG et al., 2013). Outro estudo demonstrou que a 2'-hidroxi-4',6'-dimetoxichalcona (Flavokawain B) elevou os níveis de EROs em células de câncer de cólon HCT116, com subsequente ativação de apoptose por via intrínseca (KUO et al., 2010). Interessantemente, em todos esses estudos o pré-tratamento com NAC (antioxidante e precursor da síntese de GSH) reverteu o aumento de EROs e a citotoxicidade destes chalconas.

Para várias chalconas hidroxiladas têm-se demonstrado efeitos antitumorais possivelmente decorrentes da inativação da topoisomerase I e II com a consequente quebra do DNA (GUL et al., 2009; KIM et al., 2013; PARK et al., 2009b). Por exemplo, a 2',4',4'-tri-hidroxichalcona (isoliquiritigenina) mostrou efeitos anti-proliferativos em células HeLa associados a sua capacidade de aumentar a expressão de p21 como consequência da inativação da topoisomerase II (PARK et al., 2009b).

Em células de câncer de pulmão A549 expostas à 2'-hidroxichalcona, assim como a vários dos seus derivados hidroxilados nas posições 5', 2, 4 e 3 nas concentrações 10  $\mu$ M, reduziram os níveis de GSH em 75-90% após apenas 2 horas de exposição. Também, nestas mesmas células, observou-se na presença de 2',5'-dihidroxichalcona na concentração 25  $\mu$ M (24 horas de incubação), uma significativa depleção de GSH (95%). Porém nestas mesmas condições, a depleção em células de próstata (PC-3) foi de apenas 23%, o que evidencia que o efeito destes compostos pode diferir dependendo também da linhagem celular (KACHADOURIAN, 2006).

### 2.6.2 Chalconas nitradas

Vários fármacos nitrados como nimesulida, flutamida, cloranfenicol, entre outros, são exemplos de moléculas nitro-aromáticas usados para tratamento de diversas doenças (BOELSTERLI et al., 2006). A presença do grupo funcional nitro altera várias propriedades intrínsecas da molécula como reatividade, solubilidade, etc (PATTERSON; WYLLIE, 2014). Uma das características deste grupo é sua susceptibilidade para ser bioativado por enzimas celulares que podem agir como nitroredutases, incluindo a tioredoxina reductase, NAD(P)H:quinona oxidoreductase, xantina oxidase, entre outras (ARLT et al., 2005; CENAS et al., 2006). Uma destas vias de redução envolve a transferência sequencial de dois elétrons ao grupo nitro que resulta na formação do grupo amino na etapa final, porém gerando vários intermediários com alta reatividade como o radical nitroso e hidroxilamino. Adicionalmente, estes intermediários podem ser ainda conjugados com outras moléculas endógenas gerando compostos com alto potencial tóxico para as células (ARLT et al., 2005; KOVACIC; SOMANATHAN, 2014; STIBOROVÁ et al., 2014a). De fato, este é um dos mecanismos que explica alguns efeitos adversos apresentados por fármacos nitrados como o cloranfenicol (HOLT; BAJORIA, 1999). Por outro lado, a transferência ao grupo nitro de apenas um elétron gera o instável ânion nitro que na presença de oxigênio inicia um ciclo fútil regenerando o grupo nitro, porém com a resultante formação de radical superóxido (CHIN CHUNG; LONGHIN BOSQUESI; LEANDRO DOS SANTOS, 2011).

Comparado ao grande número de estudos que demonstram promissores efeitos antitumorais de chalconas com grupos funcionais tais como hidroxila,

metoxila; existem poucos trabalhos que avaliaram o potencial de chalconas nitradas. Um estudo mostrou que a toxicidade da 2'-hidroxi-4',6'-dimetoxichalcona ( $IC_{50} > 100 \mu M$ ) em células HeLa aumentou pela inclusão do grupo nitro na posição 4 ( $IC_{50} \sim 43 \mu M$ ) (MAI et al., 2014). Zhang et al., (2015) comparando a citotoxicidade de uma série de chalconas substituídas com os grupos nitro, metila, metoxila e hidroxila na posição 3, também em células HeLa, evidenciaram que a chalcona nitrada foi o composto mais citotóxico com um  $IC_{50}$  de  $8 \mu M$ . Adicionalmente, seu efeito foi associado à sua capacidade para inibir a enzima TrxR-1 com a consequente geração de EROs.

## 2.6 Nanopartículas como sistema de entrega de fármacos

Apesar dos relatos na literatura demonstrarem promissores efeitos antitumorais de inúmeras chalconas em experimentos *in vitro*, existem poucos estudos sobre sua eficácia e o seu potencial tóxico em modelo *in vivo*. CABRERA et al., (2010) em ensaios de toxicidade aguda em ratos, demonstram que a 2'-hidroxichalcona e a 2'-hidroxi-4-metoxichalcona quando administradas em dose oral única de 250 mg/kg, não evidenciaram toxicidade após três dias de observação. Porém outros estudos tem mostrado que algumas chalconas podem gerar efeitos adversos. Por exemplo, ZHOU et al., (2010) demonstraram que uma dose diária (25 mg/kg) de 2'-hidroxi-4',6'-dimetoxichalcona (flavokawain B) administrada a camundongos, por via oral durante uma semana, produziu dano hepático associado à depleção de GSH e ao aumento de EROs. Adicionalmente, este composto também inibiu a atividade do fator de transcrição NF- $\kappa$ B (*Nuclear factor kappa B*) envolvido na ativação de vias de sinalização pró-sobrevivência. Um estudo de WINTER et al., (2014) verificou efeitos hepatotóxicos induzidos por naftilchalconas administradas diariamente por via intraperitoneal (5 mg/Kg) durante 14 dias em camundongos. Estes estudos revelam que algumas chalconas podem gerar efeitos adversos. Com isso, seriam necessárias estratégias que permitissem reduzir o risco de exposição sistêmica de tecidos normais a este tipo de compostos.

O encapsulamento de fármacos em nano-formulações permite reduzir a exposição de células normais à moléculas com potencial tóxico. Estes tipos de formulações se beneficiam da permeabilidade aumentada do tecido vascular



tumoral que facilita a entrega de fármacos de forma preferencial às células alvos (MATSUMOTO et al., 2016).

Uma estratégia para acrescentar a seletividade de nanopartículas é a incorporação na superfície da formulação de ligantes que possam ser reconhecidos preferencialmente por células tumorais. Por exemplo, estudos têm demonstrado a captação preferencial por células tumorais de nanopartículas funcionalizadas com transferrina, lactoferrina e também galactose, aproveitando a expressão aumentada de receptores para essas moléculas (KUMARI; KONDAPI, 2017; WANG et al., 2016; YHEE et al., 2013).

Nanopartículas funcionalizadas com ácido fólico (AF) têm sido descritas como eficientes para entrega de drogas às células com altos níveis de expressão de receptores de folato como células de adenocarcinoma de pulmão (DRIVER et al., 2016), carcinomas de mama, ovário (CHEUNG et al., 2016) e cérvix (LIU et al., 2017). De fato, em células HeLa formulações de nanopartículas com AF contendo quimioterápicos como cisplatina (ALVAREZ-BERRÍOS; VIVERO-ESCOTO, 2016), 5-fluorouracil (CHOWDHURI et al., 2016) ou topotecam (LÓPEZ et al., 2017) têm demonstrado resultados promissores.

## **2.7 Justificativa**

Devido à necessidade de contar com novas drogas para tratamento do câncer cérvico uterino, e ainda os interessantes efeitos citotóxicos que já foram demonstrados por chalconas sobre algumas linhagens de células tumorais, no presente trabalho foram propostos os seguintes objetivos:



## Capítulo 3: OBJETIVOS

## Capítulo 3. OBJETIVOS

### 3.1 OBJETIVO GERAL

Avaliar comparativamente os efeitos citotóxicos e pró-oxidantes de chalconas sintéticas contendo grupo hidroxila e/ou nitro sobre células HeLa e investigar seus mecanismos de ação /alguns parâmetros biológicos.

### 3.2 OBJETIVOS ESPECÍFICOS

- Realizar um *screening* através da avaliação dos efeitos das chalconas (CH, 3NC, 2HC e HNC) na viabilidade de células de câncer cérvico uterino (HeLa) para verificar possíveis efeitos em relação à presença dos grupamentos nitro e/ou hidroxila na estrutura básica das chalconas;
- Selecionar as chalconas mais promissoras e determinar as concentrações adequadas para estudar seus efeitos sobre os seguintes parâmetros:
  - Viabilidade celular;
  - Mecanismo de morte celular;
  - Ciclo celular;
  - Níveis de Espécies Reativas de Oxigênio (EROs);
  - Níveis de Glutathiona reduzida (GSH);
- Verificar a formação de adutos entre nitrochalconas e GSH em sistema livre de células e em extratos celulares;
- Verificar se a superexpressão de transportadores MRP-1 em células BHK21 confere resistência aos efeitos gerados por HNC;
- Avaliar os efeitos sobre a viabilidade de células HeLa da 4-nitrochalcona encapsulada em nanopartículas de PMMA funcionalizadas com AF e compará-los com os obtidos com 4-nitrochalcona livre;
- Verificar a via de internalização desta formulação de nanopartículas e determinar a influência da funcionalização com AF para a entrada preferencial em células HeLa.

## Capítulo 4: ARTIGO 1

## **Capítulo 4: Prooxidant and cytotoxic effect of 4–nitrochalcone on HeLa cells**

Juan Marcelo Carpio Arévalo<sup>1</sup>, Diogo Henrique Kita<sup>2</sup>, Glaucio Valdameri<sup>2</sup>, Silvia Maria Suter C. Cadena<sup>1</sup>, Guilhermina Rodrigues Noleto<sup>1</sup>, Glaucia Regina Martinez<sup>1</sup> and Maria Eliane Merlin Rocha<sup>1</sup>

<sup>1</sup>Department of Biochemistry and Molecular Biology of Federal University of Parana, Brazil

<sup>2</sup>Laboratory of Cancer Drug Resistance, Pharmaceutical Sciences Program, Federal University of Paraná, 80210-170 Curitiba, PR, Brazil

### **Corresponding author:**

Maria Eliane Merlin Rocha, Ph.D. Profa.

Department of Biochemistry and Molecular Biology

Federal University of Paraná, 81531-990, CP 19046,, Curitiba - PR, Brazil

Phone: 55+ 41 3361 1664

Fax: 55+ 41 3266 2042

E-mail: [maelimerlin.rocha@gmail.com](mailto:maelimerlin.rocha@gmail.com) or [memrocha@ufpr.br](mailto:memrocha@ufpr.br)

## Abstract

In this study the pro-oxidant effects of synthetic 4-nitrochalcone (4NC), and its relationship with cytotoxicity on HeLa cells were evaluated. 4NC induced a dose-dependent reduction in cell viability starting from the 15  $\mu$ M concentration, with an  $IC_{50}$  value of 32.92  $\mu$ M. Apart from inducing morphological features of cell death; 4NC did not produce effects on cell cycle. Regarding the action of 4NC, we found a rapid increase in the cellular ROS levels. The time-course of ROS accumulation revealed a sharp elevation (< 30 min), followed by a rapid return to control levels, without further increase. In addition, we also observed that preincubating with NAC reverts the cytotoxicity of 4NC (15  $\mu$ M) and increases the survival of the cells exposed to the 30  $\mu$ M concentration, which is likely to decrease the ROS elevation. On the contrary, the cells preincubated with BSO were sensitized to 4NC effects at these same concentrations. Moreover, 4NC decreased the reduced glutathione (GSH) content after only 1h of exposure, suggesting that the GSH depletion could be a consequence of the early ROS increase. The adduct formation between 4NC and GSH, as an additional GSH depletion mechanism was also verified in free-cell system, however, in cell extracts the adduct appearance was not detected. Finally, the role of MRP1 transporter was investigated, however; the results suggest the absence of 4NC transport mediated by MRP1 and that 4NC or the adduct did not trigger a collateral sensitivity mediated by GSH efflux.

**Keywords:** 4-nitrochalcone, cytotoxicity, HeLa, ROS, GSH, chalcone - glutathione adduct

#### 4.1. Introduction

Cancer remains one of the major challenges in the field of medicine with broad social and economic impacts [1]. Cervical cancer is one of the most frequent types of cancer in women worldwide, being especially prevalent in developing countries, where it occurs in approximately 85% of all cases [2]. Despite the effectiveness of surgical and non-surgical therapeutic approaches such as chemotherapy and radiotherapy, there are still low survival rates in the more advanced stages of the disease. Therefore, there is an increasing need to develop more effective drugs with fewer adverse reactions.

One of the most successful approaches in the drug discovery field has been the search for bioactive molecules from natural sources [3]. Chalcones are secondary plant metabolites that have demonstrated cytotoxic effects on various cancer cell lines [4,5]. Their simple chemical structure and easy synthesis make these compounds very attractive to the development of potential drug candidates [6].

Structurally chalcones consist of two six-membered aromatic rings linked by a  $\alpha,\beta$ -unsaturated keto-enone system of three carbons. The electron deficient  $\beta$ -carbon gives them their electrophilic character and is prone to nucleophilic attack by the thiol groups (-SH) [7,8]. In fact, some cytotoxic effects of the chalcones can be explained by their ability to react with the SH groups of antioxidant components, weakening the redox buffering capacity of the cells [9,10]. In addition to this intrinsic reactivity, the functionalization of the backbone with chemical groups modify their biological activities [4,11]. Some structure-activity studies have revealed that the nitro substituent, especially on the B ring, can generate chalcone derivatives with higher cytotoxicity compared to the parent compounds. [9,12].

On the other hand, the toxicity of nitroaromatic compounds can be correlated to the propensity of the functional group to undergo futile cycles of oxidation-reduction, increasing the concentration of potentially harmful reactive oxygen species or by generating toxic metabolites [13–15]. In fact, it is precisely these nitro aromatic properties that could be exploited to reposition these types of drugs as options for cancer therapy [16,17].

In the present study we evaluated the cytotoxicity of 4NC on HeLa cells and found a potential relationship between these effects with their capacity to

increases the levels of reactive oxygen species followed by a decrease in reduced glutathione levels. Additionally, the adduct formation between glutathione and 4NC was examined in a free cell system, as well as in cell extracts. Finally, we also assessed the possible influence of MRP1 transporter on cell death trigger by 4NC.

## **4.2. Material and Methods**

### **4.2.1 Material**

For the experiments with HeLa cells the following reagents were used: minimum essential medium (MEM), phosphate-buffered saline (PBS) and fetal bovine serum (FBS) purchased from Cultilab (São Paulo, SP, Brazil). 4-nitrochalcone (4NC), 3-(4,5-dimethylthiazol-2-yl)-2,5-diphenyltetrazolium bromide (MTT), 2'7'-dichlorofluorescein diacetate (DCFH-DA), propidium iodide (PI), N-acetyl-L-cysteine (NAC) and L-buthionine sulfoximine (BSO) were purchased from Sigma-Aldrich (St. Louis, MO, USA). Monochlorobimane (mBCl) were purchased from Fluka-Thermo Fisher Scientific (Switzerland). 4',6-diamidino-2-phenylindole (DAPI) and Prolong Gold with DAPI were purchased from Thermo Fisher (Waltham, MA, USA). Hoechst 33342 was purchased from Invitrogen (Carlsbad, CA, USA). Entellan was purchased from Merck Millipore (Billerica, MA, USA). Dimethyl sulfoxide (DMSO) was purchased from Merck (Darmstadt, Germany). All reagents were commercial products of the highest available purity grade.

### **4.2.2 Biological assays**

The human cervix adenocarcinoma cell line (HeLa) was obtained from Institute Adolfo Lutz (São Paulo, Brazil). BHK21-MRP1 (BHK21 cells stably transfected with MRP1) and BHK21 wild-type cells were kindly provided by Dr. Attilio Di Pietro (IBCP, Lyon, France). In all experiments, the cells were grown in MEM medium containing 10% FBS, 100 U/mL of penicillin/streptomycin and maintained under culture condition (37°C in a humidified atmosphere with 5% CO<sub>2</sub>). The treatments with 4NC were prepared from the DMSO stock solutions and further diluted in MEM to reach the respective concentrations (4 - 45 µM).

The maximum concentration of DMSO in the treatments and controls was 0.1% (v/v).

#### **4.2.3 *In vitro* cytotoxicity assay**

To assess the effect of 4NC on the viability of HeLa cells, the cells were seeded in 96-well plate ( $1 \times 10^4$ /well) and maintained under culture conditions for 24 h. Subsequently, they were exposed to 4NC (4 - 45  $\mu$ M) or vehicle control for an additional 24 h. Then, treatments were discarded and substituted by 200  $\mu$ L of MTT solution (0.5 mg/mL) prepared in PBS (pH 7.4) and incubated for an additional 2 h. Lastly, MTT was carefully discarded and the formazan crystals dissolved in 200  $\mu$ L of DMSO. Absorbance was read at 550 nm using an Epoch microplate spectrophotometer. The experiments were performed in triplicate with three wells for each condition and the results were expressed as the percentage of viable cells in comparison to control cells (100%). To assess the effect of 4NC on MRP1 transporter, BHK21-MRP1 and BHK21 wild-type cells were seeded at a density of  $1 \times 10^4$  cells/well into 96-well culture plates and allowed to attach for 24 h at 37°C in 5% CO<sub>2</sub>. The treatment was done with various concentrations of 4NC in a final volume of 200  $\mu$ L and allowed to grow for 48 h at 37°C in 5% CO<sub>2</sub>. After the appropriate treatment time, 20  $\mu$ L of MTT solution (5 mg/ mL) was added to each well and incubated for 4 h at 37°C in 5% CO<sub>2</sub>. Then the culture medium was discarded, each well was washed with PBS, and 100  $\mu$ L of DMSO was added to each well and mixed by gentle shaking for 10 min. Absorbance was measured in a microplate reader at 560 nm (Glomax multi – Promega). Experimental conditions were set in triplicate, and control experiments were performed with DMEM high glucose containing 0.1% DMSO (v/v). Data are plotted as a percentage of reduced cell viability compared to control (untreated cells) that was taken as 100%.

#### **4.2.4 Fluorescence microscopy analysis**

For fluorescence micrographs using Hoechst and PI,  $1 \times 10^4$  HeLa cells were seeded in 96-well black-walled microplate and incubated under culture conditions for 24 h. Posteriorly, they were exposed to free 4NC (4 - 45  $\mu$ M) for 24 h, incubated for 30 min with the membrane-permeable nucleic acid stain Hoechst 33342 (3.5  $\mu$ g/mL), and for an additional 5 min with the membrane-impermeant



nucleic acid stain PI (2.5 µg/mL). The analysis was performed with a microscope Zeiss LSM 410 equipped with a fluorescent lamp and the suitable filter for the respective fluorescence (Hoechst 33342: ex/em = 350 / 461 nm; PI: ex/em = 493/636 nm).

#### **4.2.5 Morphological analysis of cells stained with hematoxylin and eosin (H&E)**

HeLa cells were cultivated on glass coverslips at a density of  $1.2 \times 10^5$  cells/well in 24-well culture plates for 24 h and subsequently exposed to the vehicle control or 4NC (20 and 30 µM) for 24 h. Then, the coverslips were washed twice with PBS, exposed to Bouin's fixative solution for 5 min, stained with hematoxylin for 1 min, exposed to eosin for 30 s, and finally dehydrated in acetone. The coverslips were then mounted with Entellan and examined under bright field light with a Zeiss LSM 410 microscope.

#### **4.2.6 Assessment of the effect of 4NC on the cell cycle**

HeLa cells were cultivated at a density of  $2 \times 10^5$  cells/well onto a 6-well culture plate for 24 h and posteriorly exposed for additional 24 h to 4NC (20 and 30 µM) or vehicle control. Both detached and trypsinized adherent cells were collected and centrifuged at  $1.000 \times g$  for 1 min. The cell pellet was resuspended in 0.3 mL of PBS containing 0.1 % Triton and 50 µg/mL propidium iodide (PI). Lastly, the samples were analyzed using a flow cytometer Accuri C5 (BD). 10,000 events were analyzed per condition.

#### **4.2.7 Assessment of reactive oxygen species**

To assess the ROS levels, we used the probe DCFH-DA (10 µM in PBS), which after intracellular hydrolysis yields a fluorescent product in the presence of ROS [18]. In brief, HeLa cells ( $1 \times 10^4$ /well) were seeded in a 96-well black-walled microplate and incubated for 24 h under culture conditions. To detect change in the ROS levels after exposure to 4NC (1, 3, 6 and 24 h), the cells were exposed at different concentrations of 4NC, followed by 25 min of incubation with DCFH-DA. Posteriorly, the probe was replaced by PBS, and the fluorescence signal was measured using a Tecan-Infinite M200 microplate reader (ex/em: 485/525 nm). For the detection of change in the ROS levels during a short exposure time to

4NC (0-30 min), we followed the protocol provided by the Abcam manufacturer, with minor modifications. In brief, after adhesion, the cells were preloaded for 25 min with DCFH-DA (10  $\mu$ M in PBS). Subsequently, the probe was discarded and the cells were exposed to 4NC or vehicle control for 30 min. Lastly, the treatments were replaced by PBS, and the measurement of fluorescence was conducted as previously described. The fluorescence micrographs were obtained from these same cells using an microscope Zeiss LSM 410 equipped with a fluorescent lamp and a suitable filter to detect the oxidized DCFH product (DCF: ex/em: 485/525 nm).

#### **4.2.8 Assessment of reduced glutathione levels**

To measure the levels of reduced glutathione, we used the probe mBCI that reacts with reduced glutathione yielding a fluorescent adduct [19,20]. In brief,  $1 \times 10^4$  cells/well were seeded in a 96-well black-walled microplate and incubated for 24 h under culture conditions. Subsequently, the cells were exposed to 4NC or vehicle control for the respective times and concentrations. Posteriorly, the treatments were replaced by 100  $\mu$ L of PBS and one first measure was conducted in a TECAN-Infinite M200 microplate reader (ex/em: 385/485 nm) to obtain the blank values. Then, 100  $\mu$ L of mBCI (20  $\mu$ M) was added to each well and incubated for an additional 25 min. Lastly, the probe was replaced by 100  $\mu$ L of PBS and one new fluorescence read was conducted with the same parameters. The values of the blanks were subtracted from the fluorescence of the respective wells to perform the analyses. The fluorescence micrographs were obtained from these same cells using a microscope Zeiss LSM 410 equipped with a fluorescent lamp and the suitable filter to detect the adduct GS-mBCI (ex/em: 385/485 nm).

#### **4.2.9 Characterization of the adduct 4NC-GS by RP- HPLC and Mass Spectrometry**

In order to characterize the adduct formed by the reaction between 4NC and GSH in the free-cell system, a reaction mixture containing 4NC (30  $\mu$ M) and GSH (5 mM) in PBS was prepared and incubated at 37°C for 70 min and immediately analyzed (see below). To verify the formation of the adduct in cellular extracts, Hela cells were seeded ( $2.2 \times 10^6$  cells/plate onto a 60mm plate), incubated for

24h, and exposed to 4NC (30  $\mu$ M) for different times. Subsequently, the adherent cells were washed with 4 ml of cold PBS (three times), harvested by scraping, and centrifuged at 2,000 x g for 1 min at 4°C. Then, the cells were resuspended in 1 ml of cold PBS and centrifuged one more time. The cell pellet was subjected to two cycles of freezing (-20°C) and thawing (4°C); mixed with 450  $\mu$ L of cold methanol (100%) and kept at 4°C for 1 h with occasional vortexing. Lastly, the methanolic supernatant, obtained after centrifugation (6.800 x g by 5 min, 4°C) was used for further analysis.

Characterization and purification of the adduct (free-cell and methanolic extracts) was conducted in an HPLC Prominence LC-20 system (Shimadzu, Kyoto, Japan) equipped with a diode array detector (PDA) set to the wavelength range 200-700 nm. The oven column temperature was set to 30 °C. A column Hypersyl C<sub>18</sub> (250 x 4.6 mm, 5  $\mu$ m) was used for the chromatographic separation. The mobile phase was composed of formic acid (0.18%) (solvent A) and methanol (100%) (solvent B), with the following gradient: 5% B (0-15 min), 5-100% B (15-25 min) and 100% B (25-40 min). The flow rate was 0.72 mL/ min. The injection volume for all the experiments was 400  $\mu$ L.

The mass spectrum of the product was obtained from electrospray ionization mass spectrometry LTQ-Orbitrap-XL (Thermo Scientific, Waltham, MA), operating in positive ionization mode. The set up for detection of positive ions was: electrospray at 4.5 kV, capillary at 50 V, and tube lens at 150 V.

#### **4.2.10 Statistical analysis**

Data are presented as the mean  $\pm$  standard deviation (SD) of three independent determinations performed in technical triplicate. A One-way ANOVA was used for all analyses, with a significance level set to  $p < 0.05$ , followed by the Tukey's test as a post-hoc comparison. Statistical analyses were performed using GraphPad Prism version 5.04 (GraphPad Software, Inc. CA, USA).

### **4.3 Results**

#### **4.3.1 *In vitro* cytotoxic effect of 4NC in HeLa cells**

As shown in Figure 1A the exposure of HeLa cells to the increasing concentrations of 4NC (4 - 45  $\mu$ M) for 24 h showed a dose-dependent response, presenting a significant reduction in cell viability of ~16% at the concentration of

15  $\mu\text{M}$ , and around 39% and 71% at the concentrations of 30 and 45  $\mu\text{M}$ , respectively, with an  $\text{IC}_{50}$  value of 32.92  $\mu\text{M}$  (Figure 1B). To verify if this reduction could be associated with cell death, microscopic examinations of the cells in the presence of PI were performed. The fluorescence micrographs in Figure 1C show an absence of fluorescence in the control cells, while the cells exposed to 4NC showed, in a concentration-dependent manner, an increasing number of cells permeable to PI. This result indicates the loss of plasma membrane integrity and is a clear indication of cell death. Additionally, as shown, the images of the cells stained with H&E (Figure 1D), as a function of 4NC concentration, have morphological changes, such as cell shrinkage, membrane plasma blebbing, and apparent chromatin fragmentation were observed.

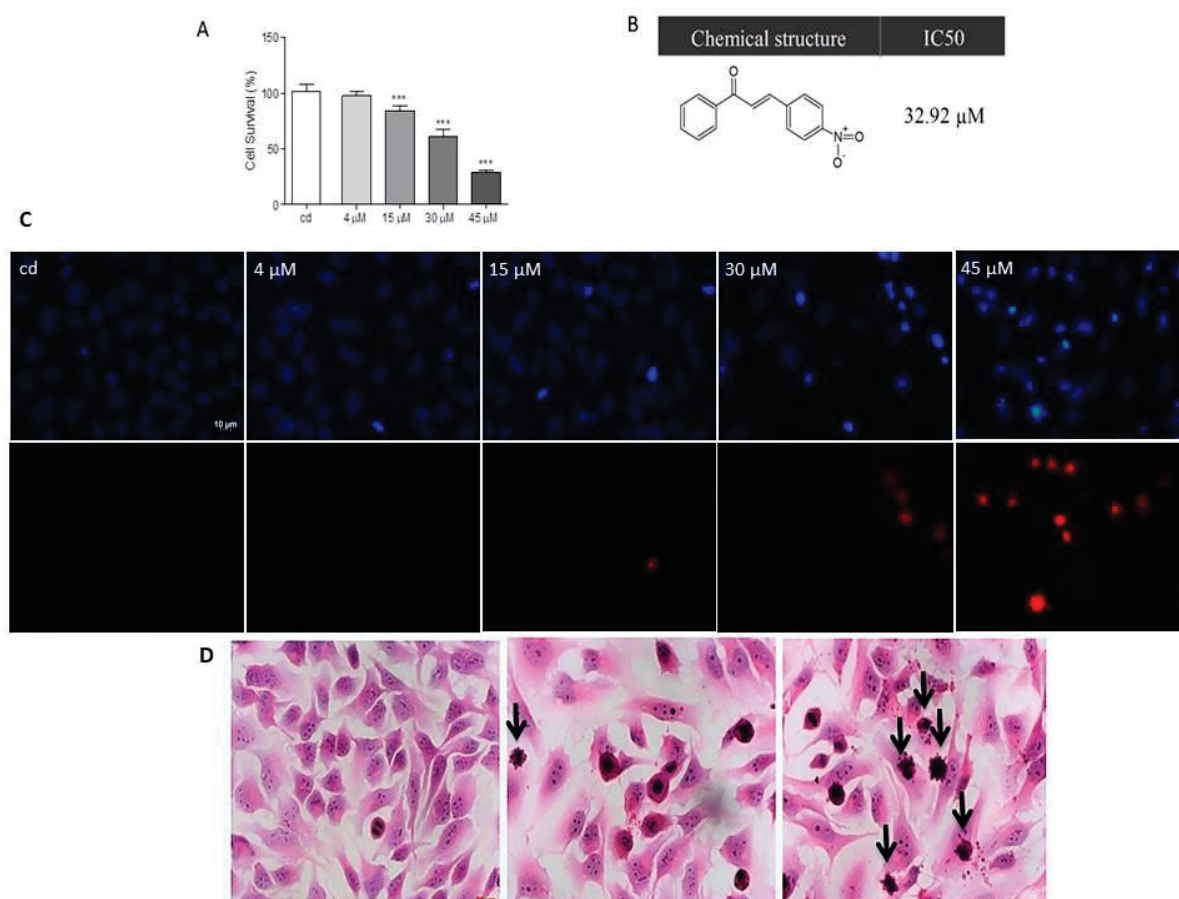


**Figure. 1.** Cytotoxic effects of 4NC evaluated by the MTT method after 24 h of exposure. Data are shown as mean  $\pm$  S.D. of three independent experiments performed in triplicate. \*\*\*  $p < 0.001$  (A). Structure and  $\text{IC}_{50}$  of 4NC in HeLa cells (B). Representative fluorescence micrographs of HeLa cells exposed for 24 h to different concentrations of 4NC, using Hoechst (blue fluorescence) and PI (red fluorescence) (C). Representative hematoxylin and eosin staining of HeLa cells incubated for 24 h with vehicle control (cd, MEM with 0.1% of DMSO) and 4NC (20 and 30  $\mu\text{M}$ ). The red arrows indicate cells with apparent chromatin fragmentation and plasma membrane blebbing (D). Magnification  $\times 200$ .

### 4.3.2 Evaluation of 4NC effect in the HeLa cell cycle

To verify whether 4NC could induce anti-proliferative effects, alterations in the cell population distribution in different cell-cycle phases were analyzed. As shown in Figure 2A, compared to the cells incubated with vehicle control (left histogram) the exposure to 4NC at 20 and 30  $\mu$ M (middle and right histograms, respectively) did not significantly increase the percentages of cells distributed into the populations G0/G1, S, and G2/M (Figure 2B). Interestingly, both concentrations, in a dose dependent manner, increased the population of hypodiploid cells (indicative of chromatin fragmentation) by roughly 12% and 18%, in relation at the control cells (6%) (Figure 2C).

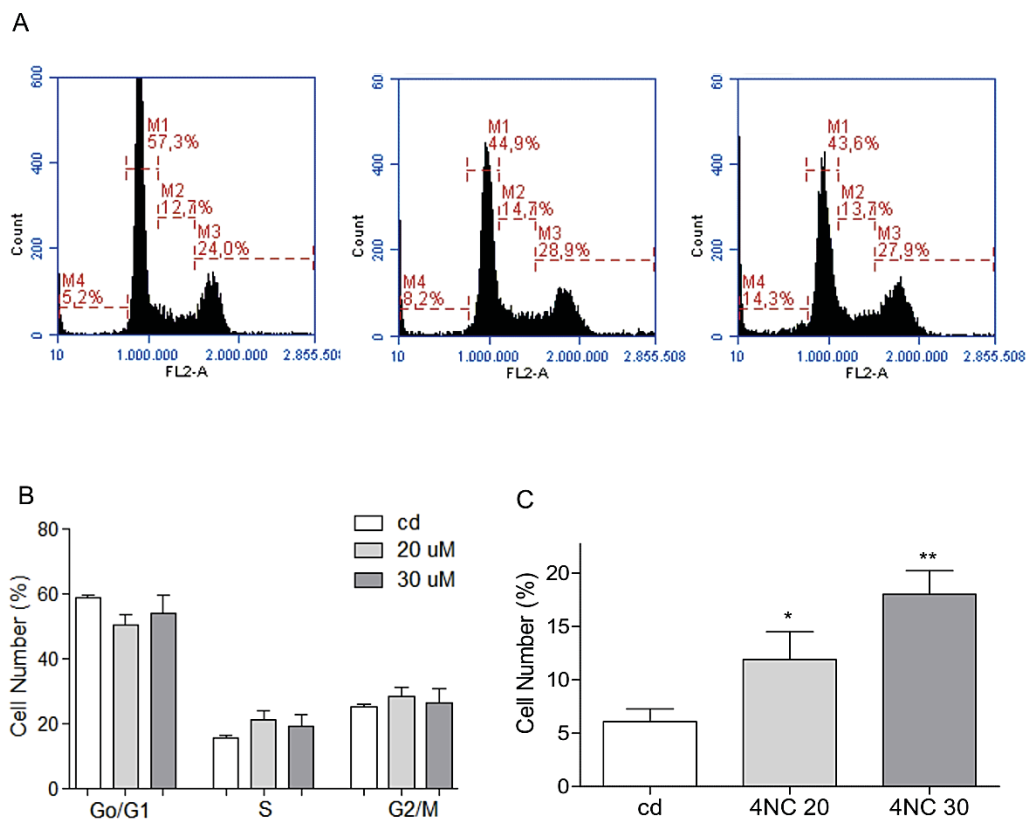


**Figure. 2.** Representative histogram analysis showing the cell cycle profiles of control cells (left), incubated with 4NC 20  $\mu$ M (middle) and 30  $\mu$ M (right) (A). Distribution in different cell cycle phases of control cells and cells exposed to 4NC at 20 and 30  $\mu$ M from three independent experiments (B). Percent of hypodiploid cells after exposure to vehicle control (cd), or at 4NC 20 and 30  $\mu$ M (C).

### 4.3.3 Effect of 4NC on the cellular levels of reactive oxygen species

The probe for ROS detection DCFH-DA was used to assess alterations in the intracellular ROS levels produced by 4NC. Our results showed that the cells exposed to 4NC (15 and 30  $\mu$ M) for 1, 3, 6, and 24 h, did not undergo alterations in the ROS levels when compared to cells incubated with vehicle control (data not shown). However, when the cells were preloaded with DCFH-DA and subsequently exposed to 4NC (15 and 30  $\mu$ M) to assess early ROS alterations, a significant accumulation was detected at both concentrations, reaching approximately 2.7 times higher ROS levels in the cells exposed at the concentration 30  $\mu$ M than in the control cells (Figure 3A and B).

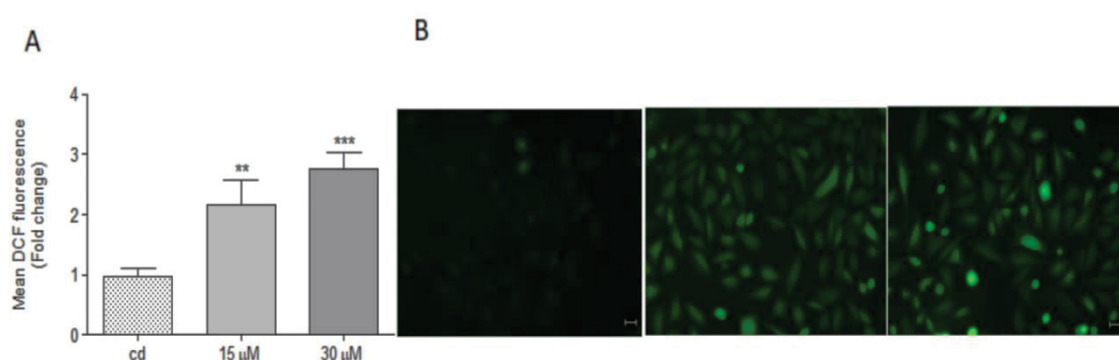


**Figure. 3.** ROS levels (fold change of DCF fluorescence) in HeLa cells preloaded with DCFH-DA and exposed for 30 min to 4NC (15 and 30  $\mu$ M) or vehicle control (cd) (A). Representative fluorescence micrographs of these cells (B). Data shown as mean $\pm$ S.D. of three independent experiments performed in triplicate. Bar scale: 10  $\mu$ m.

In order to verify the relationship between the enhanced ROS levels and cytotoxicity, as well as considering the pivotal roles of the GSH for several cellular antioxidants systems [21,22], we evaluated the effect of 4NC on cells with modulated GSH levels. For this, after adhesion, the cells were preincubated for two hours with BSO (100  $\mu$ M) or NAC (10 mM) to inhibit or induce the *de novo* synthesis of GSH, respectively. The results in Figure 4 show that the NAC pre-treatment reverted the cytotoxicity of 4NC at the concentration 15  $\mu$ M, and increased the survival of the cells exposed to the concentration of 30  $\mu$ M by around 13% (71.8%) compared to the cells without preincubation (58.9%). On the contrary, the inhibition of GSH synthesis by BSO has sensitizer effect and increased the toxicity of 4NC by approximately 7% and 19% at the concentrations of 15 and 30  $\mu$ M, respectively. Interestingly, as shown in Figure 5,



when the cells were preincubated with NAC, the intracellular ROS accumulation generated by the concentrations of 15 and 30  $\mu$ M of 4NC were markedly diminished.

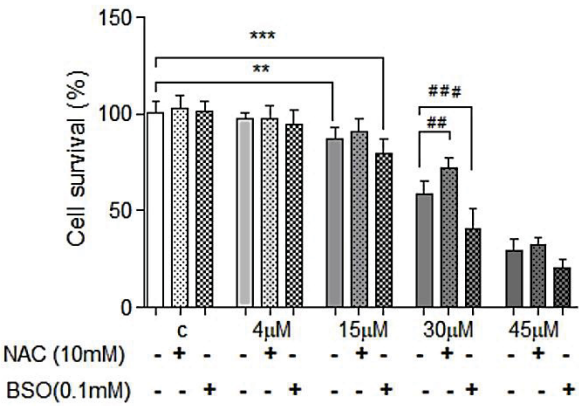


**Figure. 4.** Comparative effect of 4NC on HeLa cells with modulated GSH levels. The cells were preincubated for two hours with BSO (0.1 mM) or NAC (10 mM) and posteriorly exposed at the different concentrations of 4NC. Data showed as mean  $\pm$  S.D. of three independent experiments performed in triplicate. \*\* $p < 0.01$ ; \*\*\*  $p < 0.001$ ; ## $P < 0.01$ ; ### $P < 0.001$ .

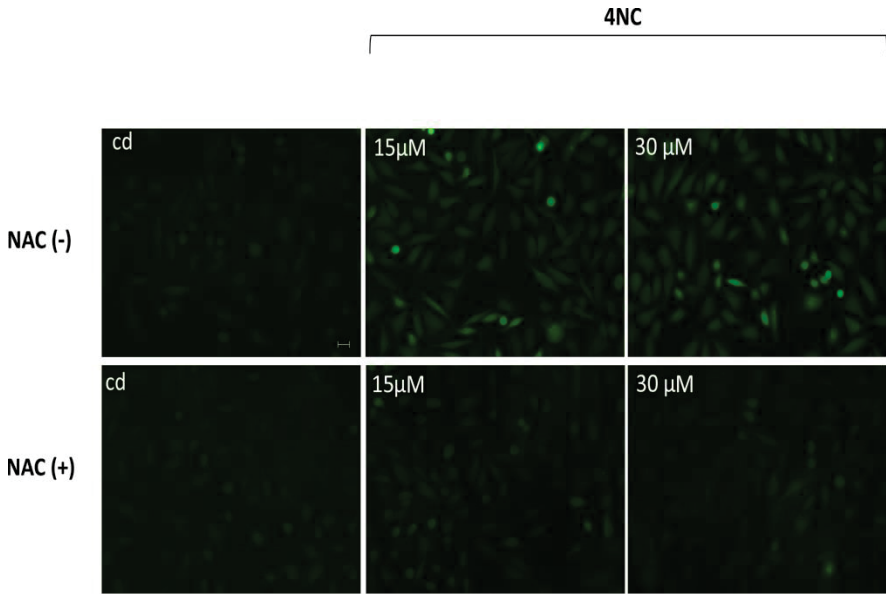


**Figure. 5.** Representative fluorescence micrographs of HeLa cells with or without preincubation with NAC (10 mM), loaded with DFCH-DA and exposed for 30 min to 4NC (15 and 30  $\mu$ M). Bar scale: 10  $\mu$ m.

**4.3.4 Effect of 4NC on the cellular glutathione levels**

Since GSH keeps the cellular redox homeostasis, their intracellular

concentration is sensitive to alterations in the ROS levels. Thus, the next step was to determine whether 4NC affected the GSH pool in the cells. The micrographs of Figure 6A show that one hour of exposure to 4NC at the concentration of 30  $\mu$ M generated a marked decrease in the intracellular GSH levels. In fact, after six hours of exposure at the concentrations of 15 and 30  $\mu$ M the reductions reached  $\sim 42\%$  and  $\sim 55\%$ , compared with the control cells (Figure 6B and C). Interestingly, at these same concentrations of 4NC, the cells exposed to only 30 minutes did not show significant alterations in the GSH pool (Figure 6D).

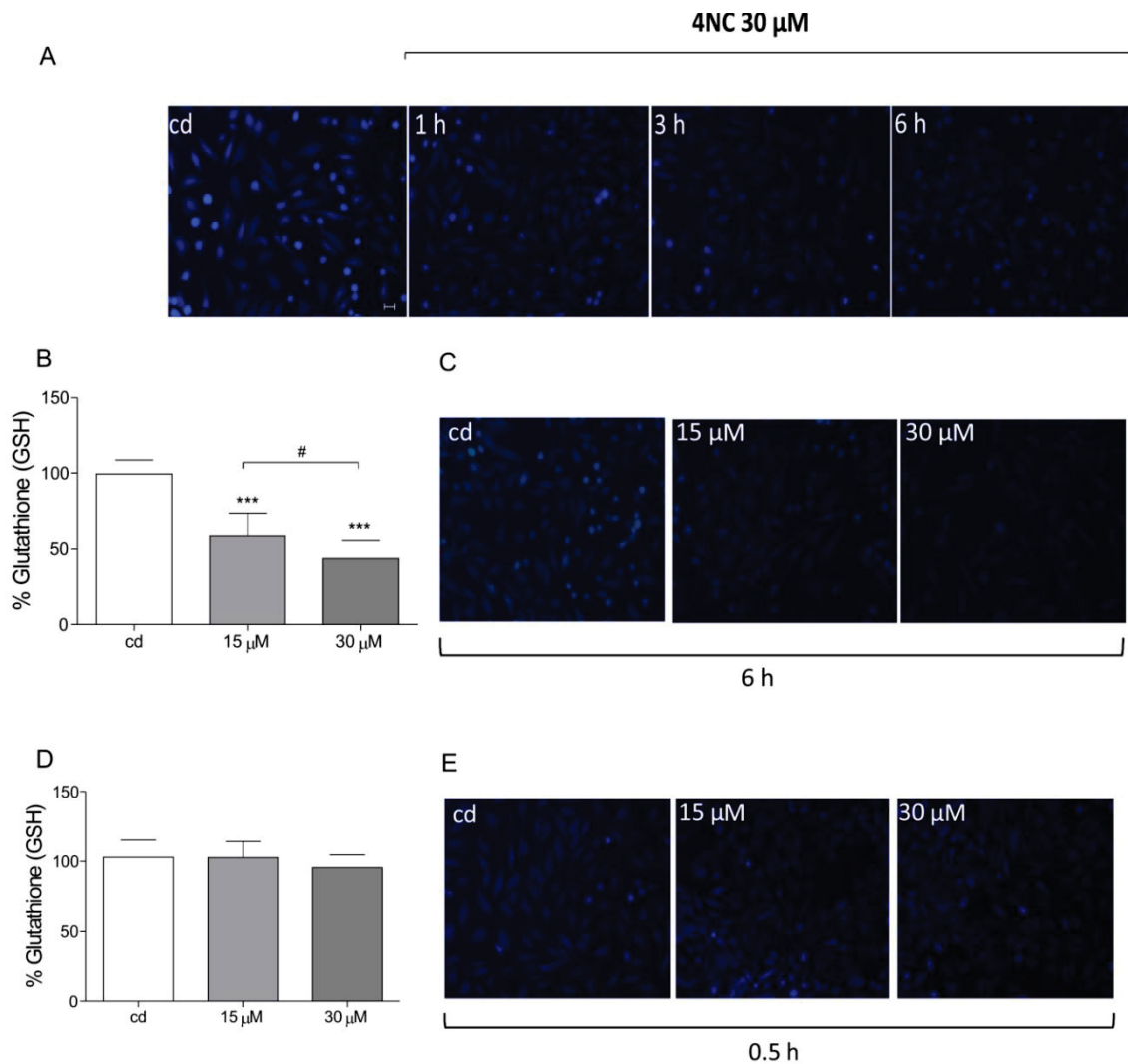


**Figure 6.** Representative fluorescence micrographs of HeLa cells exposed to 4NC (30  $\mu$ M) for the indicated times and posteriorly incubated with mBCl (magnification  $\times 200$ ) (A). Levels of reduced glutathione after 6 h of incubation with 4NC (15 and 30  $\mu$ M). Data shown as mean $\pm$ S.D. of three independent experiments performed in triplicate. \*\*\* $p < 0.001$ ; # $P < 0.05$  (B). Representative fluorescence micrographs of these cells (magnification  $\times 200$ ) (C). Levels of reduced glutathione after incubation for 0.5 h with 4NC (15 and 30  $\mu$ M) (D). Data shown as mean $\pm$ S.D. of three independent experiments performed in triplicate.



Representative fluorescence micrographs of HeLa cells exposed to 4NC (15 and 30  $\mu$ M) for 0.5 h and posteriorly incubated with mBCl (magnification  $\times 200$ ) (E).

Based on the fact that the chemical addition between electrophiles and GSH might also compromise the intracellular GSH content [23], we studied if this reaction could be involved in the reduction of the GSH level.

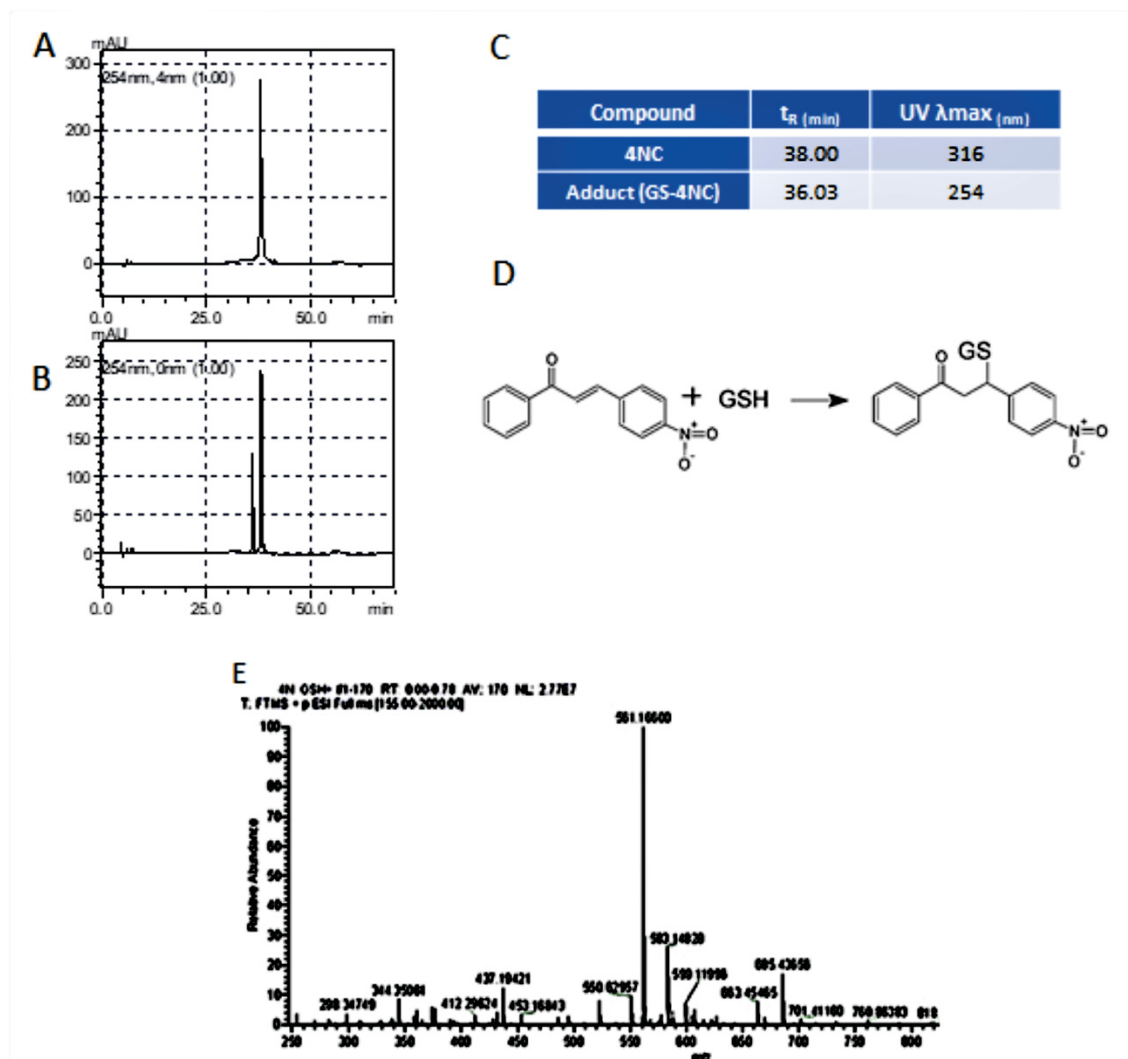


**Figure. 7.** Representative chromatogram of 4NC (30  $\mu$ M) dissolved in PBS (A). Representative chromatogram of 4NC (30  $\mu$ M) and GSH (5mM) mixture prepared in PBS (B). Retention time ( $t_R$ ) and maximum absorption wavelength ( $\lambda_{max}$ ) of 4NC and of the product of the reaction between GSH and 4NC (C). Reaction between 4NC and GSH (D). Mass Spectrum of the product of the reaction between GSH and 4NC (E).

First, the adduct formation between 4NC and GS in a free-cell system was analyzed using RP-HPLC. Figure 7A shows the chromatogram of the 4NC solution prepared in PBS (0.1% DMSO), which displayed a major peak at a

retention time of 38 min, corresponding to 4NC. In the Figure 7B the chromatogram of a 4NC and GSH mixture incubated for 70 minutes shows a new peak at a retention time of ~ 36 min, suggesting the appearance of a product. This compound was purified by RP-HPLC and analyzed by mass spectrometry (MS) to verify its chemical identity. The mass spectrum of Figure 7E shows a molecular ion at  $m/z = 561.16600$   $[M+H]^+$  which is consistent with the expected mass of the product generated from 4NC (253.073893 g/mol) and GSH (307.083806 g/mol) (Figure 7D). To verify the occurrence of this reaction in the cellular context, we analyzed the cell extracts after incubation with 4NC (30  $\mu$ M) for 0.25, 1, 3 and 6 hours; however, the presence of the adduct was not detected.

#### 4.3.5 Cytotoxicity assay using cells overexpressing MRP1 transporter

Some cancer cells overexpress ABC transporters that mediate the efflux of chemotherapeutics, and thus, contribute to the resistance to treatment. MRP1 transporter is capable of promote the efflux of free GSH and drugs conjugated with GSH. To verify if this transporter could reduce the cytotoxic effects of 4NC by a direct efflux of this compound, or trigger the MRP1-mediated collateral sensitivity by a GSH depletion, we treated BHK21 cells that overexpress MRP1 (BHK21-MRP1) and BHK21 wild-type cells (BHK21) with 4NC during 48h. Figure 8 shows that the cytotoxic effects of 4NC are not different between these cell lines, suggesting that 4NC is not a MRP1 substrate and that 4NC did not promotes cell death mediated by MRP1 activity.

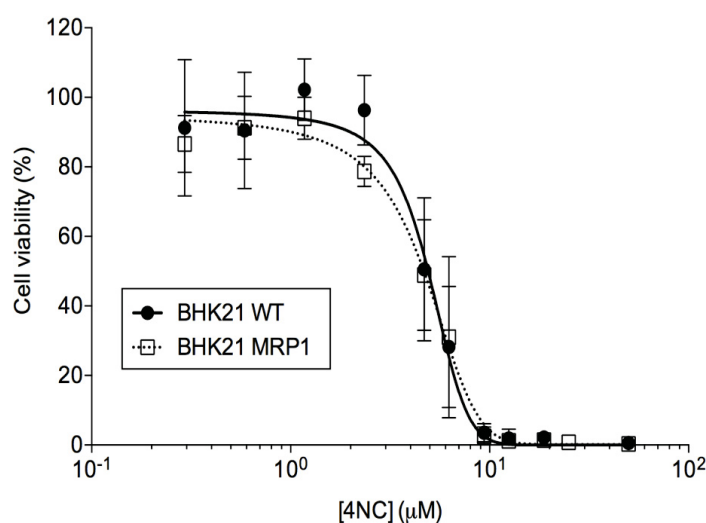


**Figure 8.** Cell viability of BHK21-MRP1 and BHK21 wild-type cells was determined upon treatment for 48 h with 4NC. The values represent the mean  $\pm$  SD of percent cell viability with respect to the untreated control. Data are the mean  $\pm$  SD of three independent experiments.

#### 4.4 Discussion

The chalcones are molecules of natural origin that exhibit a broad range of biological activities including anti-inflammatory [24], anti-diabetic [11], antifungal [25], antibacterial [26], etc. One of the more intensely studied effects is their potential antitumoral activities.

To our knowledge, this is the first time that the cytotoxic potential of the monofunctionalized 4-nitrochalcone on HeLa cells is verified. Our results show that 4NC induced a dose-dependent reduction in cell viability, which was accompanied by DNA fragmentation and clear morphological features indicative of cell death [27]. In addition, our analysis based on the cellular DNA content suggests that 4NC did not induce anti-proliferative effects. Studies in our laboratory, using the parent chalcone core structure (unfunctionalized) under the same experimental conditions, have shown roughly two times lower toxicity of this chalcone on HeLa cells when compared with 4NC, exhibiting an  $IC_{50}$  value of 66.9  $\mu$ M (data not shown). In line with this, other authors have reported that the nitration of some polyfunctionalized chalcones resulted in increased cytotoxicity on tumor cells, including HeLa cells [9]. In a previous study, Mai et al., (2014a), also found increased cytotoxicity of the 2'-hydroxy-4',6'-dimethoxy-4-nitrochalcone on some tumoral cells compared with the unnitrated derivative. Even though it is not clear the precise contribution of the nitro group to the cytotoxicity of the chalcones, are known some electronic and sterical effects of this substituent on the chalcone backbone. For example, it is a well-established fact that the inclusion of electron-withdrawing groups, such as the nitro substituent, can exert profound effects on the  $\alpha,\beta$ -unsaturated system, affecting properties such as their chemical reactivity [7,28]. Furthermore, the nitro group, specifically located on the 4-position of the ring B introduces a remarkable conformational change resulting in a chalcone with planar conformation [25]. Consequently, these effects might modify both the reversibility of chemical interactions, as well their coupling to cellular targets [29,30], which could explain their differential activity.

The higher ROS levels in cancer cells compared to non-tumoral ones is considered a vulnerability that can be exploited to kill tumor cells with higher selectivity [31]. In fact, the pro-oxidant action of some chalcones is frequently associated with their toxic effect on tumor cells. Our results showed that after a few minutes of exposure to 4NC, a rapid increase occurred in the cellular ROS levels, followed by a sharp reduction until it reached the control cell levels within one hour. Despite this short-term ROS elevation, our results suggest that their length and intensity are enough to induce cytotoxic effects. The protective effect of NAC, which reduced both the ROS accumulation and the cytotoxicity of 4NC, supports the idea of ROS involvement in cell death induced by this compound. The sudden ROS elevation could indicate that 4NC can trigger some active mechanism of ROS production. In line with this hypotheses, a previous study reported that some tumor cells exposed to the chalcone xanthohumol experienced mitochondrial dysfunction, which resulted in a rapid but transient accumulation of anion superoxide (less than 30 min) enough to induce toxicity in these cells [32]. In addition, various authors also have shown that the cytosolic antioxidant enzyme thioredoxin reductase (TrxR1), highly expressed in tumor cells, is a target of several electrophiles [33,34]. These molecules react with the catalytic selenothiol in the enzyme inhibiting their reductase activity and shifts this enzyme to a superoxide generator [35]. Knowing that one identified target of some chalcones is the TrxR1 [9,30], might be possible that 4NC increase the ROS levels through this mechanism. However, further studies are necessary to clarify both the mechanism, as well to define the identity of the ROS induced by 4NC in HeLa cells.

Importantly, besides interacting with components of the antioxidant cellular machinery, some chalcones can trigger alternative cytotoxic mechanisms, in parallel or independently from ROS generation [36,37]. Thus, the mild protection against the effects of 4NC provided by the preincubation with NAC raises the hypothesis that additional mechanism could be relevant for the overall cytotoxicity of this compound.

Glutathione is the most abundant non-protein thiol in the cell and plays crucial roles in keeping the redox homeostasis [38]. With respect to the effect of 4NC in GSH levels, we observed a dose-dependent reduction in the GSH content, with an apparent decreasing gradual rate as a function of exposure time.

Interestingly, at the time of maximal ROS generation (0 - 30 min) a decrease in the GSH pool was not found. This finding suggests that the GSH depletion is not directly involved in the ROS accumulation. Rather, this progressive reduction could reflect their consume by the antioxidant systems to restore the redox balance against the early ROS elevation [32]. However, in addition to their role in the antioxidant defense, GSH is also involved in xenobiotic detoxification pathways by scavenging electrophiles by conjugation or through GSH-dependent efflux mechanisms [39]. In line with this, an alternative interpretation for the GSH depletion could be the well-documented Michael-type addition between GSH and chalcones [8,40]. In this scenario, the 4NC entry and subsequent adduct formation in the cell could be responsible for the GSH depletion. Our experiments in free-cell system confirmed the capacity of 4NC to react with GSH. We were not, however, able to detect the adduct in the cells incubated with 4NC at different times. Nonetheless, these results not necessarily discard the occurrence of this reaction in a biological context. In fact, factors, such as adduct instability due to the reversible nature of the Michael-type addition, are considered potential drawbacks in the study of these type of compounds [41,42].

The development of multidrug resistance (MDR) involves the increased expression of members of the ATP binding cassette (ABC) transporter superfamily, many of which promote chemoresistance through the efflux of anticancer drugs from cancer cells [43]. One of the most characterized ABC transporter is MRP1 (multidrug resistance associated protein-1), which in addition to anticancer drugs, recognizes and exports several forms of glutathione, including free GSH and conjugated with drugs [44]. Some compounds have been described to induce a preferential cell death in cells overexpressing MRP1 transporter. These compounds, such as Verapamil, can stimulate a MRP1-mediated GSH efflux causing a large depletion of intracellular GSH and consequently triggering selective apoptosis of the cells, a phenomenon called collateral sensitivity [45]. To investigate if 4NC is transported by MRP1 or trigger a collateral sensitivity mediated by this ABC transporter, the cytotoxicity caused by 4NC was evaluated in BHK21 wild-type and BHK21 transfected cells overexpressing MRP1. Our results showed that both cell lines exhibited similar sensitivities at increasing concentrations of 4NC, which suggest that MRP1 does not have a significant role on effects promoted by 4NC.

#### 4.5 Conclusion

Our results show for the first time the cytotoxic effects of 4NC on HeLa cells, and establish a relationship with rapid elevation of the ROS levels. Despite the reduction in the GSH content could be associated principally with the antioxidant response of the cell, a possible involvement of the Michael addition in this GSH depletion could not be totally discarded. In addition, the overexpression of MRP1 transporter does not result in a reduction of the effect of 4NC. Taken together, our results suggest that 4NC could be considered a promising compound that deserves further investigation to clarify their action mechanism and verify their potential chemotherapeutic value.

#### Acknowledgement

The authors would like to thank the financial support from CNPq (Conselho Nacional de Desenvolvimento Científico e Tecnológico) and CAPES (Coordenação de Aperfeiçoamento de Pessoal de Nível Superior). The financial support organizations had no role in the study design, data collection and analysis, decision to publish, or preparation of the manuscript. The authors would also like to thank Dr. Guilherme L. Sassaki, Dr. Lauro Mera de Souza and the UFPR-RMN Center for the mass spectrometry analyses. We are also grateful for the National Institute of Science and Technology of Biological Nitrogen Fixation (INCT-FBN) and Dr. Emanuel Maltempi de Souza for providing access to the flow cytometer. We are also grateful to Dra. Fabiane Gomes de Moraes Rego of the Graduate Program in Pharmaceutical Sciences for the use of the laboratory and reagents for analysis with BHK21 wild-type and BHK21-MRP1 cells.

#### 4.6 References

- [1] M. Siddiqui, S. V Rajkumar, The High Cost of Cancer Drugs and What We, JMCP. 87 (2012) 935–943. doi:10.1016/j.mayocp.2012.07.007.
- [2] W. Small, M.A. Bacon, A. Bajaj, L.T. Chuang, B.J. Fisher, M.M. Harkenrider, A. Jhingran, H.C. Kitchener, L.R. Mileskin, A.N. Viswanathan, D.K. Gaffney, Cervical cancer: A global health crisis, Cancer. 123 (2017) 2404–2412. doi:10.1002/cncr.30667.
- [3] F.-S. Li, J.-K. Weng, Demystifying traditional herbal medicine with modern



approach, *Nature Plants*. 3 (2017) 17109. doi:10.1038/nplants.2017.109.

- [4] S. Padhye, A. Ahmad, N. Oswal, P. Dandawate, R.A. Rub, J. Deshpande, K.V. Swamy, F.H. Sarkar, Fluorinated 2'-hydroxychalcones as garcinol analogs with enhanced antioxidant and anticancer activities, *Bioorganic and Medicinal Chemistry Letters*. 20 (2010) 5818–5821. doi:10.1016/j.bmcl.2010.07.128.
- [5] C. Karthikeyan, N.S. Narayana Moorthy, S. Ramasamy, U. Vanam, E. Manivannan, D. Karunakaran, P. Trivedi, Advances in Chalcones with Anticancer Activities, *Recent Patents on Anti-Cancer Drug Discovery*. 10 (2015) 97–115. doi:10.2174/1574892809666140819153902.
- [6] M. Gomes, E. Muratov, M. Pereira, J. Peixoto, L. Rosseto, P. Cravo, C. Andrade, B. Neves, Chalcone Derivatives: Promising Starting Points for Drug Design, *Molecules*. 22 (2017) 1210. doi:10.3390/molecules22081210.
- [7] D. Maydt, S. De Spirt, C. Muschelknautz, W. Stahl, T.J.J. Müller, Chemical reactivity and biological activity of chalcones and other  $\alpha,\beta$ -unsaturated carbonyl compounds, *Xenobiotica*. 43 (2013) 711–718. doi:10.3109/00498254.2012.754112.
- [8] S. Amslinger, N. Al-Rifai, K. Winter, K. Wörmann, R. Scholz, P.B. and M. Wild, Reactivity Assessment of Chalcones by a Kinetic Thiol Assay, *Organic & Biomolecular Chemistry*. (2012) 2–5. doi:10.1039/b000000x.
- [9] B. Zhang, D. Duan, C. Ge, J. Yao, Y. Liu, X. Li, J. Fang, Synthesis of xanthohumol analogues and discovery of potent thioredoxin reductase inhibitor as potential anticancer agent, *Journal of Medicinal Chemistry*. 58 (2015) 1795–1805. doi:10.1021/jm5016507.
- [10] O. Sabzevari, G. Galati, M.Y. Moridani, A. Siraki, P.J. O'Brien, Molecular cytotoxic mechanisms of anticancer hydroxychalcones, *Chemico-Biological Interactions*. 148 (2004) 57–67. doi:10.1016/j.cbi.2004.04.004.
- [11] C.T. Hsieh, T.J. Hsieh, M. El-Shazly, D.W. Chuang, Y.H. Tsai, C.T. Yen, S.F. Wu, Y.C. Wu, F.R. Chang, Synthesis of chalcone derivatives as potential anti-diabetic agents, *Bioorganic and Medicinal Chemistry Letters*. 22 (2012) 3912–3915. doi:10.1016/j.bmcl.2012.04.108.
- [12] C.W. Mai, M. Yaeghoobi, N. Abd-Rahman, Y.B. Kang, M.R. Pichika, Chalcones with electron-withdrawing and electron-donating substituents: Anticancer activity against TRAIL resistant cancer cells, structure-activity relationship analysis and regulation of apoptotic proteins, *European Journal of Medicinal Chemistry*. 77 (2014) 378–387. doi:10.1016/j.ejmech.2014.03.002.
- [13] V.M. Arlt, M. Stiborova, C.J. Henderson, M.R. Osborne, C.A. Bieler, E. Frei, V. Martinek, B. Sopko, C.R. Wolf, H.H. Schmeiser, D.H. Phillips, Environmental pollutant and potent mutagen 3-nitrobenzanthrone forms DNA adducts after reduction by NAD(P)H:quinone oxidoreductase and conjugation by acetyltransferases and sulfotransferases in human hepatic

- cytosols, *Cancer Research*. 65 (2005) 2644–2652. doi:10.1158/0008-5472.CAN-04-3544.
- [14] P. Kovacic, R. Somanathan, Nitroaromatic compounds: Environmental toxicity, carcinogenicity, mutagenicity, therapy and mechanism, *Journal of Applied Toxicology*. 34 (2014) 810–824. doi:10.1002/jat.2980.
- [15] M. Chin Chung, P. Longhin Bosquesi, J. Leandro dos Santos, A Prodrug Approach to Improve the Physico-Chemical Properties and Decrease the Genotoxicity of Nitro Compounds, *Current Pharmaceutical Design*. 17 (2011) 3515–3526. doi:10.2174/138161211798194512.
- [16] S. Patterson, S. Wyllie, Nitro drugs for the treatment of trypanosomatid diseases: Past, present, and future prospects, *Trends in Parasitology*. 30 (2014) 289–298. doi:10.1016/j.pt.2014.04.003.
- [17] F.W. Hunter, B.G. Wouters, W.R. Wilson, Hypoxia-activated prodrugs: Paths forward in the era of personalised medicine, *British Journal of Cancer*. 114 (2016) 1071–1077. doi:10.1038/bjc.2016.79.
- [18] C.P. Lebel, H. Ischiropoulos, S.C. Bondys, Evaluation of the Probe 2',7'-Dichlorofluorescein as an Indicator of Reactive Oxygen Species Formation and Oxidative Stress, *Chem. Res. Toxicol.* 5 (1992) 227–231. doi:10.1021/tx00026a012.
- [19] J. Sebastia, R. Cristofol, M. Martin, E. Rodriguez-Farre, C. Sanfeliu, Evaluation of fluorescent dyes for measuring intracellular glutathione content in primary cultures of human neurons and neuroblastoma SH-SY5Y, *Cytometry A*. 51 (2003) 16–25. doi:10.1002/cyto.a.10003.
- [20] S. Chatterjee, H. Noack, H. Possel, G. Keilhoff, G. Wolf, Glutathione levels in primary glial cultures: Monochlorobimane provides evidence of cell type-specific distribution, *Glia*. 27 (1999) 152–161. doi:10.1002/(SICI)1098-1136(199908)27:2<152::AID-GLIA5>3.0.CO;2-Q.
- [21] Y. Du, H. Zhang, J. Lu, A. Holmgren, Glutathione and glutaredoxin act as a backup of human thioredoxin reductase 1 to reduce thioredoxin 1 preventing cell death by aurothioglucose, *Journal of Biological Chemistry*. 287 (2012) 38210–38219. doi:10.1074/jbc.M112.392225.
- [22] R. Brigelius-flohé, M. Maiorino, Glutathione peroxidases, *Biochimica et Biophysica Acta Journal*. 1830 (2013) 3289–3303. doi:10.1016/j.bbagen.2012.11.020.
- [23] Y. Zhang, Role of glutathione in the accumulation of anticarcinogenic isothiocyanates and their glutathione conjugates by murine hepatoma cells, *Carcinogenesis*. 21 (2000) 1175–1182.
- [24] A. Gómez-Rivera, H. Aguilar-Mariscal, N. Romero-Ceronio, L.F. Roa-De La Fuente, C.E. Lobato-García, Synthesis and anti-inflammatory activity of three nitro chalcones, *Bioorganic and Medicinal Chemistry Letters*. 23 (2013) 5519–5522. doi:10.1016/j.bmcl.2013.08.061.



- [25] S.N. Lopez, M. V Castelli, S.A. Zacchino, J.N. Domínguez, G. Lobo, J. Charris-Charris, J.C.. Cortes, J.C. Ribas, C. Devia, A.M. Rodriguez, R.D. Enriz, In vitro antifungal evaluation and structure–activity relationships of a new series of chalcone derivatives and synthetic analogues, with inhibitory properties against polymers of the fungal cell wall, *Bioorganic & Medicinal Chemistry*. 9 (2001) 1999–2013. doi:10.1016/S0968-0896(01)00116-X.
- [26] M. Siddiqui, S. V Rajkumar, The High Cost of Cancer Drugs and What We, *JMCP*. 87 (2012) 935–943. doi:10.1016/j.mayocp.2012.07.007.
- [27] W. Small, M.A. Bacon, A. Bajaj, L.T. Chuang, B.J. Fisher, M.M. Harkenrider, A. Jhingran, H.C. Kitchener, L.R. Mileschkin, A.N. Viswanathan, D.K. Gaffney, Cervical cancer: A global health crisis, *Cancer*. 123 (2017) 2404–2412. doi:10.1002/cncr.30667.
- [28] F.-S. Li, J.-K. Weng, Demystifying traditional herbal medicine with modern approach, *Nature Plants*. 3 (2017) 17109. doi:10.1038/nplants.2017.109.
- [29] S. Padhye, A. Ahmad, N. Oswal, P. Dandawate, R.A. Rub, J. Deshpande, K.V. Swamy, F.H. Sarkar, Fluorinated 2'-hydroxychalcones as garcinol analogs with enhanced antioxidant and anticancer activities, *Bioorganic and Medicinal Chemistry Letters*. 20 (2010) 5818–5821. doi:10.1016/j.bmcl.2010.07.128.
- [30] C. Karthikeyan, N.S. Narayana Moorthy, S. Ramasamy, U. Vanam, E. Manivannan, D. Karunagaran, P. Trivedi, Advances in Chalcones with Anticancer Activities, *Recent Patents on Anti-Cancer Drug Discovery*. 10 (2015) 97–115. doi:10.2174/1574892809666140819153902.
- [31] M. Gomes, E. Muratov, M. Pereira, J. Peixoto, L. Rosseto, P. Cravo, C. Andrade, B. Neves, Chalcone Derivatives: Promising Starting Points for Drug Design, *Molecules*. 22 (2017) 1210. doi:10.3390/molecules22081210.
- [32] D. Maydt, S. De Spirt, C. Muschelknautz, W. Stahl, T.J.J. Müller, Chemical reactivity and biological activity of chalcones and other  $\alpha,\beta$ -unsaturated carbonyl compounds, *Xenobiotica*. 43 (2013) 711–718. doi:10.3109/00498254.2012.754112.
- [33] S. Amslinger, N. Al-Rifai, K. Winter, K. Wörmann, R. Scholz, P.B. and M. Wild, Reactivity Assessment of Chalcones by a Kinetic Thiol Assay, *Organic & Biomolecular Chemistry*. (2012) 2–5. doi:10.1039/b000000x.
- [34] B. Zhang, D. Duan, C. Ge, J. Yao, Y. Liu, X. Li, J. Fang, Synthesis of xanthohumol analogues and discovery of potent thioredoxin reductase inhibitor as potential anticancer agent, *Journal of Medicinal Chemistry*. 58 (2015) 1795–1805. doi:10.1021/jm5016507.
- [35] O. Sabzevari, G. Galati, M.Y. Moridani, A. Siraki, P.J. O'Brien, Molecular cytotoxic mechanisms of anticancer hydroxychalcones, *Chemico-Biological Interactions*. 148 (2004) 57–67. doi:10.1016/j.cbi.2004.04.004.
- [36] C.T. Hsieh, T.J. Hsieh, M. El-Shazly, D.W. Chuang, Y.H. Tsai, C.T. Yen,

- S.F. Wu, Y.C. Wu, F.R. Chang, Synthesis of chalcone derivatives as potential anti-diabetic agents, *Bioorganic and Medicinal Chemistry Letters*. 22 (2012) 3912–3915. doi:10.1016/j.bmcl.2012.04.108.
- [37] C.W. Mai, M. Yaeghoobi, N. Abd-Rahman, Y.B. Kang, M.R. Pichika, Chalcones with electron-withdrawing and electron-donating substituents: Anticancer activity against TRAIL resistant cancer cells, structure-activity relationship analysis and regulation of apoptotic proteins, *European Journal of Medicinal Chemistry*. 77 (2014) 378–387. doi:10.1016/j.ejmech.2014.03.002.
- [38] V.M. Arlt, M. Stiborova, C.J. Henderson, M.R. Osborne, C.A. Bieler, E. Frei, V. Martinek, B. Sopko, C.R. Wolf, H.H. Schmeiser, D.H. Phillips, Environmental pollutant and potent mutagen 3-nitrobenzanthrone forms DNA adducts after reduction by NAD(P)H:quinone oxidoreductase and conjugation by acetyltransferases and sulfotransferases in human hepatic cytosols, *Cancer Research*. 65 (2005) 2644–2652. doi:10.1158/0008-5472.CAN-04-3544.
- [39] P. Kovacic, R. Somanathan, Nitroaromatic compounds: Environmental toxicity, carcinogenicity, mutagenicity, therapy and mechanism, *Journal of Applied Toxicology*. 34 (2014) 810–824. doi:10.1002/jat.2980.
- [40] M. Chin Chung, P. Longhin Bosquesi, J. Leandro dos Santos, A Prodrug Approach to Improve the Physico-Chemical Properties and Decrease the Genotoxicity of Nitro Compounds, *Current Pharmaceutical Design*. 17 (2011) 3515–3526. doi:10.2174/138161211798194512.
- [41] S. Patterson, S. Wyllie, Nitro drugs for the treatment of trypanosomatid diseases: Past, present, and future prospects, *Trends in Parasitology*. 30 (2014) 289–298. doi:10.1016/j.pt.2014.04.003.
- [42] F.W. Hunter, B.G. Wouters, W.R. Wilson, Hypoxia-activated prodrugs: Paths forward in the era of personalised medicine, *British Journal of Cancer*. 114 (2016) 1071–1077. doi:10.1038/bjc.2016.79.
- [43] C.P. Lebel, H. Ischiropoulos, S.C. Bondys, Evaluation of the Probe 2',7'-Dichlorofluorescein as an Indicator of Reactive Oxygen Species Formation and Oxidative Stress, *Chem. Res. Toxicol.* 5 (1992) 227–231. doi:10.1021/tx00026a012.
- [44] J. Sebastia, R. Cristofol, M. Martin, E. Rodriguez-Farre, C. Sanfeliu, Evaluation of fluorescent dyes for measuring intracellular glutathione content in primary cultures of human neurons and neuroblastoma SH-SY5Y, *Cytometry A*. 51 (2003) 16–25. doi:10.1002/cyto.a.10003.
- [20] S. Chatterjee, H. Noack, H. Possel, G. Keilhoff, G. Wolf, Glutathione levels in primary glial cultures: Monochlorobimane provides evidence of cell type-specific distribution, *Glia*. 27 (1999) 152–161. doi:10.1002/(SICI)1098-1136(199908)27:2<152::AID-GLIA5>3.0.CO;2-Q.
- [45] Y. Du, H. Zhang, J. Lu, A. Holmgren, Glutathione and glutaredoxin act as a backup of human thioredoxin reductase 1 to reduce thioredoxin 1

- preventing cell death by aurothioglucose, *Journal of Biological Chemistry*. 287 (2012) 38210–38219. doi:10.1074/jbc.M112.392225.
- [46] R. Brigelius-flohé, M. Maiorino, Glutathione peroxidases, *Biochimica et Biophysica Acta Journal*. 1830 (2013) 3289–3303. doi:10.1016/j.bbagen.2012.11.020.
- [47] Y. Zhang, Role of glutathione in the accumulation of anticarcinogenic isothiocyanates and their glutathione conjugates by murine hepatoma cells, *Carcinogenesis*. 21 (2000) 1175–1182.
- [48] A. Gómez-Rivera, H. Aguilar-Mariscal, N. Romero-Ceronio, L.F. Roa-De La Fuente, C.E. Lobato-García, Synthesis and anti-inflammatory activity of three nitro chalcones, *Bioorganic and Medicinal Chemistry Letters*. 23 (2013) 5519–5522. doi:10.1016/j.bmcl.2013.08.061.
- [49] S.N. Lopez, M. V Castelli, S.A. Zacchino, J.N. Domínguez, G. Lobo, J. Charris-Charris, J.C.. Cortes, J.C. Ribas, C. Devia, A.M. Rodriguez, R.D. Enriz, In vitro antifungal evaluation and structure–activity relationships of a new series of chalcone derivatives and synthetic analogues, with inhibitory properties against polymers of the fungal cell wall, *Bioorganic & Medicinal Chemistry*. 9 (2001) 1999–2013. doi:10.1016/S0968-0896(01)00116-X.
- [50] X. Fang, B. Yang, Z. Cheng, P. Zhang, M. Yang, Synthesis and antimicrobial activity of novel chalcone derivatives, *Research on Chemical Intermediates*. 40 (2014) 1715–1725. doi:10.1007/s11164-013-1076-5.
- [51] C.M. Henry, E. Hollville, S.J. Martin, Measuring apoptosis by microscopy and flow cytometry, *Methods*. 61 (2013) 90–97. doi:10.1016/j.ymeth.2013.01.008.
- [52] S.R. Spencer, L.A. Xue, E.M. Klenz, P. Talalay, The potency of inducers of NAD(P)H:(quinone-acceptor) oxidoreductase parallels their efficiency as substrates for glutathione transferases. Structural and electronic correlations, *Biochemical Journal*. 273 (1991) 711–717. doi:10.1042/bj2730711.
- [53] M.H. Johansson, Reversible Michael additions: covalent inhibitors and prodrugs, *Mini Rev Med Chem*. 12 (2012) 1330–1344. doi:10.2174/13895575112091330.
- [54] F.-F. Gan, K.K. Kaminska, H. Yang, C.-Y. Liew, P.-C. Leow, C.-L. So, L.N.L. Tu, A. Roy, C.-W. Yap, T.-S. Kang, W.-K. Chui, E.-H. Chew, Identification of Michael acceptor-centric pharmacophores with substituents that yield strong thioredoxin reductase inhibitory character correlated to antiproliferative activity., *Antioxidants & Redox Signaling*. 19 (2013) 1149–65. doi:10.1089/ars.2012.4909.
- [55] A.T. Dharmaraja, Role of Reactive Oxygen Species (ROS) in Therapeutics and Drug Resistance in Cancer and Bacteria, *Journal of Medicinal Chemistry*. 60 (2017) 3221–3240. doi:10.1021/acs.jmedchem.6b01243.
- [56] J. Strathmann, K. Klimo, S.W. Sauer, J.G. Okun, J.H.M. Prehn, C.

- Gerhäuser, Xanthohumol-induced transient superoxide anion radical formation triggers cancer cells into apoptosis via a mitochondria-mediated mechanism., *The FASEB Journal : Official Publication of the Federation of American Societies for Experimental Biology*. 24 (2010) 2938–2950. doi:10.1096/fj.10-155846.
- [57] S. Urig, K. Becker, On the potential of thioredoxin reductase inhibitors for cancer therapy, *Seminars in Cancer Biology*. 16 (2006) 452–465. doi:10.1016/j.semcancer.2006.09.004.
- [58] A. Bindoli, M.P. Rigobello, G. Scutari, C. Gabbiani, A. Casini, L. Messori, Thioredoxin reductase: A target for gold compounds acting as potential anticancer drugs, *Coordination Chemistry Reviews*. 253 (2009) 1692–1707. doi:10.1016/j.ccr.2009.02.026.
- [59] J. Fang, J. Lu, A. Holmgren, Thioredoxin reductase is irreversibly modified by curcumin: A novel molecular mechanism for its anticancer activity, *Journal of Biological Chemistry*. 280 (2005) 25284–25290. doi:10.1074/jbc.M414645200.
- [60] I. Park, K.K. Park, J.H.Y. Park, W.Y. Chung, Isoliquiritigenin induces G2 and M phase arrest by inducing DNA damage and by inhibiting the metaphase/anaphase transition, *Cancer Letters*. 277 (2009) 174–181. doi:10.1016/j.canlet.2008.12.005.
- [61] K. Lee, D. Hyun, L.J. Kim, Y. Jung, S.Y. Shin, D. Koh, Y. Han, The chalcone derivative HymnPro generates reactive oxygen species through depletion of intracellular glutathione, *Applied Biological Chemistry*. 59 (2016) 391–396. doi:10.1007/s13765-016-0168-5.
- [62] V.I. Lushchak, V.I. Lushchak, Glutathione Homeostasis and Functions: Potential Targets for Medical Interventions, *Journal of Amino Acids*. 2012 (2012) 1–26. doi:10.1155/2012/736837.
- [63] N. Ballatori, S.M. Krance, R. Marchan, C.L. Hammond, Plasma membrane glutathione transporters and their roles in cell physiology and pathophysiology, *Mol Aspects Med*. 30 (2009) 13–28. doi:10.1016/j.mam.2008.08.004.
- [64] P. Perjési, G. Maász, R. Reisch, A. Benko, (E)-2-Benzylidenebenzocyclanones: Part VII. Investigation of the conjugation reaction of two cytotoxic cyclic chalcone analogues with glutathione: An HPLC-MS study, *Monatshefte Fur Chemie*. 143 (2012) 1107–1114. doi:10.1007/s00706-012-0768-7.
- [65] Z. Rozmer, T. Berki, G. Maász, P. Perjési, Different effects of two cyclic chalcone analogues on redox status of Jurkat T cells, *Toxicology in Vitro*. 28 (2014) 1359–1365. doi:10.1016/j.tiv.2014.06.006.
- [66] T.A. Baille, J.. Slatter, Glutathione - a vehicle for the transport of chemically reactive metabolites in vivo., *Accounts of Chemical Research*. 24 (1991) 264–270. doi:10.1021/ar00009a003.

- [67] M.M. Gottesman, T. Fojo, S.E. Bates, Multidrug Resistance in Cancer: Role of Atp-Dependent Transporters, *Nature Reviews Cancer*. 2 (2002) 48–58. doi:10.1038/nrc706.
- [68] G. Szakács, M.D. Hall, M.M. Gottesman, A. Boumendjel, R. Kachadourian, B.J. Day, H. Baubichon-Cortay, A. Di Pietro, Targeting the achilles heel of multidrug-resistant cancer by exploiting the fitness cost of resistance, *Chemical Reviews*. 114 (2014) 5753–5774. doi:10.1021/cr4006236.
- [69] D. et al. Trompier, Verapamil and it derivate trigger apoptosis through gluathione extrusion by multidrug resistance protein MRP1., *Cancer research*. 64 (2004) 4950–4956.

## Capítulo 5: ARTIGO 2

**Capítulo 5: Synthesis and evaluation of a formulation of 4–nitrochalcone loaded in poly(methyl methacrylate) nanoparticles functionalized with folic acid against HeLa cells**

Juan Marcelo Carpio Arévalo<sup>1#</sup>, Paulo Emilio Feuser<sup>2#</sup>, Gustavo Rodrigues Rossi<sup>3</sup>, Edvaldo S. Trindade<sup>3</sup>, Claudia Sayer<sup>2</sup>, Pedro H. Hermes de Araújo<sup>2</sup>, Silvia Maria Suter C. Cadena<sup>1</sup>, Guilhermina Rodrigues Noletto<sup>1</sup>, Glaucia Regina Martinez<sup>1</sup> and Maria Eliane Merlin Rocha<sup>1</sup>

<sup>1</sup>Department of Biochemistry and Molecular Biology of Federal University of Parana, Brazil

<sup>2</sup>Department of Chemical Engineering and Food Engineering, Federal University of Santa Catarina, Brazil

<sup>3</sup>Department of Cellular Biology of Federal University of Parana, Brazil

**Corresponding author:**

Maria Eliane Merlin Rocha, Ph.D. Profa.

Department of Biochemistry and Molecular Biology

Federal University of Paraná, 81531-990, CP 19046,, Curitiba - PR, Brazil

Phone: 55+ 41 3361 1664

Fax: 55+ 41 3266 2042

E-mail: [maelimerlin.rocha@gmail.com](mailto:maelimerlin.rocha@gmail.com) or [memrocha@ufpr.br](mailto:memrocha@ufpr.br)

## Abstract

Chalcones are metabolites of natural origin with promissory cytotoxic effects toward several tumor cells. Chalcones functionalized with a nitro group have shown improved cytotoxic effects; nevertheless, from a structural standpoint, the presence of this chemical group in aromatic rings is frequently associated with the occurrence of adverse drug reactions. In this study, we synthesized and evaluated a formulation of poly(methyl methacrylate) (PMMA) nanoparticles functionalized with folic acid to improve the delivery of 4-nitrochalcone to folate-receptor-positive HeLa cells. PMMA synthesized using the mini emulsion polymerization technique presented spherical morphology with nanocapsule-type structure, a mean size of  $170 \pm 6$  nm, a negative zeta potential of  $-40 \pm 4$  mV at pH 7.4, and an entrapment efficiency of 80%. Empty nanoparticles, at lower concentrations, did not cause toxicity, but at these same concentrations, 4NC in PMMA nanoparticles functionalized with folic acid generated an even higher reduction in cell viability than the free chalcone. Unfunctionalized PMMA nanoparticles loaded with 4NC also reduced the viability but exhibited significantly less effect than the 4NC-folic acid-PMMA. The confocal microscopy studies showed the increased uptake of the functionalized nanoparticles and verified the critical role of folic acid in favoring uptake. Our results show that folic acid-PMMA exploits the folate receptor for their cellular uptake and is a suitable system for the delivery of 4-nitrochalcone to HeLa cells.

**Keywords:** 4-nitrochalcone, HeLa, folic acid, folate receptor, endocytosis, nanoparticles, poly (methyl methacrylate)



## 5.1 Introduction

Cancer is one of the most important unsolved health problems and accounted for nearly 1 in 6 deaths annually worldwide (WHO, 2017). Key factors to this scenario include the decreased response to the conventional chemo(radio)therapy treatments especially at more advanced disease stages or development of resistance mechanism by tumor cells, as well as severe adverse reactions associated with these treatments. For this reason, new effective drugs with potentially less toxicity are necessary.

Chalcones are metabolic intermediates in the flavonoid synthetic pathway with demonstrated biological effect (Batovska and Todorova, 2010). Many plant chalcones, as well as several synthetic derivatives, have shown cytotoxic effects on various tumor cells and act by many different mechanisms (Hsu et al., 2009; Mai et al., 2014; Shin et al., 2014; Zhou et al., 2016). Since the biosynthesis of nitrated metabolites is a process relatively infrequent in nature (Stiborová et al., 2014), nitrochalcones have comparatively been less studied than other chalcones, such as hydroxylated and methoxylated (Karthikeyan et al., 2015; Srinivasan et al., 2009). Nonetheless, the capacity of this functional group to increase the toxic effect of several chalcones in tumor cell lines including breast, liver, and cervical cancer, has been reported in the literature (Mai et al., 2014; Ramalho et al., 2013; Zhang et al., 2015). However, despite the promising cytotoxic effects of these compounds in *in vitro* assays, their potential toxicity, frequently found with various nitroaromatic drugs (Kovacic and Somanathan, 2014; Patterson and Wyllie, 2014; Stiborová et al., 2014), raises some safety concerns.

Based on the previous premises, the selective delivery of nitrochalcones to tumoral cells could be the best option for their potential utilization as a chemotherapeutic option. Polymeric nanoparticles can be an alternative when used as drug carriers, improving specific-site drug delivery. Another aspect is increasing the therapeutic efficacy and reducing the side effects of encapsulated drugs (Chopra et al., 2016; Colson and Grinstaff, 2012; Feuser et al., 2016a; Prabhu, R. H., Patravale, V. B., & Joshi, 2015; Singh et al., 2015; Sulistio et al., 2011). Polymer-based drug carrier systems are more stable than other nanocarriers, and these can be easily manipulated and adjusted to obtain

desirable proprieties, such as appropriate release profiles and surface functionalization (Colson and Grinstaff, 2012; Felice et al., 2014).

Drug loaded polymeric nanoparticles can be obtained by *in situ* miniemulsion polymerization and by pre-formed polymer (nanoprecipitation or emulsion/solvent evaporation technique) (Feuser et al., 2016b; Letchford and Burt, 2007). The miniemulsion polymerization technique has some advantages, such as the capacity to manipulate and adjust in order to produce carriers with desirable physicochemical properties in a single polymerization step at fast rates (Asua, 2002; Lorca et al., 2012). Another advantage of the miniemulsion polymerization technique is the use of low amounts of surfactant without the need to add any organic solvent (Asua, 2002). Recent works have demonstrated that waterborne polymeric nanoparticles can be a great alternative in the development of drug nanocarriers for cancer treatment, offering relevant therapeutic benefits when compared with other therapies, such as conventional chemotherapy or radiotherapy (Asua, 2002; Colson and Grinstaff, 2012; Sulistio et al., 2011; Wang et al., 2014).

Recent studies have revealed that surface functionalization of polymeric nanoparticles can improve targeted drug delivery, increase cellular uptake, and consequently, promote higher therapeutic activity (Lee et al., 2015; Scarano et al., 2013; Sulistio et al., 2011). Folic acid, also known as vitamin B9, is an example of a functionalizing agent that can be used to increase cancer cell uptake, since folate receptors are overexpressed in many human cancers, such as ovarian, lung, renal, colon, and endometrial cancers, and are present at low or negligible levels in non-cancer cells, which is its main advantage to ensure targeted drug delivery (Chen et al., 2013; Feuser et al., 2016a; Kuo and Chen, 2015; Parker et al., 2005; Yang et al., 2014). Folate receptor-mediated drug delivery is based on the uptake of folic acid functionalized nanoparticles by folate receptor-mediated endocytosis pathways (Chen et al., 2013; Scarano et al., 2013).

Herein we report the effects of 4NC on HeLa cells and the synthesis of 4-nitrochalcone loaded in folic acid poly(methyl methacrylate) (PMMA) nanoparticles by mini-emulsion polymerization. Drug-loaded PMMA nanoparticles were characterized and *in vitro* studies performed to evaluate their uptake and their potential to reduce the viability of HeLa cells.

## 5.2 Material and Methods

### 5.2.1 Material

For the synthesis of polymeric nanoparticles, the following reagents were used: methyl methacrylate (MMA) from Arinos Chemistry and azobisisobutyronitrile (AIBN), dimethyl sulfoxide (DMSO), and folic acid purchased from Vetec. 4-nitrochalcone 99% (4NC) and 6-coumarin purchased from Sigma Aldrich, lecithin from Alpha Aesar, trehalose from Dinâmica, and Crodamol GTCC (caprylic/capric triglyceride) from Croda. Distilled water was used throughout these experiments.

The human cervix adenocarcinoma cell line (HeLa) was obtained from Institute Adolfo Lutz (São Paulo, SP, Brazil). For the experiments with cells the following reagents were used: minimum essential medium (MEM), phosphate-buffered saline pH 7.4 (PBS) and fetal bovine serum (FBS) purchased from Cultilab (São Paulo, SP, Brazil). 3-(4,5-dimethylthiazol-2-yl)-2,5-diphenyltetrazolium bromide (MTT) and Methyl- $\beta$ -cyclodextrin were purchased from Sigma-Aldrich (St. Louis, MO, USA). 4',6-diamidino-2-phenylindole (DAPI) and Prolong Gold with DAPI were purchased from Thermo Fisher (Waltham, MA, USA). Dimethyl sulfoxide (DMSO) was purchased from Merck (Darmstadt, Germany). Paraformaldehyde was purchased from Electron Microscopy Science (Washington, USA). All reagents were commercial products of the highest available purity grade.

### 5.2.2 Methods

#### 5.2.2.1. Synthesis of 4NC loaded in folic acid – PMMA nanoparticles

Drug loaded polymeric nanoparticles were synthesized by miniemulsion polymerization technique in just one step as described by FEUSER et al., 2016a. Initially, we mixed 1 mL of Crodamol containing 20 mg of 4NC, 2 g of MMA, 0.15 g of lecithin and 0.04 g of AIBN (initiator), which formed the organic phase. The organic phase was added dropwise into a beaker containing 20 mL of distilled water containing 0.01% w/w (aqueous phase) of folic acid under sonication with an amplitude of 70% (Fisher Scientific, Sonic Dismembrator, 500 W). The sonication was continued for 5 min (10 s on and 1 s off) in a beaker immersed in an ice bath. The miniemulsion was transferred to glass tubes (15 mL) at 70 °C, and the polymerization was allowed to proceed for 4 h.

Afterwards, the material was cooled, centrifuged, and washed three times with phosphate buffered saline (PBS) at pH 7.4. Trehalose (2 %w/v) was added to the polymeric aqueous dispersion, transferred to glass vials, frozen in liquid nitrogen, and lyophilized (FreeZone 4.5-L Benchtop Freeze Dry System; Labconco, Kansas City, MO). The lyophilized powder was stored at room temperature before analysis. Polymeric nanoparticles without folic acid were also synthesized. The synthesis methodology was the same as previously described, but without folic acid in the aqueous phase.

#### **5.2.2.2. Synthesis of 4NC loaded in folic acid - PMMA nanoparticles labeled with 6-coumarin**

Polymeric nanoparticles with and without folic acid were synthesized with 6-coumarin, a highly fluorescent molecule. The synthesis was the same as previously described, with the addition of 6-coumarin in Crodamol (0.01% w/w). The next steps were the same as previously mentioned.

#### **5.2.3 Characterization**

The morphology of the polymeric nanoparticles was evaluated by transmission electron microscope (TEM), model JEM 2100F, operating at 80 kV. For TEM analysis, several drops of the samples, resuspended in PBS (1:10), were placed on a 300-mesh Formvar/carbon copper grid (Electron Microscopy Science). After drying, samples were sputter-coated with a thin layer of carbon film to avoid the degradation of the PMMA under the electron beam. Average particle size and polydispersity index (PDI) were measured by dynamic light scattering, and the surface charge at pH 7.4 was investigated through zeta potential measurements (in both cases using the same Malvern Zetasizer). All samples were analyzed three times, to obtain the average and standard deviation (SD). Fourier-transform infrared spectroscopy (FT-IR) was used to confirm their chemical structure using a KBr pellet. X-ray diffraction (XRD) experiments were performed to identify the crystallographic structure of the free drug and polymeric nanoparticles.

##### **5.2.3.1. Entrapment efficiency (EE %) of 4NC**

The EE (%) of 4NC was analyzed using UV-Vis spectrophotometry. 10 mg of polymeric nanoparticles was dissolved in DMSO, the common solvent for both

drug and polymer. The determination coefficient ( $R^2$ ) exceeded 0.996 with excellent linearity. The 4NC concentration was measured at 323 nm (ultraviolet region of the electromagnetic spectrum) using a calibration curve with different concentrations (0.4 – 2 µg/mL) dispersed in DMSO. The EE (%) was calculated from Eq. (1):

$$EE(\%) = M_1/M_t \times 100$$

(1)

where EE (%) is the 4NC encapsulation efficiency,  $M_1$  is the mass of 4NC in polymeric nanoparticles, and  $M_t$  is the mass of 4NC used in the formulation. The experiments were run in triplicate (n=3).

### 5.2.3.2. Controlled and kinetic release

The release was carried out in the diffusion cell. Polymeric nanoparticles (10 mg) were weighed and placed in the donor compartment of the diffusion cell. A cellulose acetate membrane (dialysis tubing cellulose membrane, Sigma-Aldrich, Ref D9652-100TF) was used for separating donor compartments containing the nanoparticles from the receptor compartment that contained 10 ml of PBS (pH 7.4) with 0.5 % SDS. The membrane was thin and porous allowing free diffusion of the solvent and drug. Receptor medium was continuously stirred (100 rpm) and the temperature was maintained at 37°C in a thermostatically controlled water bath. The release studies followed the sink conditions. At 0.3, 1, 1.5, 2, 3, 4, 20, 24, 30 and 48 hours, an aliquot was withdrawn from the receptor medium of the release studies. The release study was performed in triplicate (n=3). The drug released in the receptor medium was quantified by spectrophotometry using the ultraviolet region, as previously described. The release profile was obtained by associating the percentage of the drug released with time. The release data were fit using the mathematical models of zero order ( $Q_t = Q_0 + K_0t$ ), first order ( $\ln Q_t = \ln Q_0 + K_1t$ ), Korsmeyer–Peppas ( $\frac{M_1}{M_\infty} = Kt^n$ ), and Higuchi ( $Q_t = K_H t^{1/2}$ ) (Costa and Sousa Lobo, 2001). The linear regression analysis ( $R^2$ ) and straight line equation were determined using the software Excel. The mathematical model with the best fit is the model that provides the highest value of determination coefficient. Graphs were plotted using OriginPro 8 software.

#### 5.2.4. Biological assays

The HeLa cells were grown in MEM medium containing 10% FBS, 100 U/mL of penicillin/streptomycin, and maintained under culture condition (37°C in a humidified atmosphere with 5% CO<sub>2</sub>). The treatments with 4NC were prepared from the stock solutions in DMSO and further diluted in MEM to reach the respective concentrations (4 - 45 µM). The maximal concentration of DMSO in the treatments and controls was 0.1% (v/v). The treatments with empty nanoparticles functionalized with folic acid (PMMA-folic acid), 4NC loaded in nanoparticles functionalized with folic acid (4NC-folic acid-PMMA), and 4NC loaded in nanoparticles without folic acid (4NC-PMMA) were prepared in MEM from their respective suspension stock (1.6 mg of nanoparticles/mL) to reach the equivalent concentrations of free 4NC (4 - 45 µM).

##### 5.2.4.1. *In vitro* cytotoxicity assay

HeLa cells seeded at a density of  $1 \times 10^4$ /well in 96-well plate were incubated under culture conditions for 24h. Subsequently, the cells were exposed to additional increasing concentrations of free 4NC, 4NC folic acid-PMMA, 4NC PMMA, and folic acid-PMMA nanoparticles. Posteriorly, the cell viability using the MTT assay was performed. In brief, after exposure, the treatments were discarded, and the cells were carefully washed twice with PBS. Lastly, 200 µL of an MTT solution prepared in PBS (0.5 mg/mL) was added to each well and incubated for an additional two hours and the resulting formazan dye was solubilized with DMSO (200 µl). The absorbance was measured at 550 nm in an Epoch Microplate Spectrophotometer. The experiments were performed in triplicate with three wells for each condition. The results were expressed as the percentage of viable cells in comparison to the respective controls (MEM with or without DMSO 0.1%).

##### 5.2.4.2. Cellular uptake assay by laser scanning confocal microscopy

HeLa cells ( $5.9 \times 10^4$ ) were seeded on 13 mm diameter glass coverslips in 24 well plates and maintained under culture conditions for 24 h. For experiments with inhibition of caveolae-dependent endocytosis, the cells were pre-incubated with methyl-β-cyclodextrin (2.5 mM) dissolved in MEM and incubated for 40

minutes at 37°C. Then, the cells were exposed to 450 µg/ml of PMMA nanoparticles (with or without folic acid) loaded with 6-coumarin and incubated for one hour at either 4 or 37 °C. Subsequently, the cells were washed with PBS (three times) and fixed at room temperature with paraformaldehyde (2% in PBS) for 20 min. Coverslips were posteriorly mounted using Prolong Gold with DAPI and examined by laser scanning confocal microscopy A1RSi+MP (Nikon Corp, Tokyo, Japan). Fluorescence imaging was acquired by exciting DAPI with a 405 nm laser, and the emission was captured using the filter 450/50 (425–475 nm bandpass). The 6-coumarin was excited using the 488 nm laser, and emission was captured using the filter 515/30 (500–530 nm bandpass). The images were analyzed using Fiji software.

#### **5.2.4.3. Statistical analysis**

Data are presented as the mean  $\pm$  standard deviation (SD) of three independent determinations performed in technical triplicate. A One-way ANOVA was used for all analyses with a significance level set at  $p < 0.05$ , followed by the Tukey's test as a post-hoc comparison. Statistical analyses were performed using GraphPad Prism 5.04 version (GraphPad Software, Inc. CA, USA).

### **5.3 Results and discussion**

#### **5.3.1. Physicochemical proprieties analyses of nanoparticles**

Dynamic light scattering analysis (Figure 1) of the PMMA nanoparticles showed a mean intensity of  $170 \pm 6$  nm and a polydispersity index around 0.1. From the TEM images (Figure 1 insert) we observed a spherical core-shell morphology, nanocapsules type with an oily core (Crodamol containing 4NC) wrapped in a polymeric shell (PMMA) (Feuser et al., 2016c; Tiarks et al., 2001). The results showed a high entrapment efficiency of the 4NC ( $80\% \pm 5\%$ ). The zeta potential analyses were also performed. The nanocapsules had a negative surface charge ( $-40 \pm 4$  mV) at pH 7.4. The nanocapsules with and without folic acid did not present significant differences in relation to size, size distribution, morphology and surface charge. The high negative zeta potential was related to the presence of lecithin adsorbed on the polymeric nanoparticle surface, contributing to a higher colloidal stability (Singh et al., 2015). These



physicochemical proprieties have relevant biological implications in cellular uptake and biological processes of nanoparticles (Frohlich, 2012; He et al., 2010). Negatively charged polymeric nanoparticles tend to decrease association with the red blood cells and do not cause hemolysis, being safely administered into the bloodstream to reach cancer cells (Feuser et al., 2016a; Guo et al., 2015).

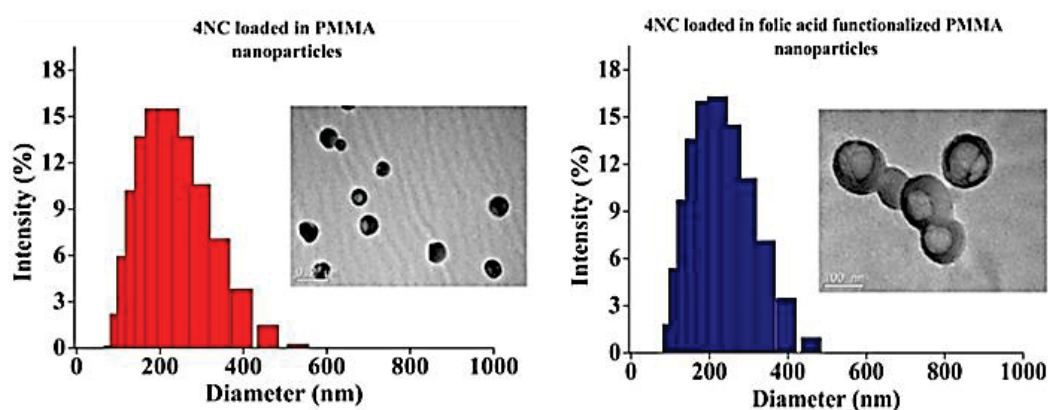


**Figure 1.** Dynamic light scattering analysis and TEM images (inserts) of polymeric nanoparticles without FA (left) and with FA (right) functionalization.

The chemical structure of nanoparticles was evaluated by the FTIR spectrum. As can be seen in Figure 2A, the peaks at  $1736\text{ cm}^{-1}$  and  $3000\text{--}2800\text{ cm}^{-1}$  correspond to C=O groups and stretching of C–H bonds (Dhana Lekshmi et al., 2010; Hazra et al., 2014) of PMMA. In addition, the FTIR spectrum indicated the presence of folic acid in the PMMA nanoparticles, with the appearance of peaks at  $1688\text{ cm}^{-1}$  (amide), whereas the FTIR spectrum of PMMA nanoparticles without folic acid did not show these peaks (Andhariya et al., 2013; Date et al., 2013; Feuser et al., 2016a; Mohapatra et al., 2007). Free 4NC presented characteristic peaks at  $3100$  and  $2909\text{ cm}^{-1}$  corresponding to the aromatic and aliphatic stretching. In addition, peaks at  $1655$ ,  $1605$ ,  $1530$  and  $1327\text{ cm}^{-1}$  correspond to the C=O stretching, C=C stretching, C-NO<sub>2</sub> asymmetric and symmetric stretching, respectively (Chandra Shekhara Shetty et al., 2016; Patil et al., 2006).

XRD patterns of free 4NC and polymeric nanoparticles were obtained and are illustrated in Figure 2B. The XRD profile of free 4NC exhibited several characteristic peaks, confirming the crystalline form of 4NC. However, 4NC loaded in PMMA nanoparticles with and without folic acid presented an amorphous state, without the crystalline peaks of 4NC. The FTIR spectrum of



free 4NC, folic acid PMMA nanoparticles, and 4NC loaded in PMMA nanoparticles with and without folic acid, confirmed that there was no significant interaction between the drug and the polymer. XRD analysis suggested that the 4NC is molecularly dispersed in the oil (Crodamol) core. The PMMA amorphous state can be seen at a broad peak between 10 and 20° (2 theta) (FEUSER et al., 2016a; LEKSHMI et al., 2010).

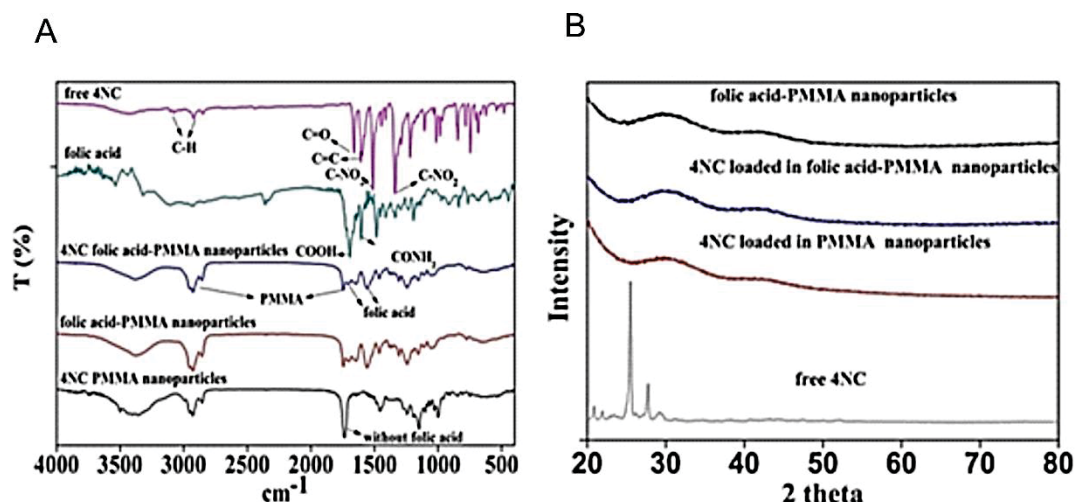


**Figure 2.** FTIR spectroscopy analyses of free 4NC and folic acid nanoparticles (A). XRD patterns of free 4NC and polymeric nanoparticles (B).

### 5.3.2. Kinetic release studies of 4NC

Release studies of 4NC loaded in folic acid - PMMA nanoparticles were performed in physiological pH (7.4). The release profile of 4NC loaded in folic acid-PMMA nanoparticles presented an initial burst effect followed by a slow and sustained release, characteristic of a biphasic release, as can be seen in Figure 3 (Dong and Feng, 2004; Hirenkumar K. Makadia and Steven J. Siegel, 2011; Rafiei and Haddadi, 2017; Zayas et al., 2013). This biphasic release profile can be attributed to the 4NC in the oily nucleus and to another part inside or near the polymer wall. The release is relatively fast (48h) due to the shell thickness of the nanocapsules, as can be seen in the TEM images (Figure 1) (Feuser et al., 2016a; Zhaparova, 2012).

Kinetic studies were performed and the zero order, first order, Korsmeyer–Peppas and Higuchi mathematical models were used. The release kinetics at physiological pH was best explained by Korsmeyer–Peppas ( $R^2 = 0.97$ ) followed by the Higuchi model ( $R^2 = 0.93$ ), the zero-order model ( $R^2 = 0.7916$ ), and finally

the first order model ( $R^2 = 0.6841$ ). The choice of model was based on the highest  $R^2$  value. From the studies of mathematical models, the release kinetics was best explained by the Korsmeyer-Peppas model and exponent  $n = 0.43$ , which implies Fickian diffusion where the release of 4NC was controlled by diffusion (Bohrey et al., 2016; Costa and Sousa Lobo, 2001; Maderuelo et al., 2011; Paul, 2011).

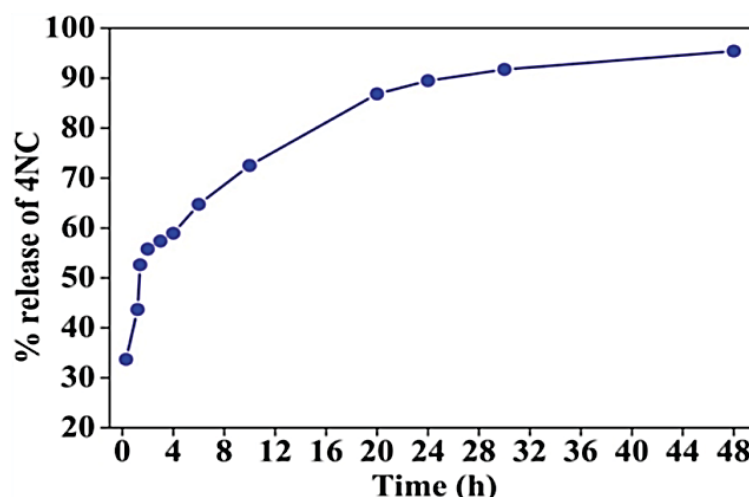


**Figure 3.** Release profiles of 4NC loaded in folic acid - PMMA nanoparticles. Data refer to mean  $\pm$  standard deviation ( $n = 3$ ) in three different experiments.

### 5.3.3. Evaluation of the effect on the cell viability of 4NC encapsulated in folic acid-PMMA nanoparticles

HeLa cells were exposed for 24 hours to increased concentrations of both free 4NC and 4NC-folic acid-PMMA nanoparticles, and the effects were analyzed by the MTT assay. The results in Figure 4 show that 4NC-folic acid-PMMA, in a dose-dependent manner, produced a reduction in the cell viability of approximately 31, 63 and 80% at the concentrations of 15, 30 and 45  $\mu\text{M}$ , respectively. Interestingly, free 4NC showed roughly 15 and 24% less cytotoxicity at the concentrations of 15 and 30  $\mu\text{M}$ , respectively. Furthermore, as shown in Figure 5, there was no toxicity found for empty folic acid-PMMA nanoparticles at the same concentrations, which indicates that the effect of 4NC-folic acid-PMMA nanoparticles could be mostly attributed to the incorporated 4NC. However, it is well-known that the nanoparticle uptake process can generate alterations in cellular physiology, without necessarily compromising the viability (Ispanixtlahuatl-Meráz et al., 2018). Therefore, the increased toxicity of 4NC-folic

acid-PMMA over the free drug could be associated, at least in part, with possible effects provoked by the nanoparticle internalization process. The cells exposed to 4NC-PMMA at the concentrations of 15  $\mu$ M were not affected in their viability, but at the concentration of 30  $\mu$ M there was a reduction in roughly 45%. In general, anionic nanoparticles can interact with positively charged molecules exposed at the plasma membrane surface enabling receptor-independent endocytosis (Kou et al., 2013). Due to the negative charge in 4NC-PMMA, the reduction in cell viability could reflect a receptor-independent uptake of these nanoparticles.

However, when compared with the reduction induced by 4NC-folic acid-PMMA at the concentrations of 15 and 30  $\mu$ M, 4NC-PMMA resulted in approximately 21 and 28% less inhibition, respectively, which highlights the influence of the folic acid functionalization in the increased toxicity.

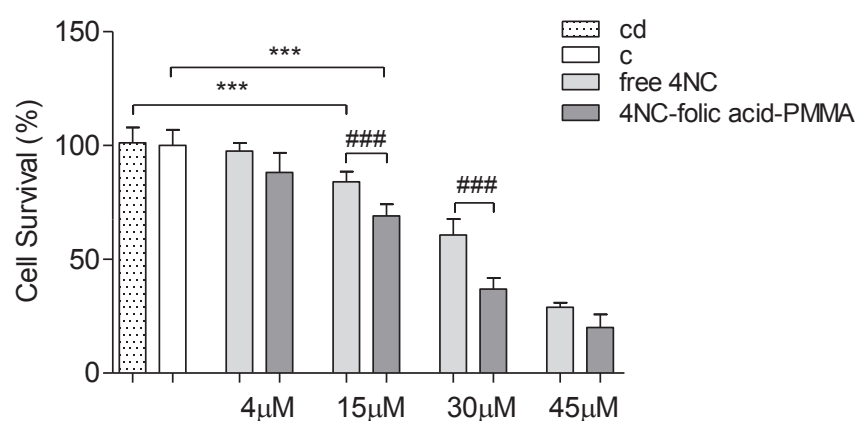


**Figure 4.** Comparative effects of free 4NC and 4NC-folic acid-PMMA nanoparticles on HeLa cell viability after 24 hours of incubation expressed as a percentage of the control cells incubated with MEM medium only (c) or MEM with 0.1% of DMSO (cd). Data shown as mean  $\pm$  S.D. of three independent experiments performed in triplicate). \*\*\* $p$  < 0.001; ### $p$  < 0.001. Cd (MEM with 0.1% of DMSO), c (MEM medium).

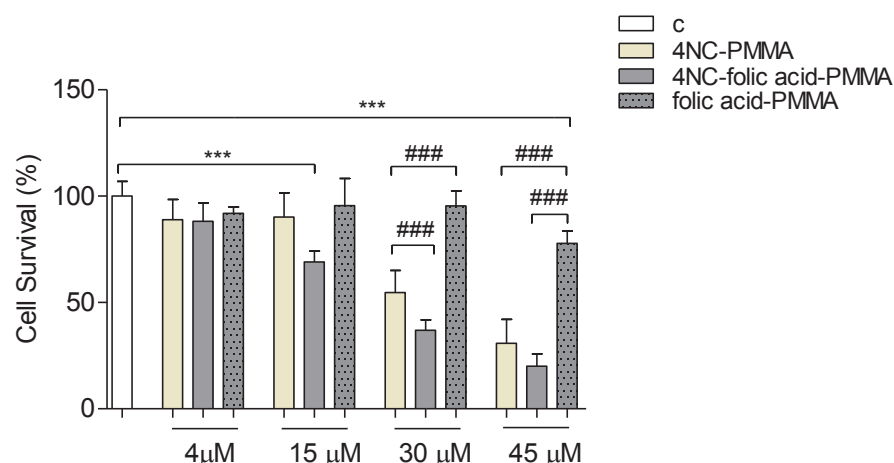


**Figure 5.** Comparative effects of 4NC-folic acid-PMMA, 4NC-PMMA and empty PMMA on HeLa cell viability expressed as a percentage of the control cells incubated with MEM medium (c). Data shown as mean  $\pm$  S.D. of three independent experiments performed in triplicate). \*\*\* $p < 0.001$ ; ### $p < 0.001$ .

#### 5.3.4. Cellular uptake of folic acid-PMMA nanoparticles

In order to verify the uptake of folic acid-PMMA by HeLa cells and further assess their preferential entry over the unfunctionalized PMMA, we loaded both types of nanoparticles with the green fluorophore 6-coumarin and detected by laser scanning confocal microscopy. Moreover, knowing that receptor-mediated endocytosis is an energy-dependent process, and hence, temperature-sensitive (Kansara et al., 2015; Weigel and Oka, 1981), we decided to further explore the uptake mechanism assessing the influence of low temperature on the entrance of the nanoparticles.

The results in the micrographs of Figures 6A and 6B show that both nanoparticles incubated at reduced temperature (4°C) were not internalized. However, when cells are incubated with PMMA and folic acid-PMMA at 37°C, they are both internalized. But incubation with folic acid-PMMA produced an evidently higher accumulation of nanoparticles (Figure 6D). These results are in line with the higher effect of the 4NC-folic acid-PMMA and support the importance of the functionalization with folic acid in nanoparticle uptake.

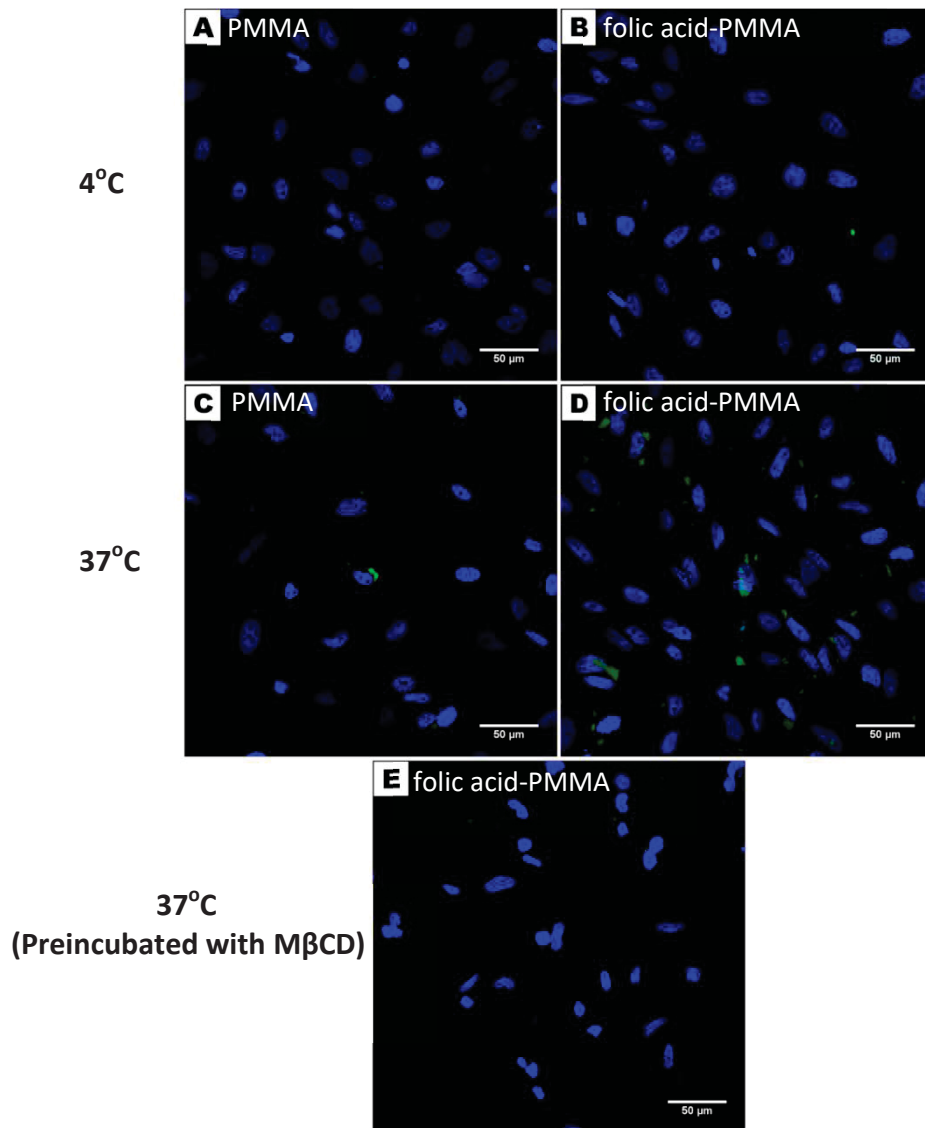


**Figure 6.** Representative fluorescence micrographs of HeLa cells incubated at 4 °C for 1 h with 6-coumarin green loaded both in (A) and in folic acid-PMMA (B). Representative fluorescence micrographs of HeLa cells incubated at 37 °C for 1 h with 6-coumarin loaded in PMMA (C) and in folic acid-PMMA (D). Representative fluorescence micrographs of HeLa cells pretreated with methyl- $\beta$ -cyclodextrin and incubated at 37°C for 1 h with 6-coumarin loaded in folic acid PMMA (E). After treatments the cells were stained with nuclear dye DAPI (blue fluorescence).

The clathrin- and caveolin-mediated endocytosis are two well-characterized mechanisms of folate receptor-mediated internalization (Kou et al., 2013). The endocytic pathway of the formulation depends on both the cell type, as well as on various inherent nanoparticles characteristics (He et al., 2010; Suen and Chau, 2014; Truong et al., 2014). As mentioned above, one of these

parameters is the nanoparticle surface charge. Previous studies have found that positively charged nanoparticles are almost exclusively endocytosed by the clathrin-dependent mechanism, whereas anionic nanoparticles could use the caveolin pathway or both pathways (Harush-Frenkel et al., 2007; Zhang and Monteiro-Riviere, 2009). Interestingly, as revealed in Figure 6E, when HeLa cells were preincubated with methyl- $\beta$ -cyclodextrin, a caveolae-mediated endocytosis inhibitor (Suen and Chau, 2014), the uptake of folic acid-PMMA nanoparticles was blocked. This finding suggests that the caveolae-mediated internalization could be involved in the uptake of our formulation. Obviously, additional studies are needed to further clarify if additional endocytic mechanisms could collaborate with the entry of our formulation into these cells.

Altogether, these observations confirm the role of folic acid in enhancing cellular uptake of folic acid-PMMA, and supports the notion that the receptor-mediated endocytic pathway could be involved in their internalization process.

## **5.4 Conclusion**

4-nitrochalcone loaded in poly (methyl methacrylate) nanoparticles functionalized with folic acid (4NC-folic acid-PMMA) was successfully synthesized by mini-emulsion polymerization technique. We verified that the internalization of PMMA nanoparticles was favored by the folic acid, suggesting that the receptor-mediated endocytic pathway was involved in nanoparticle uptake. Our results also show the potential of free 4NC to induce a reduction in the cell viability and that folic acid-PMMA is a promising encapsulation system to deliver 4NC to HeLa cells.

## **Acknowledgements**

The authors would like to thank CNPq (Conselho Nacional de Desenvolvimento Científico e Tecnológico) and CAPES (Coordenação de Aperfeiçoamento de Pessoal de Nível Superior) for their financial support, and the TEM analysis from Laboratório Central de Microscopia Eletrônica of Federal University of Santa Catarina (LCME/UFSC).

## 5.5 References

- Andhariya, N., Upadhyay, R., Mehta, R., Chudasama, B., 2013. Folic acid conjugated magnetic drug delivery system for controlled release of doxorubicin. *J. Nanoparticle Res.* 15, 1416. doi:10.1007/s11051-013-1416-9
- Asua, J.M., 2002. Miniemulsion polymerization. *Prog. Polym. Sci.* 27, 1283–1346. doi:10.1016/S0079-6700(02)00010-2
- Batovska, D.I., Todorova, I.T., 2010. Trends in utilization of the pharmacological potential of chalcones. *Curr. Clin. Pharmacol.* 5, 1–29. doi:10.2174/157488410790410579
- Bohrey, S., Chourasiya, V., Pandey, A., 2016. Polymeric nanoparticles containing diazepam: preparation, optimization, characterization, in-vitro drug release and release kinetic study. *Nano Converg.* 3, 3. doi:10.1186/s40580-016-0061-2
- Chandra Shekhara Shetty, T., Raghavendra, S., Chidan Kumar, C.S., Dharmaprakash, S.M., 2016. Crystal structure and nonlinear optical absorption of a new chalcone derivative: a promising candidate for optical switching. *Appl. Phys. B Lasers Opt.* 122, 1–9. doi:10.1007/s00340-016-6478-9
- Chen, C., Ke, J., Zhou, X.E., Yi, W., Brunzelle, J.S., Li, J., Yong, E.-L., Xu, H.E., Melcher, K., 2013. Structural basis for molecular recognition of folic acid by folate receptors. *Nature* 500, 486–9. doi:10.1038/nature12327
- Chopra, M., Jain, R., Dewangan, A.K., Varkey, S., Mazumder, S., 2016. Design of Curcumin Loaded Polymeric Nanoparticles-Optimization, Formulation and Characterization. *J. Nanosci. Nanotechnol.* 16, 9432–9442. doi:10.1166/jnn.2016.12363
- Colson, Y.L., Grinstaff, M.W., 2012. Biologically Responsive Polymeric Nanoparticles

- for Drug Delivery. *Adv. Mater.* 24, 3878–3886. doi:10.1002/adma.201200420
- Costa, P., Sousa Lobo, J.M., 2001. Modeling and comparison of dissolution profiles. *Eur. J. Pharm. Sci.* 13, 123–33.
- Date, P. V., Patel, M.D., Majee, S.B., Samad, A., Devarajan, P. V., 2013. Ionic complexation as a non-covalent approach for the design of folate anchored rifampicin gantrez nanoparticles. *J. Biomed. Nanotechnol.* 9, 765–775. doi:10.1166/jbn.2013.1581
- Dhana Lekshmi, U.M., Poovi, G., Kishore, N., Reddy, P.N., 2010. In vitro characterization and invivo toxicity study of repaglinide loaded poly (methyl methacrylate) nanoparticles. *Int. J. Pharm.* 396, 194–203. doi:10.1016/j.ijpharm.2010.06.023
- Dong, Y., Feng, S.S., 2004. Methoxy poly(ethylene glycol)-poly(lactide) (MPEG-PLA) nanoparticles for controlled delivery of anticancer drugs. *Biomaterials* 25, 2843–2849. doi:10.1016/j.biomaterials.2003.09.055
- Felice, B., Prabhakaran, M.P., Rodríguez, A.P., Ramakrishna, S., 2014. Drug delivery vehicles on a nano-engineering perspective. *Mater. Sci. Eng. C. Mater. Biol. Appl.* 41C, 178–195. doi:10.1016/j.msec.2014.04.049
- Feuser, P.E., Arévalo, J.M.C., Junior, E.L., Rossi, G.R., da Silva Trindade, E., Rocha, M.E.M., Jacques, A.V., Ricci-Júnior, E., Santos-Silva, M.C., Sayer, C., de Araújo, P.H.H., 2016a. Increased cellular uptake of lauryl gallate loaded in superparamagnetic poly(methyl methacrylate) nanoparticles due to surface modification with folic acid. *J. Mater. Sci. Mater. Med.* 27. doi:10.1007/s10856-016-5796-0
- Feuser, P.E., Bubniak, L. dos S., Bodack, C. do N., Valério, A., Silva, M.C. dos S.,



- Ricci-Júnior, E., Sayer, C., Araújo, P.H.H. de, 2016b. In Vitro Cytotoxicity of Poly(Methyl Methacrylate) Nanoparticles and Nanocapsules Obtained by Miniemulsion Polymerization for Drug Delivery Application. *J. Nanosci. Nanotechnol.* 16, 7669–7676. doi:10.1166/jnn.2016.11610
- Andhariya, N., Upadhyay, R., Mehta, R., Chudasama, B., 2013. Folic acid conjugated magnetic drug delivery system for controlled release of doxorubicin. *J. Nanoparticle Res.* 15, 1416. doi:10.1007/s11051-013-1416-9
- Asua, J.M., 2002. Miniemulsion polymerization. *Prog. Polym. Sci.* 27, 1283–1346. doi:10.1016/S0079-6700(02)00010-2
- Batovska, D.I., Todorova, I.T., 2010. Trends in utilization of the pharmacological potential of chalcones. *Curr. Clin. Pharmacol.* 5, 1–29. doi:10.2174/157488410790410579
- Bohrey, S., Chourasiya, V., Pandey, A., 2016. Polymeric nanoparticles containing diazepam: preparation, optimization, characterization, in-vitro drug release and release kinetic study. *Nano Converg.* 3, 3. doi:10.1186/s40580-016-0061-2
- Chandra Shekhara Shetty, T., Raghavendra, S., Chidan Kumar, C.S., Dharmaprakash, S.M., 2016. Crystal structure and nonlinear optical absorption of a new chalcone derivative: a promising candidate for optical switching. *Appl. Phys. B Lasers Opt.* 122, 1–9. doi:10.1007/s00340-016-6478-9
- Chen, C., Ke, J., Zhou, X.E., Yi, W., Brunzelle, J.S., Li, J., Yong, E.-L., Xu, H.E., Melcher, K., 2013. Structural basis for molecular recognition of folic acid by folate receptors. *Nature* 500, 486–9. doi:10.1038/nature12327
- Chopra, M., Jain, R., Dewangan, A.K., Varkey, S., Mazumder, S., 2016. Design of Curcumin Loaded Polymeric Nanoparticles-Optimization, Formulation and

Characterization. *J. Nanosci. Nanotechnol.* 16, 9432–9442.

doi:10.1166/jnn.2016.12363

Colson, Y.L., Grinstaff, M.W., 2012. Biologically Responsive Polymeric Nanoparticles for Drug Delivery. *Adv. Mater.* 24, 3878–3886. doi:10.1002/adma.201200420

Costa, P., Sousa Lobo, J.M., 2001. Modeling and comparison of dissolution profiles. *Eur. J. Pharm. Sci.* 13, 123–33.

Date, P. V., Patel, M.D., Majee, S.B., Samad, A., Devarajan, P. V., 2013. Ionic complexation as a non-covalent approach for the design of folate anchored rifampicin gantrez nanoparticles. *J. Biomed. Nanotechnol.* 9, 765–775. doi:10.1166/jbn.2013.1581

Dhana Lekshmi, U.M., Poovi, G., Kishore, N., Reddy, P.N., 2010. In vitro characterization and invivo toxicity study of repaglinide loaded poly (methyl methacrylate) nanoparticles. *Int. J. Pharm.* 396, 194–203. doi:10.1016/j.ijpharm.2010.06.023

Dong, Y., Feng, S.S., 2004. Methoxy poly(ethylene glycol)-poly(lactide) (MPEG-PLA) nanoparticles for controlled delivery of anticancer drugs. *Biomaterials* 25, 2843–2849. doi:10.1016/j.biomaterials.2003.09.055

Felice, B., Prabhakaran, M.P., Rodríguez, A.P., Ramakrishna, S., 2014. Drug delivery vehicles on a nano-engineering perspective. *Mater. Sci. Eng. C. Mater. Biol. Appl.* 41C, 178–195. doi:10.1016/j.msec.2014.04.049

Feuser, P.E., Arévalo, J.M.C., Junior, E.L., Rossi, G.R., da Silva Trindade, E., Rocha, M.E.M., Jacques, A.V., Ricci-Júnior, E., Santos-Silva, M.C., Sayer, C., de Araújo, P.H.H., 2016a. Increased cellular uptake of lauryl gallate loaded in superparamagnetic poly(methyl methacrylate) nanoparticles due to surface

modification with folic acid. *J. Mater. Sci. Mater. Med.* 27. doi:10.1007/s10856-016-5796-0

Feuser, P.E., Bubniak, L. dos S., Bodack, C. do N., Valério, A., Silva, M.C. dos S., Ricci-Júnior, E., Sayer, C., Araújo, P.H.H. de, 2016b. In Vitro Cytotoxicity of Poly(Methyl Methacrylate) Nanoparticles and Nanocapsules Obtained by Miniemulsion Polymerization for Drug Delivery Application. *J. Nanosci. Nanotechnol.* 16, 7669–7676. doi:10.1166/jnn.2016.11610

Feuser, P.E., Bubniak, L. dos S., Bodack, C. do N., Valério, A., Silva, M.C. dos S., Ricci-Júnior, E., Sayer, C., Araújo, P.H.H. de, 2016c. In Vitro Cytotoxicity of Poly(Methyl Methacrylate) Nanoparticles and Nanocapsules Obtained by Miniemulsion Polymerization for Drug Delivery Application. *J. Nanosci. Nanotechnol.* 16, 7669–7676. doi:10.1166/jnn.2016.11610

Frohlich, E., 2012. The role of surface charge in cellular uptake and cytotoxicity of medical nanoparticles. *Int. J. Nanomedicine* 7, 5577–5591. doi:10.2147/IJN.S36111

Guo, H., Sun, S., Yang, Z., Tang, X., Wang, Y., 2015. Strategies for ribavirin prodrugs and delivery systems for reducing the side-effect hemolysis and enhancing their therapeutic effect. *J. Control. Release* 209, 27–36. doi:10.1016/j.jconrel.2015.04.016

Hazra, C., Kundu, D., Chatterjee, A., Chaudhari, A., Mishra, S., 2014. Poly(methyl methacrylate) (core)–biosurfactant (shell) nanoparticles: Size controlled sub-100nm synthesis, characterization, antibacterial activity, cytotoxicity and sustained drug release behavior. *Colloids Surfaces A Physicochem. Eng. Asp.* 449, 96–113. doi:10.1016/j.colsurfa.2014.02.051

He, C., Hu, Y., Yin, L., Tang, C., Yin, C., 2010. Effects of particle size and surface

charge on cellular uptake and biodistribution of polymeric nanoparticles.

Biomaterials 31, 3657–66. doi:10.1016/j.biomaterials.2010.01.065

Hirenkumar K. Makadia and Steven J. Siegel, 2011. Biomedical Applications of

Biodegradable Polymers. Polymers (Basel). 3, 1377–1397.

doi:10.3390/polym3031377.Poly

Hsu, Y.L., Chia, C.C., Chen, P.J., Huang, S.E., Huang, S.C., Kuo, P.L., 2009. Shallot and licorice constituent isoliquiritigenin arrests cell cycle progression and induces apoptosis through the induction of ATM/p53 and initiation of the mitochondrial system in human cervical carcinoma HeLa cells. Mol. Nutr. Food Res. 53, 826–835. doi:10.1002/mnfr.200800288

Ispanixtlahuatl-Meráz, O., Schins, R.P.F., Chirino, Y.I., 2018. Cell type specific cytoskeleton disruption induced by engineered nanoparticles. Environ. Sci. Nano. doi:10.1039/C7EN00704C

Kansara, V., Paturi, D., Luo, S., Gaudana, R., Mitra, A.K., City, K., 2015. Folic acid transport via high affinity carrier-mediated system in human retinoblastoma cells. Int J Pharm 355, 210–219. doi:10.1016/j.ijpharm.2007.12.008.Folic

Karthikeyan, C., Narayana Moorthy, N.S., Ramasamy, S., Vanam, U., Manivannan, E., Karunagaran, D., Trivedi, P., 2015. Advances in Chalcones with Anticancer Activities. Recent Pat. Anticancer. Drug Discov. 10, 97–115. doi:10.2174/1574892809666140819153902

Kou, L., Sun, J., Zhai, Y., He, Z., 2013. The endocytosis and intracellular fate of nanomedicines: Implication for rational design. Asian J. Pharm. Sci. 8, 1–8. doi:10.1016/j.ajps.2013.07.001

Kovacic, P., Somanathan, R., 2014. Nitroaromatic compounds: Environmental

- toxicity, carcinogenicity, mutagenicity, therapy and mechanism. *J. Appl. Toxicol.* 34, 810–824. doi:10.1002/jat.2980
- Kuo, Y.-C., Chen, Y.-C., 2015. Targeting delivery of etoposide to inhibit the growth of human glioblastoma multiforme using lactoferrin- and folic acid-grafted poly(lactide-co-glycolide) nanoparticles. *Int. J. Pharm.* 479, 138–149. doi:10.1016/j.ijpharm.2014.12.070
- Lee, S.J., Shim, Y.-H., Oh, J.-S., Jeong, Y.-I., Park, I.-K., Lee, H.C., 2015. Folic-acid-conjugated pullulan/poly(DL-lactide-co-glycolide) graft copolymer nanoparticles for folate-receptor-mediated drug delivery. *Nanoscale Res. Lett.* 10, 1–11. doi:10.1186/s11671-014-0706-1
- Letchford, K., Burt, H., 2007. A review of the formation and classification of amphiphilic block copolymer nanoparticulate structures: micelles, nanospheres, nanocapsules and polymersomes. *Eur. J. Pharm. Biopharm.* 65, 259–269. doi:10.1016/j.ejpb.2006.11.009
- Lorca, B.S.S., Bessa, E.S., Nele, M., Santos, E.P., Pinto, J.C., 2012. Preparation of PMMA Nanoparticles Loaded with Benzophenone-3 through Miniemulsion Polymerization. *Macromol. Symp.* 319, 246–250. doi:10.1002/masy.201100252
- Maderuelo, C., Zarzuelo, A., Lanao, J.M., 2011. Critical factors in the release of drugs from sustained release hydrophilic matrices. *J. Control. Release* 154, 2–19. doi:10.1016/j.jconrel.2011.04.002
- Mai, C.W., Yaeghoobi, M., Abd-Rahman, N., Kang, Y.B., Pichika, M.R., 2014. Chalcones with electron-withdrawing and electron-donating substituents: Anticancer activity against TRAIL resistant cancer cells, structure-activity relationship analysis and regulation of apoptotic proteins. *Eur. J. Med. Chem.* 77, 378–387. doi:10.1016/j.ejmech.2014.03.002

- Mohapatra, S., Mallick, S.K., Maiti, T.K., Ghosh, S.K., Pramanik, P., 2007. Synthesis of highly stable folic acid conjugated magnetite nanoparticles for targeting cancer cells. *Nanotechnology* 18, 385102. doi:10.1088/0957-4484/18/38/385102
- Parker, N., Turk, M.J., Westrick, E., Lewis, J.D., Low, P.S., Leamon, C.P., 2005. Folate receptor expression in carcinomas and normal tissues determined by a quantitative radioligand binding assay. *Anal. Biochem.* 338, 284–293. doi:10.1016/j.ab.2004.12.026
- Patil, P.S., Dharmaprakash, S.M., Fun, H.K., Karthikeyan, M.S., 2006. Synthesis, growth, and characterization of 4-OCH<sub>3</sub>-4-nitrochalcone single crystal: A potential NLO material. *J. Cryst. Growth* 297, 111–116. doi:10.1016/j.jcrysgro.2006.09.017
- Patterson, S., Wyllie, S., 2014. Nitro drugs for the treatment of trypanosomatid diseases: Past, present, and future prospects. *Trends Parasitol.* 30, 289–298. doi:10.1016/j.pt.2014.04.003
- Paul, D.R., 2011. Elaborations on the Higuchi model for drug delivery. *Int. J. Pharm.* 418, 13–17. doi:10.1016/j.ijpharm.2010.10.037
- Prabhu, R. H., Patravale, V. B., & Joshi, M.D., 2015. Polymeric nanoparticles for targeted treatment in oncology : current insights. *Int. J. Nanomedicine*, 10, 1001–1018. doi:10.2147/IJN.S56932
- Rafiei, P., Haddadi, A., 2017. Docetaxel-loaded PLGA and PLGA-PEG nanoparticles for intravenous application: Pharmacokinetics and biodistribution profile. *Int. J. Nanomedicine* 12, 935–947. doi:10.2147/IJN.S121881
- Ramalho, S.D., Bernades, A., Demetrius, G., Noda-Perez, C., Vieira, P.C., Dos Santos, C.Y., Da Silva, J.A., De Moraes, M.O., Mousinho, K.C., 2013. Synthetic

- chalcone derivatives as inhibitors of cathepsins K and B, and their cytotoxic evaluation. *Chem. Biodivers.* 10, 1999–2006. doi:10.1002/cbdv.201200344
- Scarano, W., Duong, H.T.T., Lu, H., De Souza, P.L., Stenzel, M.H., 2013. Folate conjugation to polymeric micelles via boronic acid ester to deliver platinum drugs to ovarian cancer cell lines. *Biomacromolecules* 14, 962–975. doi:10.1021/bm400121q
- Shin, S.Y., Lee, J.M., Lee, M.S., Koh, D., Jung, H., Lim, Y., Lee, Y.H., 2014. Targeting Cancer Cells via the Reactive Oxygen Species-Mediated Unfolded Protein Response with a Novel Synthetic Polyphenol Conjugate. *Clin. Cancer Res.* 20, 4302–4313. doi:10.1158/1078-0432.CCR-14-0424
- Singh, R., Kesharwani, P., Mehra, N.K., Singh, S., Banerjee, S., Jain, N.K., 2015. Development and characterization of folate anchored Saquinavir entrapped PLGA nanoparticles for anti-tumor activity. *Drug Dev. Ind. Pharm.* 0, 1–14. doi:10.3109/03639045.2015.1019355
- Srinivasan, B., Johnson, T.E., Lad, R., Xing, C., 2009. Structure - Activity Relationship Studies of Chalcone Leading to Factor K B Inhibitors and Their Anticancer Activities 7228–7235. doi:10.1021/jm901278z
- Stiborová, M., Frei, E., Schmeiser, H.H., Arlt, V.M., Martínek, V., 2014. Mechanisms of enzyme-catalyzed reduction of two carcinogenic nitro-aromatics, 3-nitrobenzanthrone and aristolochic acid I: Experimental and theoretical approaches. *Int. J. Mol. Sci.* 15, 10271–10295. doi:10.3390/ijms150610271
- Suen, W.L.L., Chau, Y., 2014. Size-dependent internalisation of folate-decorated nanoparticles via the pathways of clathrin and caveolae-mediated endocytosis in ARPE-19 cells. *J. Pharm. Pharmacol.* 66, 564–573. doi:10.1111/jphp.12134

- Sulistio, A., Lowenthal, J., Blencowe, A., Bongiovanni, M.N., Ong, L., Gras, S.L., Zhang, X., Qiao, G.G., 2011. Folic acid conjugated amino acid-based star polymers for active targeting of cancer cells. *Biomacromolecules* 12, 3469–3477. doi:10.1021/bm200604h
- Tiarks, F., Landfester, K., Antonietti, M., 2001. Preparation of polymeric nanocapsules by miniemulsion polymerization. *Langmuir* 17, 908–918. doi:10.1021/la001276n
- Truong, N.P., Whittaker, M.R., Mak, C.W., Davis, T.P., Truong, N.P., Whittaker, M.R., Mak, C.W., Davis, T.P., 2014. Expert Opinion on Drug Delivery The importance of nanoparticle shape in cancer drug delivery The importance of nanoparticle shape in cancer drug delivery 12, 129–142. doi:10.1517/17425247.2014.950564
- Wang, B., Dong, J., Li, Q., Xiong, Z., Xiong, C., Chen, D., 2014. Mechanism of inhibition on L929 rat fibroblasts proliferation induced by potential adhesion barrier material poly(p-dioxanone-co-  $\alpha$ -phenylalanine) electrospun membranes. *J. Biomed. Mater. Res. Part A* 102, 4062–4070. doi:10.1002/jbm.a.35077
- Weigel, P.H., Oka, J.A., 1981. Temperature dependence of endocytosis mediated by the asialoglycoprotein receptor in isolated rat hepatocytes. Evidence for two potentially rate-limiting steps. *J. Biol. Chem.* 256, 2615–2617.
- WHO, 2017. Cervical cancer [WWW Document].
- Yang, H., Li, Y., Li, T., Xu, M., Chen, Y., Wu, C., Dang, X., Liu, Y., 2014. Multifunctional Core/Shell Nanoparticles Cross-linked Polyetherimide-folic Acid as Efficient Notch-1 siRNA Carrier for Targeted Killing of Breast Cancer. *Sci. Rep.* 4, 7072. doi:10.1038/srep07072



- Zayas, H. a., Truong, N.P., Valade, D., Jia, Z., Monteiro, M.J., 2013. Narrow molecular weight and particle size distributions of polystyrene 4-arm stars synthesized by RAFT-mediated miniemulsions. *Polym. Chem.* 4, 592. doi:10.1039/c2py20709e
- Zhang, B., Duan, D., Ge, C., Yao, J., Liu, Y., Li, X., Fang, J., 2015. Synthesis of xanthohumol analogues and discovery of potent thioredoxin reductase inhibitor as potential anticancer agent. *J. Med. Chem.* 58, 1795–1805. doi:10.1021/jm5016507
- Zhaparova, L., 2012. Synthesis of nanoparticles and nanocapsules for controlled release of the antitumor drug “Arglabin” and antituberculosis drugs. doi:10.6100/IR731636
- Zhou, B., Yu, X., Zhuang, C., Villalta, P., Lin, Y., Lu, J., Xing, C., 2016. Unambiguous Identification of  $\beta$ -Tubulin as the Direct Cellular Target Responsible for the Cytotoxicity of Chalcone by Photoaffinity Labeling. *ChemMedChem* 11, 1436–1445. doi:10.1002/cmdc.201600150.

## Capítulo 6: ARTIGO 3

## **Capítulo 6: Prooxidant and cytotoxic effects of nitrochalcones on HeLa cells**

Juan Marcelo Carpio Arévalo<sup>a</sup>, Diogo Henrique Kita<sup>b</sup>, Glaucio Valdameri<sup>b</sup>, Silvia Maria Suter C. Cadena<sup>a</sup>, Glaucia R. Martinez<sup>a</sup>, Guilhermina Rodrigues Noletto<sup>a</sup>, Alfredo R. M. de Oliveira<sup>c</sup>, Maria E.M. Rocha<sup>a,\*</sup>

<sup>a</sup> Department of Biochemistry and Molecular Biology, Federal University of Paraná, Curitiba, PR, Brazil

<sup>b</sup> Department of Clinical Analysis, Federal University of Paraná, Curitiba, PR, Brazil

<sup>c</sup> Department of Chemistry, Federal University of Paraná, Curitiba, PR, Brazil

\*Corresponding author. Tel.: +55 41 3361 1664; fax: +55 41 3266 2042.

E-mail addresses: maelimerlin.rocha@gmail.com (M.E.M.Rocha).

## Abstract

Hydroxylated and nitrated chalcones were evaluated for their cytotoxic and pro-oxidant effects in HeLa cells. Structure-activity relationship (SAR) studies have demonstrated the importance of electron withdrawing and electron donating groups in the chalcone core structure in order to improve their biological activities. In this study, chalcones containing either a 3-nitro group in the B ring, a hydroxyl group at 2' position of the A ring, or a newly-synthesized chalcone harboring both substituents were tested for their cytotoxic effects on HeLa cells. In addition, we investigated the role of reactive oxygen species. The results revealed that chalcones containing a nitro group were the most potent compounds. The bifunctionalized chalcone (HNC) exhibited better water-solubility and yielded an  $IC_{50} = 24 \mu M$ . The results of the annexin V-FITC/propidium iodide double labeling assay, as well as morphological alterations and the increase in the percentage of hypodiploid cells suggested that cell death mechanism induced by HNC could be apoptosis. We assessed the HNC effects (20 and 30  $\mu M$ ) on levels of reactive oxygen species, and only at the higher concentration a significant increase was observed. Moreover, when the cells were pre-incubated with NAC, no protective effect against HNC was found. These results suggest that reduction of cell viability induced by HNC might not be, at least in part, associated with ROS increase. Additionally, after few minutes of exposure to HNC, the adduct between GSH and HNC was detected in cell extracts. Lastly, we showed that the overexpression of MRP1 transporters in cells does not confer resistance to the effects of HNC. Thus, HNC could be a promising adjuvant in cancer treatment since it can reduce the GSH pool availability, promoting HeLa cell death possibly through an apoptotic mechanism, and its cytotoxic effect is not even reduced in cells that overexpress MRP1.

**Keywords:** Nitrochalcones, Hela cells, ROS, GSH and nitrochalcone-glutathione conjugate

## 6.1 Introduction

The chalcones are a group of flavonoids that have shown important biological activities, such as antioxidant <sup>1</sup>, anti-inflammatory <sup>2</sup>, as well as cytotoxic and anti-proliferative effects in several tumoral cells <sup>3,4</sup>. Previous studies have shown the straightforward relation between their potential antitumoral effects with the interaction of several cellular targets such as  $\beta$ -tubulin <sup>5</sup>, proteasome <sup>6</sup>, topoisomerases <sup>7,8</sup>, as well as several antioxidant enzymes <sup>9,10</sup>.

Structurally chalcone consist of two aromatic rings (A and B) linked by an three-carbon  $\alpha$ ,  $\beta$ -unsaturated carbonyl system, which gives them their electrophilic character and enables the chemical attack on thiolate groups in several of their targets <sup>9,11,12</sup>. The broad spectrum of biological activity that these molecules exhibit can be explained by the type and substitution pattern of the different chemical groups on the aromatics rings, which exert sterical modifications and alter the electron-deficient  $\beta$ -carbon reactivity <sup>8,13,14</sup>. Remarkably, the most abundant non-protein thiol, glutathione (GSH), has been reported among the various targets of chalcones <sup>4,9</sup>. GSH plays an essential role in keeping the redox balance through their direct ROS scavenger activity and as co-substrate for some antioxidant enzymes <sup>15</sup>. Similarly, it is critically involved in various xenobiotic detoxification pathways <sup>16</sup>.

The nitro group has been used to functionalize various drugs used to treat different types of diseases <sup>17</sup>. This small functional group, with electron withdrawing effects and moderate polarity <sup>18,19</sup>, is prone to bioactivation yielding toxic metabolites and reactive oxygen species <sup>20-22</sup>.

Another functional group with remarkable effects on the cytotoxicity of chalcones is the hydroxyl, especially in the 2' position (ortho of the A ring), which is supported by some studies that demonstrated increased effects toward some cancer cell lines including HeLa cells <sup>19</sup>. This functionalization can make the chalcone more reactive by forming an intramolecular hydrogen bond between the hydroxyl and the carbonyl group that results in increased electrophilicity <sup>23</sup>. Moreover, 2'-hydroxychalcones and some of their derivatives exhibit the capacity to deplete cellular glutathione and to also induce their oxidation <sup>24,25</sup>.

Interestingly, hydroxy-methoxilated chalcones<sup>19</sup> and some methoxy-chalcones <sup>4</sup> when substituted with the nitro group have shown improved cytotoxic effects on tumoral cells including HeLa.

Cancer cells, in general, exhibit increased ROS levels compared to normal cells <sup>26,27</sup>. Therefore, therapeutic agents that increase ROS levels to toxic levels or reduces antioxidant defenses may induce tumor cell death and have less effect on normal cells <sup>28</sup>.

Cervical cancer is the fourth most frequent type of cancer in women worldwide, and is especially important in developing countries, in which it accounts for approximately 85% of cases <sup>29</sup>. Despite the effectiveness of surgical treatment and radiotherapy in the early stages, in the more advanced stages of the disease the survival rates are low <sup>30</sup>. The appearance of serious adverse effects, as well as the development of resistance to several of the drugs applied in chemotherapy regimens, such as cisplatin <sup>31</sup>, paclitaxel <sup>32</sup>, 5-fluorouracil <sup>33</sup>, topotecan <sup>34</sup>, results in a poor prognosis <sup>35</sup>. Thus, there is a growing interest in the development of new drugs potentially more effective and with less toxicity.

Since the effect of a nitro group substituent in the chalcone core structure remains unclear and some 2'-hydroxychalcone derivatives has the potential to affect the redox status of the cells, in this work was studied a chalcone core without functional groups (CH) and the derivatives, namely, 2' hydroxyl chalcone (2HC), 3'-nitrochalcone (3NC), 2'-hydroxy-3-nitrochalcone (HNC), and comparatively evaluated their cytotoxic activity in HeLa cells. The chalcone that had the best results was the HNC that was analyzed for the first time in HeLa cells in order to elucidate the role of ROS, GSH depletion, and possible GSH adduct formation in cell death induced by this chalcone.

## **6.2 Material and Methods**

### **6.2.1 Materials**

Minimum essential medium (MEM) and fetal bovine serum (FBS) were obtained from Cultilab (São Paulo, Brazil). 3-(4,5-dimethylthiazol-2-yl)-2,5-diphenyltetrazolium bromide (MTT), 2'7'-dichlorofluorescein diacetate (DCFH-DA), N-acetylcysteine (NAC), L-buthionine sulfoximine (BSO), and monochlorobimane (mBCI) were obtained from Sigma-Aldrich (St. Louis, MO, USA). Annexin V-FITC, propidium iodide was obtained from Fluka-ThermoFisher Scientific (Switzerland). Dimethyl sulfoxide (DMSO) was obtained from Merck (Darmstadt, Germany). All other reagents were commercial products of the highest available purity grade.

Chalcone, 2'-hydroxychalcone, 3-nitrochalcone and 2'-hydroxy-3-nitrochalcone were synthesized and kindly provided by Dr. Alfredo S. E. Bates (Chemistry Department, UFPR, Curitiba, Parana, BR). The compounds were dissolved at 100 mM in DMSO and, stored at - 20 °C. The respective treatments were prepared in MEM immediately before use. The maximal concentration of DMSO was 0.1% in all the treatments and controls.

## **6.2.2 Cell cultures**

The human cervical carcinoma-derived cell line HeLa was obtained from Institute Adolfo Lutz (São Paulo-Brazil). For all the experiments cells were maintained in MEM medium, supplemented with 10% FBS and 100 U/ml penicillin/streptomycin, and incubated at 37°C and 5% CO<sub>2</sub>, under controlled humidity.

## **6.2.3 Methods**

### **6.2.3.1 Cell viability assays**

HeLa cells were cultivated at a density of  $1 \times 10^4$  cells/well onto 96-well culture plates for 24 h. Afterwards cells were treated with CH, 2HC, 3NC (10-20  $\mu$ M) and HNC (10–50  $\mu$ M) for 24 h, and the viability was evaluated through the MTT assay <sup>36</sup>. In brief, after 24 h of exposure at the compounds or vehicle control, the supernatants were replaced by 200  $\mu$ L of a solution of MTT prepared in PBS (0.5mg/ml) and incubated for an additional 2 h. Lastly, MTT was discarded and the formazan dye was dissolved with 200  $\mu$ L of DMSO. The absorbance at 550 nm was measured using a microplate reader (Epoch Bioteck). Cytotoxicity was also assayed with and without pre-incubation with NAC (10 mM) or BSO (100  $\mu$ M). For this, after two hours of pre-incubation, the medium with NAC or BSO were replaced by the respective treatments or vehicle control and incubated by 24 hours. Lastly, the MTT assay was performed as above-described. MEM media containing 0.1 % DMSO was used as control (CD). The results were expressed as the percentage of viable cells in comparison to CD (100 %). To assess the effect of HNC on MRP1 transporter, BHK21-MRP1 and BHK21 wild-type cells were seeded at a density of  $1 \times 10^4$  cells/well into 96-well culture plates and allowed to attach for 24 h at 37°C in 5% CO<sub>2</sub>. The treatment was done with various concentrations of HNC in a final volume of 200  $\mu$ L and

allowed to grow for 48 h at 37°C in 5% CO<sub>2</sub>. After the appropriate treatment time, 20 µL of MTT solution (5 mg/ mL) was added to each well and incubated for 4 h at 37°C in 5% CO<sub>2</sub>. Then the culture medium was discarded, each well was washed with PBS, and 100 µL of DMSO was added to each well and mixed by gentle shaking for 10 min. Absorbance was measured in a microplate reader at 560 nm (Glomax multi – Promega). Experimental conditions were set in triplicate, and control experiments were performed with DMEM high glucose containing 0.1% DMSO (v/v). Data are plotted as a percentage of reduced cell viability compared to control (untreated cells) that was taken as 100%.

#### **6.2.3.2 Morphological analysis of HeLa cells treated with HNC**

HeLa cells were cultivated on glass coverslips at a density of  $1.2 \times 10^5$  cells/well onto 24-well culture plates for 24 h. The cells were incubated with HNC (20–30 µM) for 24 h. The coverslips were then washed twice with PBS pH 7.4, exposed for 5 min to Bouin's fixative, stained with hematoxylin for 1 min and with eosin for 30 s and dehydrated in acetone. The slides were then mounted with Entellan and examined microscopically using a Zeiss LSM 410 microscope.

#### **6.2.3.3 Cell cycle analysis**

For the analysis of the cell cycle,  $2 \times 10^5$ /well were cultivated in 6-well culture plates for 24 h and posteriorly treated with HNC (20 and 30 µM) for 24 h. Both detached and trypsinized adherent cells were collected and centrifuged at  $1.000 \times g$  for 1 min. The cell pellet was resuspended in 0.3 mL of PBS containing 0.1 % Triton and 50 µg/mL propidium iodide (PI). The samples were analyzed in a flow cytometer Accuri C5 (BD) and the results were calculated using their software.

#### **6.2.3.4 Annexin V-FITC/Propidium iodide double labeling assay**

The double labeling using annexin V that binds to phosphatidylserine externalized and PI that enters in cells with loss of membrane integrity was performed. For this,  $2 \times 10^5$  cells HeLa cells were seeded in 6-well culture plates. After 24 h the medium was removed, HNC (20–30 µM) diluted in medium was added and incubated for 24 h. A combined incubation with quercetin (50 µM) and cisplatin (10 µM) was used as a positive control for apoptosis<sup>37,38</sup>. Both



detached and adherent cells were collected. Apoptosis was determined using the PI- Annexin-V Apoptosis Detection Kit I from BD Biosciences. Briefly, after centrifugation, the pellet was resuspended in 100  $\mu$ L of Annexin binding buffer, and stained with 5  $\mu$ L of Annexin-V and 5  $\mu$ L of PI for 15 min at 25°C in the dark. Samples were diluted in additional 400  $\mu$ L of binding buffer and analyzed using a flow cytometer Accuri C5 BD.

#### **6.2.3.5 Measurement of intracellular ROS generation**

HeLa cells were cultivated at a density of  $1 \times 10^4$  cells/well in 96-well black walled culture plates for 24 h. After, the cells were exposed for 24 h to HNC (20–30  $\mu$ M) or vehicle control. For ROS detection in cells pre-incubated with NAC, cells were exposed for 2 h to NAC solution (10 mM) prepared in MEM adjusted to pH 7.4 with NaOH. Posteriorly, the medium was discarded and replaced by HNC (20–30  $\mu$ M) and vehicle control, and incubated for 24 h. Lastly, the treatments were replaced by a solution of DCFH-DA in PBS (5  $\mu$ M) and incubated for an additional 30 min at 37°C. The fluorescence was measured using an Infinite 200 TECAN microplate reader at excitation and emission wavelengths of 485 and 525 nm, respectively. The fluorescence of cells incubated with vehicle control was considered as 100%, and the fluorescence of the cells treated with HNC was normalized on the viability of the remaining cells determined by the MTT assay.

#### **6.2.3.6 Fluorescence microscopy analysis**

For fluorescence images using Hoechst and PI, the HeLa cells were incubated for 24 h with HNC (20 and 30  $\mu$ M) and subsequently stained with Hoechst 33342 solution (3.5  $\mu$ g/ml) and incubated for 30 min at 37°C. This solution was replaced by PI solution (50  $\mu$ g/ml) and incubated for 5 min at 37°C.

To evaluate the GSH content, we used the probe mBCI which yields a fluorescent adduct with GSH that allows to estimate the intracellular concentrations of GSH<sup>39,40</sup>. For this assay, after 24 hours of incubation with HNC (20 and 30  $\mu$ M), the treatments were replaced by 200  $\mu$ L of a solution of mBCI (10  $\mu$ M) prepared in PBS and incubated for additional 25 min. Finally, the probe was replaced by PBS and analyzed under a fluorescence microscope.

All the analyses were conducted with an microscope Zeiss LSM 410 equipped with a fluorescent lamp and the suitable filter for each fluorophore

used: Hoechst: ex/em 350 / 461 nm, PI: ex/em 493 / 636 nm, mbcl-GS: ex/em 385/ 485 nm.

#### **6.2.3.7 Characterization of the adduct by RP- HPLC and mass spectrometry**

To identify the adduct (GS-HNC) in the free-cell system a reaction mixture containing HNC 30  $\mu$ M and GSH 5 mM in PBS was prepared and incubated at 37°C for 15, 70 and 280 min. 280  $\mu$ L of the respective mixtures were injected onto a column of Hypersyl C<sub>18</sub> (250 x 4.6 mm, 5  $\mu$ m) using a Prominence LC-20 HPLC system (Shimadzu, Kyoto, Japan). The mobile phase was composed of formic acid (0.18 %) (solvent A) and methanol (100%) (solvent B), using the following gradient: 5% B (0-15 min), 100% B (15-25 min), and 100% B isocratic (25-40 min). The flow rate was set at 0.72 mL/min and the column temperature at 30°C. Detection was performed with a diode array detector (PDA) in the 200-700 nm wavelength range.

To detect the adduct in cellular extracts, HeLa cells ( $2 \times 10^6$ ) were incubated for 24h and posteriorly exposed to HNC (30  $\mu$ M) or vehicle control for 15, 70 and 280 min. Then, the supernatant was discarded and the adherent cells were washed with 5ml of cold PBS (three times). Subsequently, the cells were scraped into 3 ml of cold PBS and centrifuged ( $1,000 \times g$ , 2 min). Afterwards, the pellet was subjected to three freezing/thawing cycles ( $-20^\circ\text{C}$  /  $4^\circ\text{C}$ ) and mixed with 600  $\mu$ L of cold methanol. The mixture was kept at  $4^\circ\text{C}$  for 1h with occasional vortexing and centrifuged ( $6,800 \times g$ , 5 min,  $4^\circ\text{C}$ ) to obtain the methanolic supernatant. Finally, 280  $\mu$ L of each extract was destined to HPLC analyses performed as already mentioned above.

The mass spectrum of the adduct GS-HNC purified by RP-HPLC from the free-cell experiments, was obtained using an LTQ-Orbitrap-XL electrospray ionization mass spectrometer (Thermo Scientific, Waltham, MA), operated on positive ionization. The set up for detection of positive ions was: electrospray at 4.5 kV, capillary at 50 V, and tube lens at 150 V.

#### **6.2.3.8 Statistical analysis**

An analysis of variance (one-way ANOVA) followed by a Tukey test was used to compare means, using the Graph Pad Prism 5.0 software. Values of

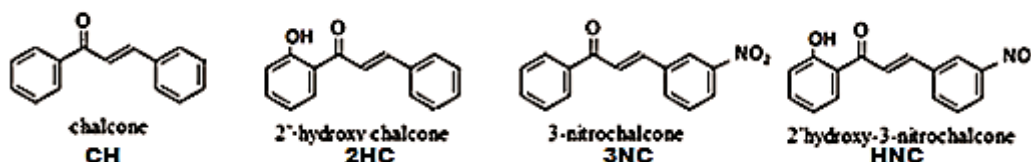
mean  $\pm$  SD were used. For all comparisons,  $p$  values less than 0.05 were considered statistically significant.

## 6.3 Results

### 6.3.1 Effects of chalcones on the viability of HeLa cells

Initially, the effects on the viability of HeLa cells was conducted by exposing the cells for 24 hours to different chalcones at the concentrations of 10 and 20  $\mu$ M to assess the effect of the functionalization, and to verify which of the derivatives (hydroxylated or nitrated) would be more toxic to HeLa cells. Figure 1B shows that the nitrated chalcones were the most efficient in reducing the viability of HeLa cells. Neither CH nor 2HC induced effects at the tested doses, while 3NC and HNC at the concentration of 20  $\mu$ M reduced cell viability by approximately 23%. However, 3NC is not soluble at concentrations higher than 20  $\mu$ M, which was previously verified by solubility tests using a DMSO concentration 0.1% in MEM. Due to the cytotoxic effect exhibited by HNC and its greater water-solubility, we chose this chalcone to continue studies of the mechanism of action.

A



B

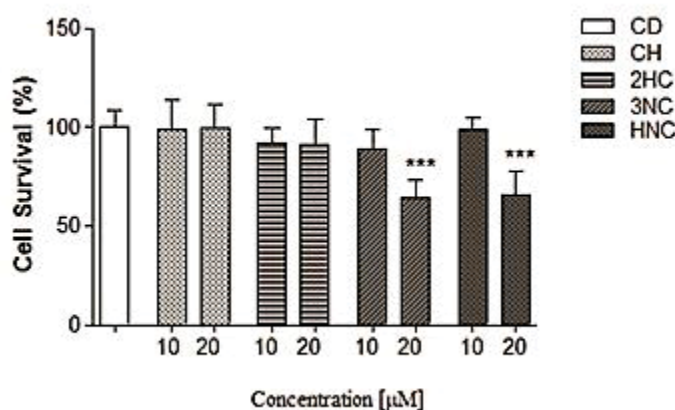


**FIGURE 1.** Chemical structure of the chalcones (A) and cytotoxic effect of chalcones on HeLa cells assessed by MTT assay (B). The results are

expressed as a percentage of cells in relation to the control (CD, MEM with 0.1% of DMSO) and represent the mean  $\pm$  standard deviation of three independent experiments performed in triplicate. \*\*\* $p < 0.001$ .

Figure 2 shows the effect of increasing concentrations of HNC on cell viability after 24 hours of incubation. HNC reduced the viability in a dose-dependent manner. At higher concentrations (30 and 50  $\mu\text{M}$ ) the reduction was around 67 and 87%, respectively, yielded an  $\text{IC}_{50} = 24 \mu\text{M}$ . These results were similar with the cell counting using PI and analyzed by flow cytometry (data not showed).

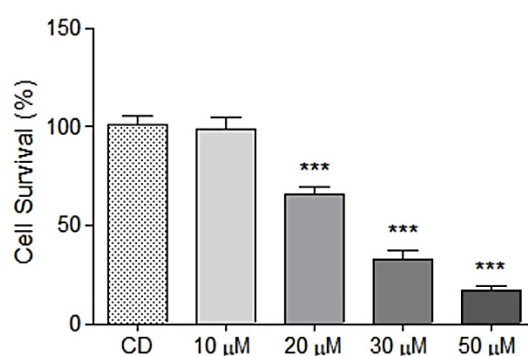


**FIGURE 2. Cytotoxic effect of HNC on HeLa cells assessed by MTT assay.** Results are expressed as a percentage of the control exposed to MEM with 0.1% of DMSO (CD) and represent the mean  $\pm$  standard deviation of three independent experiments performed in triplicate, \*\*\* $p < 0.001$ .

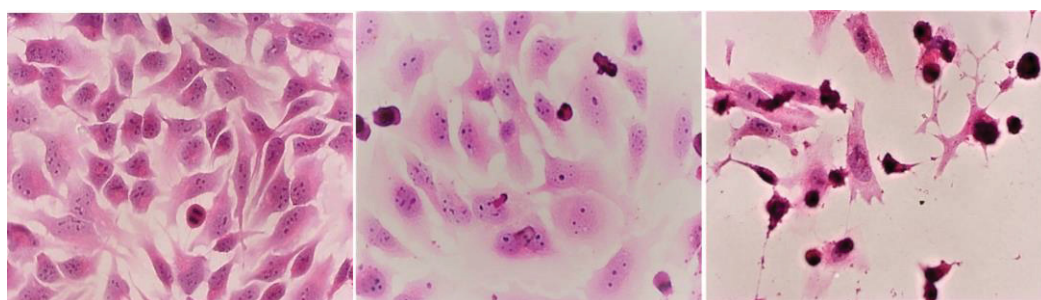
We also conducted the microscopic analyses of cells incubated with HNC and stained with hematoxylin and eosin. Figure 3A shows the light-field images of control cells forming a semi-confluent monolayer and displaying their typical elongated triangular morphology. The images of the cells treated with HNC at the concentrations of 20 and 30  $\mu\text{M}$ , show a dose-dependent reduction in the cellular volume and the appearance of an increased number of cells with hypercondensed chromatin and rounded morphology. Additionally, we also performed microscopic examination of cells exposed to the same concentrations of HNC using the membrane-impermeant dye PI to stain the nucleus of cells with loss of the membrane integrity. The fluorescence micrographs in the Figure 3B demonstrated that in a concentration-dependent manner, HNC also provoked loss of membrane integrity shown by the entry of the PI (red fluoresce).

**A**

CD

HNC 20  $\mu\text{M}$

HNC 30  $\mu\text{M}$



**B**

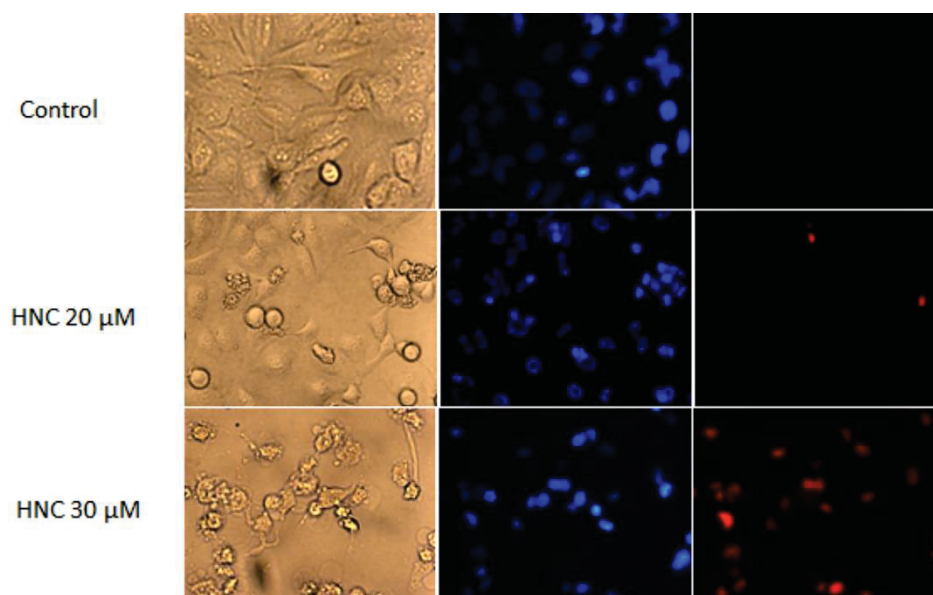


**FIGURE 3. Morphological changes induced by HNC in HeLa cells.** Bright field micrographs of HeLa cells incubated for 24 hours with HNC (20 and 30  $\mu\text{M}$ ) or with vehicle control and stained with H & E (magnification:  $\times 200$ ) (A). Fluorescence micrographs of HeLa cells incubated for 24 hours with HNC (20 and 30  $\mu\text{M}$ ), or vehicle control and posteriorly stained with Hoechst and PI (blue and red fluorescence, respectively) (magnification:  $\times 200$ ). The images were captured with a Zeiss LSM 410 microscope coupled to a UV lamp and are representative of at least two independent experiments (B).

### 6.3.2 Effects of HNC on cell cycle

Previous studies have associated the effects of some chalcones on tumoral cells with their capacity to activate checkpoints involved in proliferation control, generating cell cycle arrest<sup>41–43</sup>. In order to verify anti-proliferative activity, we assessed by flow cytometry the effect of HNC on the cell cycle distribution based on the cellular DNA content. As shown in Figure 4D, the exposure for 24 hours to HNC 20 (B) and 30  $\mu\text{M}$  (C) did not significantly increase the percentages of cells distributed into the populations G0/G1, S, and

G2/M, when compared to the cells incubated with vehicle control (Figure 4A). However, both treatments produced an approximately two-fold increase in the percentage of hypodiploid cells ("sub-G1" population) (4E), which is indicative of chromatin fragmentation.

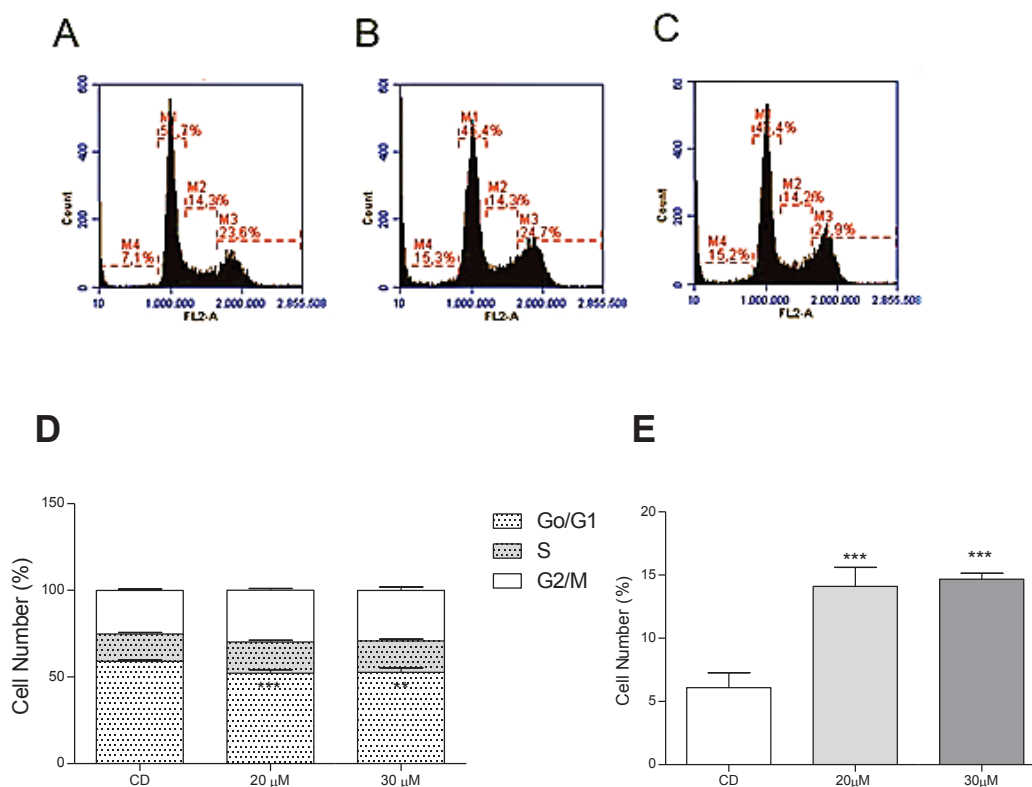


**FIGURE 4. Analysis by flow cytometry of the effect of HNC on the HeLa cell cycle.** HeLa cells were incubated for 24 hours with vehicle control (A) or with HNC at the concentrations 20 (B) and 30  $\mu$ M (C). Results in bars of three independent experiments (D), percentage of cells in sub G1 (E). The results are expressed as a percentage of the CD as the mean  $\pm$  standard deviation of three independent experiments, \*\*p < 0.01 and \*\*\*p < 0.001.

### 6.3.3 Annexin V-FITC/Propidium iodide double labeling assay

Based on the above results, we decided to assess if apoptosis could be the cell death mechanism induced by HNC. Phosphatidylserine externalization is an early event widely considered as an apoptosis marker and is detected using annexin V-FICT. Figure 5 shows that the rate of apoptosis (annexin  $^{+}$  / PI  $^{-}$ ) in cells incubated with vehicle control was 3.2%, while the rates for cells exposed to HNC 20 and 30  $\mu$ M were  $\sim$  13% and  $\sim$  7%, respectively. In addition, both concentrations significantly increased the percentage of double-labeled cells (annexin-V+/PI+) reaching 58% (20  $\mu$ M) and 45% (30  $\mu$ M). Importantly, both



concentrations also increased the percentage of cells positive to PI and negative to annexin (annexin-V-/PI+) in 7% (20  $\mu$ M) and 11% (30  $\mu$ M).

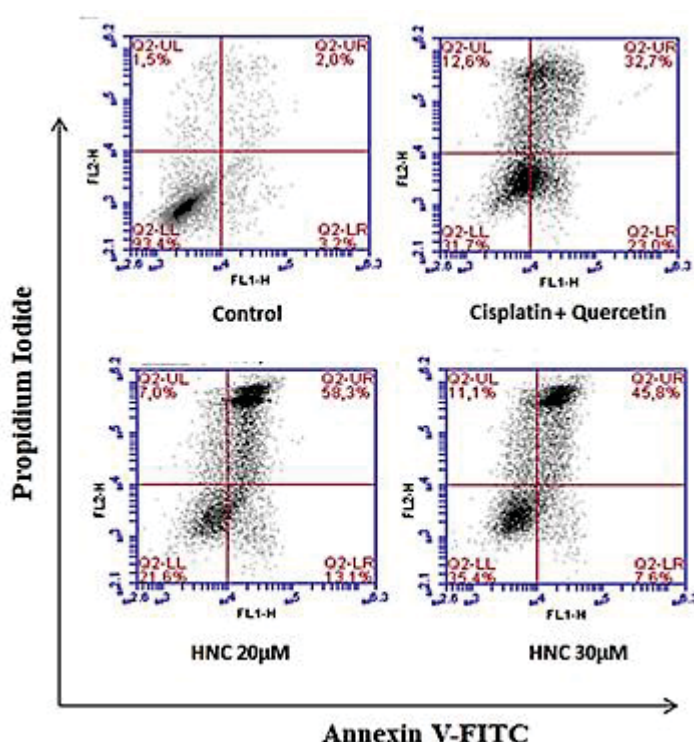


**FIGURE 5. Flow cytometry analysis of cell death by Annexin v and PI staining.** HeLa cells were incubated for 24 hours with vehicle control (MEM with DMSO (0.1%)), HNC (20 and 30  $\mu$ M) or with a mixture of quercetin (50  $\mu$ M) with cisplatin (10  $\mu$ M) (positive control to apoptosis) and subsequently incubated with Annexin V-FITC and PI. The data are representative results of three independent experiments.

#### 6.3.4 Effect of HNC on the ROS levels

Since several chalcones are well known inducers of ROS in many cells, the capacity of HNC to increase the intracellular concentration of ROS in HeLa cells was assessed. The results of Figure 6 show that after 24 hours of exposure to HNC at the concentration of 20  $\mu$ M, no differences existed when compared with the control cells; however, at the concentration of 30  $\mu$ M there was a significant increase in the ROS levels of approximately 2.3 times.

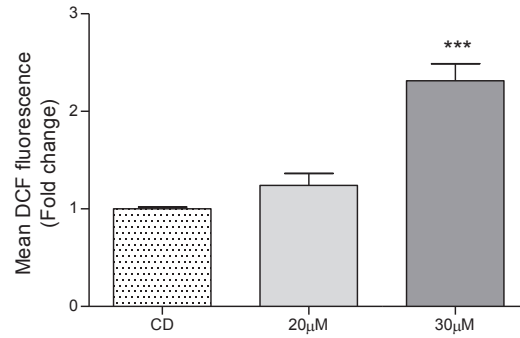


**FIGURE 6. Effect of HNC in the cellular levels of ROS.** HeLa cells were incubated for 24 hours with HNC at the indicated concentrations or with vehicle control (CD) and posteriorly with DCFH-DA to ROS detection. The results are expressed as a percentage of the control and expressed as the mean  $\pm$  standard deviation of three independent experiments performed in triplicate, \*\*\* $p < 0.001$ .

Due to a ROS accumulation could be either cause or consequence of cell death and given the relevance of GSH in keeping the cellular redox equilibrium, we evaluated the effect of HNC on the viability of cells with modulated concentrations of GSH. For this purpose, HeLa cells were incubated for two hours with BSO (a GSH synthesis inhibitor) or NAC (a GSH precursor and free radical-scavenging agent) and subsequently exposed to increasing concentrations of HNC. Figure 7A shows that the pretreatment with BSO sensitized the cells and increased the effect of HNC at the concentrations of 10 and 20  $\mu$ M. When HNC was used at 30 and 50  $\mu$ M, no differences were observed. On the other hand, the NAC pre-incubation provided no decrease in the effect of HNC (7B).

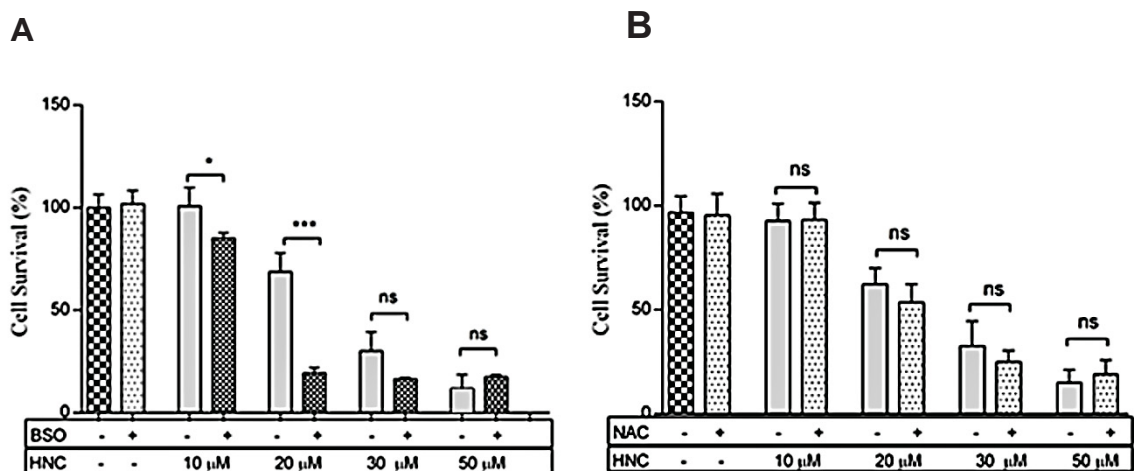




**FIGURE 7. Cytotoxic effect of HNC in cells preincubated with BSO and NAC.** HeLa cells were pre-incubated with BSO (100  $\mu$ M) (A) or NAC 10mM for 2 h and posteriorly incubated for 24 h with HNC at the indicated concentrations or with vehicle control. The results are expressed as a percentage of the control and expressed as the mean  $\pm$  standard deviation of three independent experiments performed in triplicate; \*p <0.05; \*\*\*p <0.001.

### 6.3.5 Effect of HNC on the reduced GSH levels

To ascertain whether HNC could modify the intracellular concentrations of GSH, we used the probe monochlorobimane (mBCI), which reacts with reduced glutathione yielding a blue fluorescent adduct. The micrographs of Figure 8 show that HNC at the concentration of 20  $\mu$ M did not induce evident alterations in the GSH level compared to the control cells. In contrast, the cells treated with HNC at the concentration of 30  $\mu$ M there was a marked reduction in the GSH content.

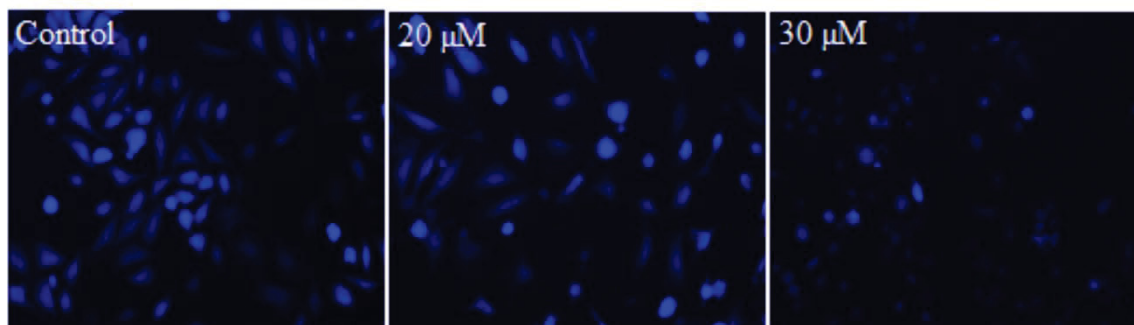
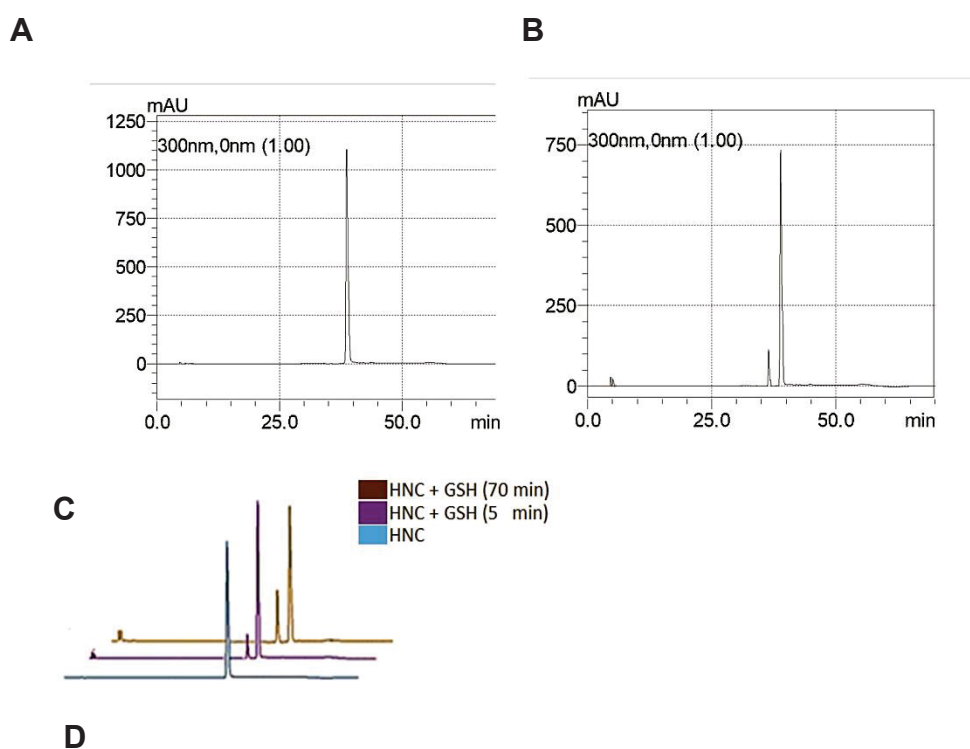


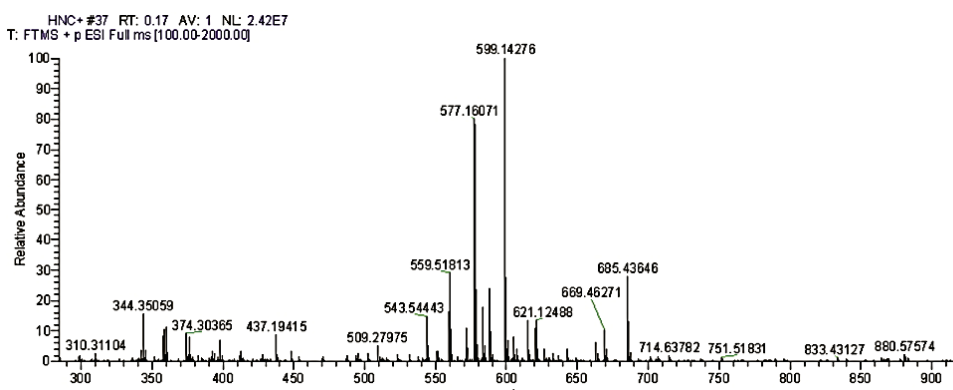
**FIGURE 8. EFFECT OF HNC ON INTRACELLULAR CONCENTRATION OF REDUCED GSH.** HeLa cells were incubated for 24 hours HNC (20 and 30  $\mu$ M) or vehicle control and posteriorly incubated with monochlorobimane (10  $\mu$ M) for 10 minutes. Fluorescence images were captured using the UV filter for the detection of the adduct GSH-mbcl (Ex./Em = 380nm / 461nm). (magnification  $\times$ 200). The images are representative of three independent experiments..

### 6.3.6 Formation of adduct between HNC and GSH

Due to the chemical addition between GSH and chalcones is one of the mechanisms that could decrease the concentration of reduced glutathione, we decided to verify if this reaction could explain the reduction in the GSH concentration. First, we conducted an analysis to characterize the product of the reaction between GSH and HNC in a free-cell system. The chromatogram of Figure 9A shows that the HNC yields a peak with a retention time of 38.5 minutes. Figure 9B shows the chromatogram of the HNC and GSH mixture, which reveals a new peak with a lower  $t_R$  (36.1 min), which suggests the

formation of an adduct. Furthermore, as a function of incubation time, the intensity of this peak increased and a concomitant reduction of the HNC peak was observed (9C). To verify the chemical identity of this product, we isolated this compound by RP-HPLC and posteriorly analyzed it by mass spectrometry. Figure 9D shows the mass spectrum of this compound exhibiting a molecular ion at  $m/z$  577.16  $[M + H]^+$ , which is consistent with the mass calculated from the reactants HNC (MW 270) and GSH (MW 306). The next step was to verify the formation of this adduct at the cellular level. The analysis of the cell extracts after 24 h of incubation with HNC (30  $\mu$ M) did not reveal the presence of the adduct (data not shown). In contrast, as shown in the chromatogram in Figure 9E, when the cells were incubated with HNC for 15 minutes, a peak consistent with the chromatographic characteristic of the adduct appeared. Interestingly, from 70 until 280 minutes of incubation there was no further accumulation of the adduct in the cells.





E

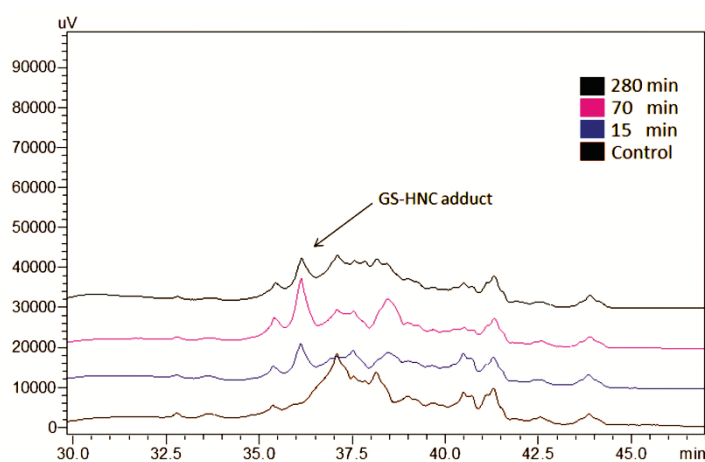


**FIGURE 9. CHARACTERIZATION OF ADDUCTS BETWEEN HNC AND GSH USING HPLC AND MASS SPECTROMETRY.** Chromatograms of a solution 30  $\mu$ M of HNC prepared in PBS (0.1% DMSO) (A) or mixed with GSH 5 mM (B). Comparison of the chromatograms of HNC with GSH mixture incubated by 5 and 70 min (C). Mass Spectrum of the product of the reaction between GSH and HNC (D). Representative stack chromatograms at 254 nm of methanolic cells extracts obtained from cell incubated with vehicle control or treated by 5, 70 and 280 min with HNC 30  $\mu$ M (E).

### 6.3.7 Influence of the overexpression of MRP1 transporters in the HNC effect

MRP1 (ABCC1) is a type of transporter involved in the efflux of many endogens an exo/exogens substrates conjugated with GSH. Since this mechanism could be a possible explanation to the reduction of the intracellular concentration of the adduct, we assessed whether the effects of HNC on the viability of BHK21 cells that overexpress MRP1 (BHK21-MRP1) are lower than wild cells (BHK21). The results in the Figure 10, shows that HNC induced a comparable reduction in the cell viability in both wild-type and in BHK21-MRP1.

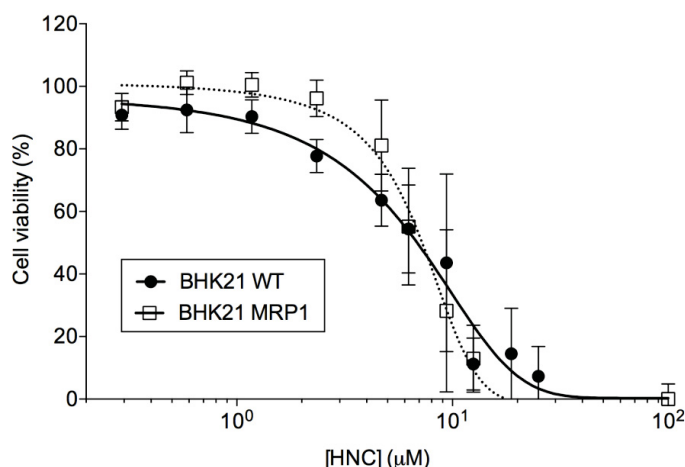


**Figure 10. Cytotoxic effect of HNC in BHK21-MRP1 and BHK21 cells**

Cell viability of BHK21-MRP1 and BHK21 wild type cells was determined upon treatment for 48 h with HNC. The values represent the mean  $\pm$  SD of percent cell viability with respect to the untreated control. Data are the mean  $\pm$  SD of five independent experiments.

#### 6.4. Discussion

In this study, we describe for the first time the effects of the bifunctionalized chalcone 2'-hydroxy-3-nitrochalcone (HNC) in HeLa cells. The functional groups used in this molecule have a documented capacity to alter the redox equilibrium and induce toxic effects in various types of tumor cells<sup>19,44</sup>. In the range of concentrations used, our results show that the inclusion of the substituent hydroxyl in the chalcone backbone did not improve the toxic effect of the chalcone toward HeLa cells. This result is not unexpected in view of the well-known hormetic effect of several chalcones, exhibiting toxicity only at relatively high doses, and acting as cytoprotectives at low concentrations<sup>45,46</sup>. On the other hand nitrated chalcones (3NC and HNC) in low doses are capable of reducing cell viability after 24 hours of incubation in HeLa cells. These results indicate that the increased effect of HNC could be principally attributed to the nitro substituent.

HNC, dependent on dose, provoked reduction in cell viability, accompanied by morphological alterations strongly suggestive of cytotoxic effects. The increase in the number of hypodiploid cells and the externalization of phosphatidylserine, which are events related to the activation of caspases<sup>47,48</sup>, suggest that the cell death mechanism induced by HNC could be apoptosis. However, other analyses are necessary to confirm these preliminary results.

Since several nitroaromatic drugs are well-known inducers of oxidative stress in many cells, we decided verify whether the toxic effect of our compound on HeLa cells could be correlated to the elevation in levels of ROS. An increase in the ROS levels and a reduction in the concentration of GSH were exhibited when the cells were incubated with a concentration of 30  $\mu\text{M}$  of HNC. Interestingly, when the cells were exposed to 20  $\mu\text{M}$  of HNC, they did not exhibit ROS increase or a reduction in the GSH content. Considering that this HNC concentration reduced the viability by 23%, this result suggests that the toxicity of our compound to HeLa cells could be, at least in part, independent of an increase in ROS levels. Additionally, when the cells were pre-incubated with NAC, no protective effect against HNC (20-50  $\mu\text{M}$ ) was found. These results further suggest that reduction of cell viability induced by HNC might be associated with another alternative mechanism. The electrophilic characteristic of chalcones explains their chemical reactivity toward thiol groups located in several of their targets. Our experiments in a cell-free system confirmed that the reaction of HNC with GSH could take place in an enzyme-independent manner. However, in a cellular context the inactivation of diverse electrophiles by conjugation with GSH largely relies on enzymes of the glutathione-S transferases family (GST), which play a critical role in the detoxification mechanisms <sup>49</sup>. In our experiments, the appearance of the adduct (HNC-GS) in cell lysates was detected as soon as 15 minutes after exposure to HNC, however, interestingly, from 70 minutes of incubation we did not find a trend toward further intracellular accumulation. One possible explanation could be that followed by an initial conjugation of HNC catalyzed by GST, the progressive increase in the intracellular concentration of HNC could affect the activity of GST preventing additional conjugation. Furthermore, hydroxylated chalcones such as 2-hydroxychalcone and 2',3,4,4'-tetrahydroxychalcone have shown potent inhibitory activity toward GST, which is reflected in their  $\text{IC}_{50}$  values in the low micromolar range (6.7 and 9  $\mu\text{M}$ , respectively) <sup>50,51</sup>.

In line with this hypothesis, the ineffectiveness of the NAC pretreatment to protect the cells against HNC was verified in our experiments, and could also be explained by the incapacity of the inhibited GST to conjugate and inactivate HNC, despite the increased GSH levels induced by NAC.

Importantly, the detoxification of electrophiles through this pathway relies on the concerted action of both GST and MRP1 transporters, which ultimately mediate the efflux of the conjugates. Furthermore, conditions that affect the GST activity makes this enzyme rate-limiting and can prevent the detoxification process, even in MRP1 overexpressing cells <sup>52,53</sup>. Thus, whether HNC could act as a GST inhibitor, the loss of the capacity of the cells to conjugate the chalcone could be an explanation for the equal sensitivity toward HNC exhibited by both BHK21 wild-type cells and BHK21 overexpressing MRP1.

Previous studies have also shown the potential of several derivatives of 2'-hydroxychalcone to deplete GSH by promoting their efflux through MRP1 transporters, and thus, sensitized the cells to several drugs <sup>54</sup>. In our experiments, the pre-incubation of HeLa cells with the GSH synthesis inhibitor BSO revealed that the reduction in the cellular levels of GSH turns HNC into a compound with higher toxicity. Based on this observation and on the fact that the overexpression of MRP1 in BHK21 did not provoke an increased toxicity, it is also possible that HCN does not promote the GSH efflux. Together these results could indicate that the reduction in the concentration of reduced GSH observed in the cells treated with HNC at 30  $\mu$ M apparently could not be related to GSH efflux or conjugation, but could be associated to oxidation by the increase in ROS levels.

Aside from their roles in detoxification mechanisms, GST is also involved in the regulation of cell signaling pathways such as JNK (Jun N-terminal kinases). The mammalian JNKs belong to the superfamily of mitogen activated protein kinases (MAP kinases) that, in response to different stimulus, can activate opposite responses, such as proliferation or cell death <sup>55</sup>. GST has showed anti-apoptotic activity through their ability to inhibit JNK by forming a heterocomplex GST-JNK <sup>56</sup>. Interestingly, some inhibitors of GST, some of them nitrated (eg. 7-nitrobenzodiazol derivatives), have shown the capacity to prevent the formation of this complex, triggering the activation of JNK/c-Jun-mediated pathway and inducing apoptosis even in the absence of an additional stressor, such as ROS <sup>57,58</sup>.

Obviously, the identification of the precise mechanism whereby HNC induce cell death, as well as the verification that GST is a possible target of our compound will require additional assays.

## 6.5. Conclusion

Despite several reports demonstrating the antitumoral potential of chalcone derivatives, very few studies were conducted to define the precise contribution of their cytotoxic effects. In this study, for the first time, we demonstrated that a chalcone derivative, HNC, carrying the hydroxyl and the nitro substituents produce remarkable toxic effects on HeLa cells. When comparing with the effects of the unfunctionalized and hydroxylated derivatives, the increased cytotoxicity can be attributed to the nitro group. Despite the reported pro-oxidant potential of the nitroaromatic drugs, our results suggest that the induction of oxidative stress could not represent the main mechanism that explains the effects of HNC in HeLa cells. However further studies are needed to assess potential additional mechanisms of bioactivation of the nitro group, as well as to verify their effect on the intrinsic properties of the chalcone backbone.

Although it is difficult at this point to determine if GST is a potential target of HNC, some of our experiments provide clues that prompted us to further explore this hypothesis due to the importance of GST inhibitors in the development of new chemotherapeutics.

Therefore, HNC could be a promising adjuvant in cancer treatment since its cytotoxic effect is not reduced even in cells that overexpress MRP1. Moreover, additional studies are needed, but these results open up new possibilities to investigate this nitrochalcone derivative as an anticancer drug.

## Conflicts of interest

The authors declare that they have no conflicts of interest.

## Acknowledgments

Grant support was provided by Coordenação de Aperfeiçoamento de Pessoal de Nível Superior – CAPES, FINEP (CT-Infra), Conselho Nacional de Pesquisa Científica – CNPq (Process: 311629/2013-0 and 310107/2015-6), and INCT Redoxoma (Process 573530/2008-4). The financial support organizations had no role in the study design, data collection and analysis, decision to publish, or preparation of the manuscript. The authors would also like to thank Dr. Guilherme L. Sasaki, Dr. Lauro Mera de Souza and the UFPR-RMN Center for



the mass spectrometry analyses. We are also grateful for the National Institute of Science and Technology of Biological Nitrogen Fixation (INCT-FBN) and Dr. Emanuel Maltempi de Souza for providing access to the flow cytometer. We are also grateful to Dra. Fabiane Gomes de Moraes Rego of the Graduate Program in Pharmaceutical Sciences for the use of the laboratory and reagents for MRP1 analysis.

## 6.6. References

1. Padhye S, Ahmad A, Oswal N, et al. Fluorinated 2'-hydroxychalcones as garcinol analogs with enhanced antioxidant and anticancer activities. *Bioorganic Med Chem Lett*. 2010;20(19):5818-5821. doi:10.1016/j.bmcl.2010.07.128.
2. Chen YH, Wang WH, Wang YH, Lin ZY, Wen CC, Chern CY. Evaluation of the anti-inflammatory effect of chalcone and chalcone analogues in a Zebrafish model. *Molecules*. 2013;18(2):2052-2060. doi:10.3390/molecules18022052.
3. Lee DH, Jung Y, Koh D, Lim Y, Lee YH, Shin SY. A synthetic chalcone, 2'-hydroxy-2,3,5'-trimethoxychalcone triggers unfolded protein response-mediated apoptosis in breast cancer cells. *Cancer Lett*. 2016;372(1):1-9. doi:10.1016/j.canlet.2015.12.017.
4. Zhang B, Duan D, Ge C, et al. Synthesis of xanthohumol analogues and discovery of potent thioredoxin reductase inhibitor as potential anticancer agent. *J Med Chem*. 2015;58(4):1795-1805. doi:10.1021/jm5016507.
5. Martel-Frchet V, Keramidas M, Nurisso A, et al. IPP51, a chalcone acting as a microtubule inhibitor with *in vivo* antitumor activity against bladder carcinoma. *Oncotarget*. 2015;6(17):14669-14686. doi:10.18632/oncotarget.4144.
6. Orlikova B, Tasdemir D, Golais F, Dicato M, Diederich M. The aromatic ketone 4'-hydroxychalcone inhibits TNF  $\alpha$ -induced NF- $\kappa$ B activation via proteasome inhibition. *Biochem Pharmacol*. 2011;82(6):620-631. doi:10.1016/j.bcp.2011.06.012.
7. Park I, Park KK, Park JHY, Chung WY. Isoliquiritigenin induces G2 and M phase arrest by inducing DNA damage and by inhibiting the metaphase/anaphase transition. *Cancer Lett*. 2009;277(2):174-181.



- doi:10.1016/j.canlet.2008.12.005.
8. Kim SH, Lee E, Baek KH, et al. Chalcones, inhibitors for topoisomerase  $\alpha$  and cathepsin B and L, as potential anti-cancer agents. *Bioorganic Med Chem Lett*. 2013;23(11):3320-3324. doi:10.1016/j.bmcl.2013.03.106.
  9. Gan F-F, Kaminska KK, Yang H, et al. Identification of Michael acceptor-centric pharmacophores with substituents that yield strong thioredoxin reductase inhibitory character correlated to antiproliferative activity. *Antioxid Redox Signal*. 2013;19(11):1149-1165. doi:10.1089/ars.2012.4909.
  10. Perjési P, Maász G, Reisch R, Benko A. (E)-2-Benzylidenebenzocyclohexanones: Part VII. Investigation of the conjugation reaction of two cytotoxic cyclic chalcone analogues with glutathione: An HPLC-MS study. *Monatshefte für Chemie*. 2012;143(8):1107-1114. doi:10.1007/s00706-012-0768-7.
  11. Dinkova-Kostova AT, Abeygunawardana C, Talalay P. Chemoprotective properties of phenylpropenoids, bis(benzylidene)cycloalkanones, and related Michael reaction acceptors: Correlation of potencies as phase 2 enzyme inducers and radical scavengers. *J Med Chem*. 1998;41(26):5287-5296. doi:10.1021/jm980424s.
  12. Amslinger S, Al-Rifai N, Winter K, Wörmann K, Scholz R, Wild PB and M. Reactivity Assessment of Chalcones by a Kinetic Thiol Assay. *Org Biomol Chem*. 2012;2-5. doi:10.1039/b000000x.
  13. Maydt D, De Spirt S, Muschelknautz C, Stahl W, Müller TJJ. Chemical reactivity and biological activity of chalcones and other  $\alpha,\beta$ -unsaturated carbonyl compounds. *Xenobiotica*. 2013;43(8):711-718. doi:10.3109/00498254.2012.754112.
  14. Raghav N, Garg S. SAR studies of o-hydroxychalcones and their cyclized analogs and study them as novel inhibitors of cathepsin B and cathepsin H. *Eur J Pharm Sci*. 2014;60:55-63. doi:10.1016/j.ejps.2014.04.006.
  15. Saydam N, Kirb A, Hazanc E, Giinep G. Determination of glutathione , glutathione reductase , glutathione peroxidase and glutathione S-transferase levels in human lung cancer tissues. 1997;119:13-19.
  16. Arabia S. Cancer and Phase II Drug-Metabolizing Enzymes. 2003:45-58.
  17. Chin Chung M, Longhin Bosquesi P, Leandro dos Santos J. A Prodrug

- Approach to Improve the Physico-Chemical Properties and Decrease the Genotoxicity of Nitro Compounds. *Curr Pharm Des.* 2011;17:3515-3526. doi:10.2174/138161211798194512.
18. Meanwell NA. Synopsis of some recent tactical application of bioisosteres in drug design. *J Med Chem.* 2011;54(8):2529-2591. doi:10.1021/jm1013693.
  19. Mai CW, Yaeghoobi M, Abd-Rahman N, Kang YB, Pichika MR. Chalcones with electron-withdrawing and electron-donating substituents: Anticancer activity against TRAIL resistant cancer cells, structure-activity relationship analysis and regulation of apoptotic proteins. *Eur J Med Chem.* 2014;77:378-387. doi:10.1016/j.ejmech.2014.03.002.
  20. Patterson S, Wyllie S. Nitro drugs for the treatment of trypanosomatid diseases: Past, present, and future prospects. *Trends Parasitol.* 2014;30(6):289-298. doi:10.1016/j.pt.2014.04.003.
  21. Squella JA, Bollo S, Nunez-Vergara LJ. Recent Developments in the Electrochemistry of Some Nitro Compounds of Biological Significance. *Curr Org Chem.* 2005;9:565-581. doi:10.2174/1385272053544380.
  22. Zhang C, Liu K, Yao K, et al. HOI-02 induces apoptosis and G2-M arrest in esophageal cancer mediated by ROS. *Cell Death Dis.* 2015;6:e1912. doi:10.1038/cddis.2015.227.
  23. Amslinger S, Al-Rifai N, Winter K, Wörmann K, Scholz R, Wild PB and M. Reactivity assessment of chalcones by a kinetic thiol assay. *Org Biomol Chem.* 2012;2-5. doi:10.1039/b000000x.
  24. Jin YL, Jin XY, Jin F, Sohn DH, Kim HS. Structure activity relationship studies of anti-inflammatory TMMC derivatives: 4-Dimethylamino group on the B ring responsible for lowering the potency. *Arch Pharm Res.* 2008;31(9):1145-1152. doi:10.1007/s12272-001-1281-7.
  25. Sabzevari O, Galati G, Moridani MY, Siraki A, O'Brien PJ. Molecular cytotoxic mechanisms of anticancer hydroxychalcones. *Chem Biol Interact.* 2004;148(1-2):57-67. doi:10.1016/j.cbi.2004.04.004.
  26. Trachootham D, Alexandre J, Huang P. Targeting cancer cells by ROS-mediated mechanisms: a radical therapeutic approach? *Nat Rev Drug Discov.* 2009;8(7):579-591. doi:10.1038/nrd2803.
  27. Zhang L, Li J, Zong L, et al. Reactive Oxygen Species and Targeted

- Therapy for Pancreatic Cancer. *Oxid Med Cell Longev*. 2016;2016:1616781. doi:10.1155/2016/1616781.
28. Galadari S, Rahman A, Pallichankandy S, Thayyullathil F. Reactive oxygen species and cancer paradox: To promote or to suppress? *Free Radic Biol Med*. 2017;104(December 2016):144-164. doi:10.1016/j.freeradbiomed.2017.01.004.
  29. WHO. Cervical cancer.
  30. SOCIETY AC. Cervical cancer survival.
  31. Astolfi L, Ghiselli S, Guaran V, et al. Correlation of adverse effects of cisplatin administration in patients affected by solid tumours: A retrospective evaluation. *Oncol Rep*. 2013;29(4):1285-1292. doi:10.3892/or.2013.2279.
  32. Chan JK, Brady MF, Penson RT, et al. Weekly vs. Every-3-Week Paclitaxel and Carboplatin for Ovarian Cancer. *N Engl J Med*. 2016;374(8):738-748. doi:10.1056/NEJMoa1505067.
  33. Tsuchiya Y, Ushijima K, Noguchi T, et al. Influence of a dosing-time on toxicities induced by docetaxel, cisplatin and 5-fluorouracil in patients with oral squamous cell carcinoma; a cross-over pilot study. *Chronobiol Int*. 2017;0(0):1-6. doi:10.1080/07420528.2017.1392551.
  34. Robati M, Holtz D, Dunton CJ. A review of topotecan in combination chemotherapy for advanced cervical cancer. *Ther Clin Risk Manag*. 2008;4(1):213-218.
  35. National Cancer Institute. Cervical cancer treatment. [https://www.cancer.gov/types/cervical/hp/cervical-treatment-pdq#link/\\_605](https://www.cancer.gov/types/cervical/hp/cervical-treatment-pdq#link/_605). Published 2017. Accessed December 12, 2018.
  36. Mosmann T. Rapid colorimetric assay for cellular growth and survival: Application to proliferation and cytotoxicity assays. *J Immunol Methods*. 1983;65(1-2):55-63. doi:10.1016/0022-1759(83)90303-4.
  37. Liu Y, Xing H, Han X, et al. The mechanism of cisplatin-induced apoptosis in HeLa cells. *Chinese J Clin Oncol*. 2005;2(6):866-869. doi:10.1007/BF02789656.
  38. Zhao JL, Zhao J, Jiao HJ. Synergistic growth-suppressive effects of quercetin and cisplatin on HepG2 human hepatocellular carcinoma cells. *Appl Biochem Biotechnol*. 2014;172(2):784-791. doi:10.1007/s12010-013-

0561-z.

39. Chatterjee S, Noack H, Possel H, Keilhoff G, Wolf G. Glutathione levels in primary glial cultures: Monochlorobimane provides evidence of cell type-specific distribution. *Glia*. 1999;27(2):152-161. doi:10.1002/(SICI)1098-1136(199908)27:2<152::AID-GLIA5>3.0.CO;2-Q.
40. Sebastia J, Cristofol R, Martin M, Rodriguez-Farre E, Sanfeliu C. Evaluation of fluorescent dyes for measuring intracellular glutathione content in primary cultures of human neurons and neuroblastoma SH-SY5Y. *Cytom A*. 2003;51(1):16-25. doi:10.1002/cyto.a.10003.
41. Hsu YL, Kuo PL, Tzeng WS, Lin CC. Chalcone inhibits the proliferation of human breast cancer cell by blocking cell cycle progression and inducing apoptosis. 2006;44:704-713. doi:10.1016/j.fct.2005.10.003.
42. Hsu YL, Chia CC, Chen PJ, Huang SE, Huang SC, Kuo PL. Shallot and licorice constituent isoliquiritigenin arrests cell cycle progression and induces apoptosis through the induction of ATM/p53 and initiation of the mitochondrial system in human cervical carcinoma HeLa cells. *Mol Nutr Food Res*. 2009;53(7):826-835. doi:10.1002/mnfr.200800288.
43. Rozmer Z, Berki T, Perjési P. Different effects of two cyclic chalcone analogues on cell cycle of Jurkat T cells. *Toxicol Vitro*. 2006;20(8):1354-1362. doi:10.1016/j.tiv.2006.05.006.
44. Kachadourian R. Flavonoid-induced glutathione depletion: Potential implications for cancer treatment. *Free Radic Biol Med*. 2006;41(1):65-76. doi:10.1016/j.freeradbiomed.2006.03.002.Flavonoid-induced.
45. Calabrese EJ. Cancer Biology and Hormesis: Human Tumor Cell Lines Commonly Display Hormetic (Biphasic) Dose Responses. *Crit Rev Toxicol*. 2005;35(6):463-582. doi:10.1080/10408440591034502.
46. Son TG, Camandola S, Mattson MP. Hormetic Dietary Phytochemicals. *Neuromolecular Med*. 2008;10(4):236-246. doi:10.1007/s12017-008-8037-y.
47. Wolf BB, Schuler M, Echeverri F, Green DR. Caspase-3 is the primary activator of apoptotic DNA fragmentation via DNA fragmentation factor-45/inhibitor of caspase-activated DNase inactivation. *J Biol Chem*. 1999;274(43):30651-30656. doi:10.1074/jbc.274.43.30651.
48. Mariño G, Kroemer G. Mechanisms of apoptotic phosphatidylserine

- exposure. *Cell Res.* 2013;23(11):1247-1248. doi:10.1038/cr.2013.115.
49. Townsend DM, Tew KD. The role of glutathione- S -transferase in anti-cancer drug resistance. 2003;7369-7375. doi:10.1038/sj.onc.1206940.
  50. Zhang K, Ping K, Chow P. Conjugation of chlorambucil with GSH by GST purified from human colon adenocarcinoma cells and its inhibition by plant polyphenols. 2003;72:2629-2640. doi:10.1016/S0024-3205(03)00173-5.
  51. Zhang KAI, Das NP. Inhibitory effects of plant polyphenols on rat liver glutathione s-transferases. *Biochem Pharmacol.* 1994;47(11):2063-2068.
  52. Morrow CS, Smitherman PK, Diah SK, Schneider E, Townsend AJ. Coordinated Action of Glutathione S-Transferases ( GSTs ) and Multidrug Resistance Protein 1 ( MRP1 ) in Antineoplastic. *Biochemistry.* 1998;273(32):20114-20120.
  53. Sibhatu MB, Smitherman PK, Townsend AJ, Morrow CS. Expression of MRP1 and GSTP1-1 modulate the acute cellular response to treatment with the chemopreventive isothiocyanate, sulforaphane. *Carcinogenesis.* 2008;29(4):807-815. doi:10.1093/carcin/bgn013.
  54. Kachadourian R. Flavonoid-induced glutathione depletion: Potencial implications for cancer treatment. *Free Radic Biol Med.* 2014;41(1):65-76. doi:10.1016/j.freeradbiomed.2006.03.002.Flavonoid-induced.
  55. Dhanasekaran DN, Reddy EP. JNK-signaling : A multiplexing hub in programmed cell death. 2017;8(September).
  56. Asakura T, Sasagawa A, Takeuchi H, et al. Conformational change in the active center region of GST P1-1, due to binding of a synthetic conjugate of DXR with GSH, enhanced JNK-mediated apoptosis. *Apoptosis.* 2007;12(7):1269-1280. doi:10.1007/s10495-007-0053-0.
  57. Turella P, Cerella C, Filomeni G, et al. Proapoptotic Activity of New Glutathione S -Transferase Inhibitors. 2005;(9):3751-3762.
  58. Laborde E. Glutathione transferases as mediators of signaling pathways involved in cell proliferation and cell death. *Cell Death Differ.* 2010;17(9):1373-1380. doi:10.1038/cdd.2010.80

## Capítulo 7: Considerações finais

## Capítulo 7. CONSIDERAÇÕES FINAIS

Vários são os exemplos de fármacos que possuem o grupo nitro (-NO<sub>2</sub>) na sua estrutura (PATTERSON & WYLLIE, 2014). Existem evidências de que algumas das moléculas nitradas usadas no tratamento de várias doenças se comportam como pró-drogas (PATTERSON & WYLLIE, 2014). Este grupamento tem sido utilizado também na síntese de alguns derivados de flavonóides na busca de modificar as suas propriedades biológicas (CÁRDENAS et al., 2006).

As chalconas podem ser sintetizadas e modificadas com relativa facilidade para obter derivados biologicamente ativos (GAONKAR; VIGNESH, 2017; LEÓN-GONZÁLEZ; AUGER; SCHINI-KERTH, 2015). As atividades citotóxicas de algumas chalconas podem ser observadas em concentrações que apresentam baixa toxicidade para células normais tornando estas moléculas fontes promissoras de novos medicamentos (LEE et al., 2016; MAI et al., 2014). Neste trabalho foram analisadas as propriedades pro-oxidantes e potenciais atividades antitumorais de chalconas nitradas e/ou hidroxiladas. Entre as chalconas estudadas duas se destacaram por seus efeitos citotóxicos sobre células HeLa que foram a 4NC e a HNC.

A 4NC reduziu a viabilidade de células HeLa de forma dependente da concentração. Foi possível observar uma rápida elevação dos níveis de EROs que poderia estar associado a este efeito citotóxico. Este aumento foi transitório, já que após 30 minutos de exposição à 4NC os níveis de EROs voltaram as condições basais, possivelmente porque a célula deve ter aumentado a expressão de suas enzimas antioxidantes como forma de defesa contra o dano oxidativo (LEÓN-GONZÁLEZ; AUGER; SCHINI-KERTH, 2015). Porém, apesar da curta duração esta elevação foi suficiente para produzir dano celular e morte. A importância do estresse oxidativo e da redução dos níveis de GSH na indução da morte celular induzida por 4NC pode ser demonstrada pelo aumento do efeito citotóxico desta chalcona com adição de BSO e pelo efeito protetor gerado pela pré-incubação com NAC, revertendo a elevação de EROs e diminuindo a citotoxicidade da 4NC.

A progressiva redução dos níveis de GSH verificada com a 4NC poderia ser consequência da oxidação pelo aumento de EROs ou pela formação de aduto entre 4NC e GSH. Em experimentos em sistema livre de célula foi observada a formação deste aduto. Contudo, em extratos de células incubadas com 4NC não foi possível detectar a formação deste aduto, possivelmente porque esta conjugação é



reversível, o que poderia provocar a sua decomposição durante as etapas de isolamento (ROZMER et al., 2014). Uma explicação alternativa poderia ser o efluxo do aduto da célula por sistemas de transporte (ex.: MRP1), que permitem a exclusão de compostos conjugados com GSH (WEEN et al., 2015). Verificou-se, contudo, que a 4NC promoveu morte celular mesmo em células que super-expressam o transportador MRP1 (BHK21 MRP1), podendo indicar que outro mecanismo pode também estar envolvido.

Em relação ao encapsulamento de 4NC em nanopartículas de PMMA funcionalizadas com AF, os resultados sugerem que a endocitose do receptor de folato dependente de caveolina estaria envolvido na internalização destas nanopartículas em células HeLa, as quais super-expressam esse receptor (FENG et al., 2013). Também foi possível observar que a 4NC encapsulada apresentou maior toxicidade do que a 4NC livre. Assim, 4NC em PMMA funcionalizado com AF é uma formulação promissora para a entrega de 4NC a estas células. Várias outras células tumorais super-expressam este receptor (SUDIMACK; LEE, 2000). Desta forma poderia se fazer a entrega de 4NC em especial para células que super-expressam esse receptor (KELEMEN, 2006), colaborando assim para evitar efeitos colaterais.

A avaliação do efeito da CH, 2CH, 3NC e HNC sobre a viabilidade de células HeLa permitiu verificar que, nas concentrações usadas, a presença do grupo nitro é mais eficiente do que o hidroxila para aumentar a toxicidade das chalconas. A ordem crescente desses valores de citotoxicidade foi:  $HNC \approx 3NC > 2CH \approx CH$ . Também foi possível verificar que a HNC apresenta efeito semelhante ao da 3NC, porém é mais hidrossolúvel, o que permitiu testar este composto em concentrações mais elevadas. Foi possível verificar que a HNC (10-50  $\mu M$ ), após 24 horas de incubação, também de forma dependente da concentração, reduz a viabilidade das células HeLa.

A HNC (30  $\mu M$ ) também promoveu a diminuição dos níveis de GSH. Porém, diferente do que aconteceu com 4NC, quando as células foram pré-incubadas com NAC e expostas a HNC não foram observadas diferenças nos efeitos citotóxicos, quando comparadas com as células sem pré-incubação. Contudo, quando foi adicionado BSO as células se tornaram mais sensíveis a HNC de forma semelhante ao observado com 4NC. Adicionalmente foi detectada, em sistema livre de células, a formação de aduto entre HNC e GSH, porém neste caso foi possível verificar a presença deste aduto também em extratos celulares após poucos minutos (15 min) de exposição à HNC. A concentração deste aduto aumentou até 70 minutos de



incubação. Porém, a partir deste tempo, não existiu acumulação adicional. Estes resultados sugerem que este conjugado poderia estar sendo transportado da célula por transportadores (ex: MRP1) ou a sua formação poderia estar sendo comprometida pela redução da atividade das enzimas GSTs, as quais catalisam a reação entre GSH e vários xenobióticos (PAUMI et al., 2001). De fato entre os inibidores desta enzima se encontram várias chalconas com hidroxilação na posição 2' (ZHANG; DAS, 1994). Adicionalmente, devido ao papel anti-apoptótico de GST (GSTP) através da inativação de MAP quinase JNK, a inibição da sua atividade poderia representar um mecanismo indutor de morte celular. Contudo, para esclarecer melhor se uma possível inibição da GST poderia explicar a redução da formação de aduto, assim como a indução da morte por HNC, novas análises estão sendo realizadas e resultados preliminares indicam que a HNC poderia inibir a atividade desta enzima (dados não mostrados).

Foi observado que chalconas hidroxiladas, em especial na posição 2' (como na HNC) e seus análogos, promovem colapso do potencial de membrana mitocondrial em mitocôndrias isoladas de fígado de rato (SABZEVARI et al., 2004). Não se poderia, portanto descartar a possibilidade da HNC promover efeitos mitocondriais semelhantes e que poderiam levar a promoção da morte celular por via intrínseca (Guzy et al., 2010), entretanto mais análises seriam necessárias para poder confirmar esta hipótese.

A detecção e o aumento da formação do aduto entre GSH e HNC no interior da célula sugerem que este processo poderia ser responsável, pelo menos em parte, pela redução de GSH e aumento de EROs. Porém, como não foi possível observar aumento de EROs na concentração de 20  $\mu$ M após 24h de incubação e a citotoxicidade não foi diminuída com a adição de NAC nesta concentração, possivelmente o aumento de EROs observado com a concentração 30  $\mu$ M poderia ser consequência da morte celular. De forma similar ao observado com a 4NC, a HNC promove citotoxicidade semelhante em células BHK21 que super-expressam o receptor MRP1 assim como células BHK21 selvagens. Este resultado indica que apesar da possibilidade do efluxo do aduto formado entre GSH e HNC, os efeitos sobre a indução de morte celular não foram reduzidos.

Desta forma pode-se verificar que as chalconas nitradas possuem a capacidade de reduzir os níveis de GSH, gerar efeitos pro-oxidantes e promover a

morte de células HeLa sendo assim, moléculas promissoras com potencial atividade antitumoral.

## Capítulo 8: Conclusões

## Capítulo 8: CONCLUSÕES

Em relação a 4-nitrochalcona (4NC) pode-se concluir que:

- Induz morte em células HeLa de forma dependente da concentração;
- Não provoca alteração na progressão do ciclo celular;
- Aumenta os níveis de EROs que colaboram, pelo menos em parte, para a indução da morte celular, o que foi demonstrado pela redução dos efeitos citotóxicos pela pré-incubação com NAC;
- Induz a diminuição de GSH que poderia ser explicada por oxidação, sem descartar a conjugação com 4NC.

Em relação a 4NC encapsulada em nanopartículas de PMMA funcionalizadas com AF concluiu-se que:

- Induz maior citotoxicidade do que a 4NC livre;
- O ácido fólico (AF) na superfície das nanopartículas promove a sua internalização celular, provavelmente por interagir com o receptor de folato encontrado superexpresso nas células HeLa, colaborando para entrega da 4NC e para seus efeitos citotóxicos.

Em relação a papel dos grupos hidroxila e nitro na toxicidade das chalconas,

- A presença do grupo 3-nitro na chalcona aumenta a toxicidade do composto;
- A introdução da hidroxila na posição 2' da 3-nitrochalcona não modificou o efeito citotóxico sobre as células HeLa, porém resulta num composto mais solúvel;
- O tipo de morte celular induzida por HNC possivelmente é por apoptose;
- O mecanismo de ação citotóxico do HNC possivelmente é independente, pelo menos em parte, da geração de EROs e de alterações nos níveis de GSH.
- 4NC e HNC não são transportados.

# Referências

## REFERÊNCIAS

- ADLER, V.; PINCUS, M. R. Effector Peptides from Glutathione-S-Transferase-pi Affect the Activation of jun by jun-N-Terminal Kinase. **Annals of Clinical and Laboratory Science**, v. 34, n. 1, p. 35–46, 2004.
- ALGECIRAS-SCHIMNICH, A. et al. Molecular Ordering of the Initial Signaling Events of CD95 Molecular Ordering of the Initial Signaling Events of CD95. v. 22, n. 1, p. 207–220, 2002.
- ALVAREZ-BERRÍOS, M. P.; VIVERO-ESCOTO, J. L. In vitro evaluation of folic acid-conjugated redox-responsive mesoporous silica nanoparticles for the delivery of cisplatin. **International Journal of Nanomedicine**, v. 11, p. 6251–6265, 2016.
- AMSLINGER, S. et al. Reactivity assessment of chalcones by a kinetic thiol assay. **Organic & Biomolecular Chemistry**, p. 2–5, 2012.
- ARLT, V. M. et al. Environmental pollutant and potent mutagen 3-nitrobenzantrone forms DNA adducts after reduction by NAD(P)H:quinone oxidoreductase and conjugation by acetyltransferases and sulfotransferases in human hepatic cytosols. **Cancer Research**, v. 65, n. 7, p. 2644–2652, 2005.
- BALLATORI, N. et al. Plasma membrane glutathione transporters and their roles in cell physiology and pathophysiology. **Mol Aspects Med.**, v. 30, p. 13–28, 2009.
- BATRA, P.; SHARMA, A. K. Anti-cancer potential of flavonoids: recent trends and future perspectives. **3 Biotech**, v. 3, n. 6, p. 439–459, 2013.
- BOELSTERLI, U. A et al. Bioactivation and hepatotoxicity of nitroaromatic drugs. **Current drug metabolism**, v. 7, n. 7, p. 715–727, 2006.
- BRAUN, K. et al. HPV18 E6 and E7 genes affect cell cycle, pRB and p53 of cervical tumor cells and represent prominent candidates for intervention by use peptide nucleic acids (PNAs). **Cancer Letters**, v. 209, n. 1, p. 37–49, 2004.
- BRECHBUHL, H. M. et al. Chrysin enhances doxorubicin-induced cytotoxicity in human lung epithelial cancer cell lines: The role of glutathione. **Toxicology and Applied Pharmacology**, v. 258, n. 1, p. 1–9, 2012.
- BRIGELIUS-FLOHÉ, R.; MAIORINO, M. Glutathione peroxidases. **Biochimica et Biophysica Acta journal**, v. 1830, n. 5, p. 3289–3303, 2013.
- CABRERA, M. et al. Identification of chalcones as in vivo liver monofunctional phase II enzymes inducers. **Bioorganic and Medicinal Chemistry**, v. 18, n. 14, p. 5391–5399, 2010.
- CADET, J. et al. Hydroxyl radicals and DNA base damage. **Mutation Research - Fundamental and Molecular Mechanisms of Mutagenesis**, v. 424, n. 1–2, p. 9–21, 1999.
- CAI, Z. et al. Plasma membrane translocation of trimerized MLKL protein is required for TNF-induced necroptosis. **Nature Cell Biology**, v. 16, n. 1, p. 55–65, 2014.
- CENAS, N. et al. Interactions of nitroaromatic compounds with the mammalian selenoprotein thioredoxin reductase and the relation to induction of apoptosis in human cancer cells. **Journal of Biological Chemistry**, v. 281, n. 9, p. 5593–5603, 2006.
- CHEN, J. et al. Downregulation of glutathione transferase  $\pi$  sensitizes lymphoma/leukaemia cells to platinum-based chemotherapy. **British Journal of**

**Haematology**, v. 162, n. 1, p. 135–137, 2013.

CHEN, L. et al. Differential targeting of prosurvival Bcl-2 proteins by their BH3-only ligands allows complementary apoptotic function. **Molecular Cell**, v. 17, n. 3, p. 393–403, 2005.

CHEUNG, A. et al. Targeting folate receptor alpha for cancer treatment. **Oncotarget**, v. 7, n. 32, p. 52553–52574, 2016.

CHIN CHUNG, M.; LONGHIN BOSQUESI, P.; LEANDRO DOS SANTOS, J. A Prodrug Approach to Improve the Physico-Chemical Properties and Decrease the Genotoxicity of Nitro Compounds. **Current Pharmaceutical Design**, v. 17, p. 3515–3526, 2011.

CHOWDHURI, A. R. et al. One-pot synthesis of folic acid encapsulated upconversion nanoscale metal organic frameworks for targeting, imaging and pH responsive drug release. **Dalton Trans.**, v. 45, n. 45, p. 18120–18132, 2016.

COLE, S. P. C. Multidrug Resistance Protein 1 (MRP1, ABCC1), a “Multitasking” ATP-binding Cassette (ABC) Transporter. **Journal of Biological Chemistry**, v. 289, n. 45, p. 30880–30888, 2014.

DI PIETRO, G.; MAGNO, L. A. V; RIOS-SANTOS, F. Glutathione S-transferases: an overview in cancer research. **Expert opinion on drug metabolism & toxicology**, v. 6, n. 2, p. 153–170, 2010.

DIAZ VIVANCOS, P. et al. A nuclear glutathione cycle within the cell cycle. **The Biochemical journal**, v. 431, n. 2, p. 169–178, 2010.

DINNEN, R. D. et al. Activation of targeted necrosis by a p53 peptide: A novel death pathway that circumvents apoptotic resistance. **Journal of Biological Chemistry**, v. 282, n. 37, p. 26675–26686, 2007.

DONG, J.; SULIK, K. K.; CHEN, S. Nrf2-Mediated Transcriptional Induction of Antioxidant Response in Mouse Embryos Exposed to Ethanol *in vivo*: Implications for the Prevention of Fetal Alcohol Spectrum Disorders. **Antioxidants & Redox Signaling**, v. 10, n. 12, p. 2023–2033, 2008.

DOSKEY, C. M. et al. Tumor cells have decreased ability to metabolize H<sub>2</sub>O<sub>2</sub>: Implications for pharmacological ascorbate in cancer therapy. **Redox Biology**, v. 10, n. October, p. 274–284, 2016.

DRIVER, B. R. et al. Folate receptor a expression level correlates with histologic grade in lung adenocarcinoma. **Archives of Pathology and Laboratory Medicine**, v. 140, n. 7, p. 682–685, 2016.

FALCONE FERREYRA, M. L.; RIUS, S. P.; CASATI, P. Flavonoids: biosynthesis, biological functions, and biotechnological applications. **Frontiers in Plant Science**, v. 3, n. September, p. 1–15, 2012.

FOSTER, I. Cancer: A cell cycle defect. **Radiography**, v. 14, n. 2, p. 144–149, 2008.

FULDA, S.; DEBATIN, K. M. Extrinsic versus intrinsic apoptosis pathways in anticancer chemotherapy. **Oncogene**, v. 25, n. 34, p. 4798–4811, 2006.

GALADARI, S. et al. Reactive oxygen species and cancer paradox: To promote or to suppress? **Free Radical Biology and Medicine**, v. 104, n. December 2016, p. 144–164, 2017.

GALATI, G. et al. Prooxidant activity and cellular effects of the phenoxyl radicals of dietary flavonoids and other polyphenolics. **Toxicology**, v. 177, n. 1, p. 91–104,

2002.

GALLUZZI, L. et al. Molecular mechanisms of cell death: recommendations of the Nomenclature Committee on Cell Death 2018. **Cell Death & Differentiation**, 2018.

GAN, F.-F. et al. Identification of Michael acceptor-centric pharmacophores with substituents that yield strong thioredoxin reductase inhibitory character correlated to antiproliferative activity. **Antioxidants & redox signaling**, v. 19, n. 11, p. 1149–65, 2013.

GORDILLO, G. M. et al. Multidrug Resistance-associated Protein-1 (MRP-1)-dependent Glutathione Disulfide (GSSG) Efflux as a Critical Survival Factor for Oxidant-enriched Tumorigenic Endothelial Cells. **Journal of Biological Chemistry**, v. 291, n. 19, p. 10089–10103, 2016.

GORRINI, C.; HARRIS, I. S.; MAK, T. W. Modulation of oxidative stress as an anticancer strategy. **Nature Reviews Drug Discovery**, v. 12, n. 12, p. 931–947, 2013.

GREK, C. L. et al. Causes and consequences of cysteine s-glutathionylation. **Journal of Biological Chemistry**, v. 288, n. 37, p. 26497–26504, 2013.

GUL, H. I. et al. Cytotoxic activity of 4'-hydroxychalcone derivatives against Jurkat cells and their effects on mammalian DNA topoisomerase I. v. 6366, n. December 2017, 2009.

HAJJ HUSSEIN, I. et al. Vaccines Through Centuries: Major Cornerstones of Global Health. **Frontiers in Public Health**, v. 3, n. November, p. 1–16, 2015.

HAMADA, S. et al. **Expression of glutathione S-transferase-pi in human ovarian cancer as an indicator of resistance to chemotherapy.** **Gynecologic oncology**, 1994. Disponível em: <<http://www.ncbi.nlm.nih.gov/pubmed/8157188>>

HANDY, D. E.; LOSCALZO, J. Redox Regulation of Mitochondrial Function. **Antioxidants & Redox Signaling**, v. 16, n. 11, p. 1323–1367, 2012.

HARTWELL, L. H.; KASTAN, M. B. Cell cycle control and cancer. **Science**, v. 266, n. 5192, p. 1821–8, 1994.

HOLT, D. E.; BAJORIA, R. The role of nitro-reduction and nitric oxide in the toxicity of chloramphenicol. **Human and Experimental Toxicology**, v. 18, n. 2, p. 111–118, 1999.

HWANG, C.; SINSKEY, A.; LODISH, H. Oxidized redox state of glutathione in the endoplasmic reticulum. **Science**, v. 257, n. 5076, p. 1496–1502, 1992.

INCA. **Estimativas de câncer de colo de útero no Brasil**. Disponível em: <[http://www2.inca.gov.br/wps/wcm/connect/tiposdecancer/site/home/colo\\_uterio/definicao](http://www2.inca.gov.br/wps/wcm/connect/tiposdecancer/site/home/colo_uterio/definicao)>. Acesso em: 1 jan. 2017.

JIANG, L. et al. Monitoring the progression of cell death and the disassembly of dying cells by flow cytometry. **Nature protocols**, v. 11, n. 4, p. 655–663, 2016.

JIN, Y. L. et al. Structure activity relationship studies of anti-inflammatory TMMC derivatives: 4-Dimethylamino group on the B ring responsible for lowering the potency. **Archives of Pharmacal Research**, v. 31, n. 9, p. 1145–1152, 2008.

JORDAN, M. A. et al. Mitotic Block Induced in HeLa Cells by Low Concentrations of Paclitaxel (Taxol) Results in Abnormal Mitotic Exit and Apoptotic Cell Death Mitotic Block Induced in HeLa Cells by Low Concentrations of Paclitaxel (Taxol) Results in Abnormal Mitotic Exit. **Cancer Research**, v. 56, p. 816–825, 1996.



- KACHADOURIAN, R. Flavonoid-induced glutathione depletion: Potencial implications for cancer treatment. **Free radical biology & medicine**, v. 41, n. 1, p. 65–76, 2006.
- KHOO, K. H. et al. Drugging the p53 pathway: understanding the route to clinical efficacy. **Nature reviews. Drug discovery**, v. 13, n. 3, p. 217–36, 2014.
- KIM, S. H. et al. Genistein inhibits cell growth by modulating various mitogen-activated protein kinases and AKT in cervical cancer cells. **Annals of the New York Academy of Sciences**, v. 1171, p. 495–500, 2009.
- KIM, S. H. et al. Chalcones, inhibitors for topoisomerase i and cathepsin B and L, as potential anti-cancer agents. **Bioorganic and Medicinal Chemistry Letters**, v. 23, n. 11, p. 3320–3324, 2013.
- KONG, Q.; LIN, C. G. Oxidative damage to RNA: mechanisms, consequences, and diseases. **Cellular and molecular life sciences : CMLS**, v. 67, n. 11, p. 1817–1829, 11 jun. 2010.
- KOO, G. B. et al. Methylation-dependent loss of RIP3 expression in cancer represses programmed necrosis in response to chemotherapeutics. **Cell Research**, v. 25, n. 6, p. 707–725, 2015.
- KOVACIC, P.; SOMANATHAN, R. Nitroaromatic compounds: Environmental toxicity, carcinogenicity, mutagenicity, therapy and mechanism. **Journal of Applied Toxicology**, v. 34, n. 8, p. 810–824, 2014.
- KRYSKO, O. et al. Necroptotic cell death in anti-cancer therapy. **Immunological Reviews**, v. 280, n. 1, p. 207–219, 2017.
- KUMARI, S.; KONDAPI, A. K. Lactoferrin nanoparticle mediated targeted delivery of 5-fluorouracil for enhanced therapeutic efficacy. **International Journal of Biological Macromolecules**, v. 95, p. 232–237, 2017.
- KUO, Y. et al. Flavokawain B , a novel chalcone from *Alpinia pricei* Hayata with potent apoptotic activity: Involvement of ROS and GADD153 upstream of mitochondria-dependent apoptosis in HCT116 cells. **Free Radical Biology and Medicine**, v. 49, n. 2, p. 214–226, 2010.
- LAZZE, M. C. et al. Anthocyanins induce cell cycle perturbations and apoptosis in different human cell lines. **Carcinogenesis**, v. 25, n. 8, p. 1427–1433, 2004.
- LEE, D. H. et al. A synthetic chalcone, 2'-hydroxy-2,3,5'-trimethoxychalcone triggers unfolded protein response-mediated apoptosis in breast cancer cells. **Cancer Letters**, v. 372, n. 1, p. 1–9, 2016.
- LI, F.-S.; WENG, J.-K. Demystifying traditional herbal medicine with modern approach. **Nature Plants**, v. 3, n. July, p. 17109, 2017.
- LI, P. et al. Cytochrome c and dATP-dependent formation of Apaf-1/caspase-9 complex initiates an apoptotic protease cascade. **Cell**, v. 91, n. 4, p. 479–489, 1997.
- LIU, C. et al. Folate receptor alpha is associated with cervical carcinogenesis and regulates cervical cancer cells growth by activating ERK1/2/c-Fos/c-Jun. **Biochemical and Biophysical Research Communications**, v. 491, n. 4, p. 1083–1091, 2017.
- LIU, Y. et al. Apoptosis of HeLa cells induced by cisplatin and its mechanism. **Journal of Huazhong University of Science and Technology - Medical Science**, v. 28, n. 2, p. 197–199, 2008.
- LOE, D. W.; DEELEY, R. G.; COLE, S. P. Verapamil stimulates glutathione transport

by the 190-kDa multidrug resistance protein 1 (MRP1). **The Journal of pharmacology and experimental therapeutics**, v. 293, n. 2, p. 530–538, 2000.

LÓPEZ, V. et al. Janus Mesoporous Silica Nanoparticles for Dual Targeting of Tumor Cells and Mitochondria. **ACS Applied Materials & Interfaces**, v. 9, n. 32, p. 26697–26706, 2017.

LU, S. C. Glutathione Synthesis. **Biochim Biophys Acta**, v. 1830, n. 5, p. 3143–3153, 2014.

MAI, C. W. et al. Chalcones with electron-withdrawing and electron-donating substituents: Anticancer activity against TRAIL resistant cancer cells, structure-activity relationship analysis and regulation of apoptotic proteins. **European Journal of Medicinal Chemistry**, v. 77, p. 378–387, 2014.

MARÍ, M. et al. Mitochondrial Glutathione, a Key Survival Antioxidant. **Antioxidants & Redox Signaling**, v. 11, n. 11, p. 2685–2700, nov. 2009a.

MARÍ, M. et al. Mitochondrial Glutathione, a Key Survival Antioxidant. **Antioxidants & Redox Signaling**, v. 11, n. 11, p. 2685–2700, 2 nov. 2009b.

MARTEL-FRACHET, V. et al. IPP51, a chalcone acting as a microtubule inhibitor with *in vivo* antitumor activity against bladder carcinoma. **Oncotarget**, v. 6, n. 17, p. 14669–14686, 2015.

MATSUMOTO, Y. et al. Vascular bursts enhance permeability of tumour blood vessels and improve nanoparticle delivery. **Nature Nanotechnology**, v. 11, n. 6, p. 533–538, 2016.

MENON, S. G.; GOSWAMI, P. C. A redox cycle within the cell cycle: ring in the old with the new. **Oncogene**, v. 26, n. 8, p. 1101–1109, 2007.

MOHANA, K.; ACHARY, A. Human cytosolic glutathione-S-transferases: quantitative analysis of expression, comparative analysis of structures and inhibition strategies of isozymes involved in drug resistance. **Drug Metabolism Reviews**, v. 49, n. 3, p. 318–337, 2017.

MORENO-GONZALEZ, G.; VANDENABEELE, P.; KRYSKO, D. V. Necroptosis: A novel cell death modality and its potential relevance for critical care medicine. **American Journal of Respiratory and Critical Care Medicine**, v. 194, n. 4, p. 415–428, 2016.

MURRAY-ZMIJEWSKI, F.; SLEE, E. A.; LU, X. A complex barcode underlies the heterogeneous response of p53 to stress. **Nature Reviews Molecular Cell Biology**, v. 9, n. 9, p. 702–712, 2008.

NCI. **Cervical Cancer Treatment.** Disponível em: <[https://www.cancer.gov/types/cervical/hp/cervical-treatment-pdq#link/\\_284\\_toc%3E2017](https://www.cancer.gov/types/cervical/hp/cervical-treatment-pdq#link/_284_toc%3E2017)>.

NGUYEN, H.; ZHANG, S.; MORRIS, M. E. Effect of flavonoids on MRP1-mediated transport in Panc-1 cells. **Journal of Pharmaceutical Sciences**, v. 92, n. 2, p. 250–257, 2003.

NIMSE, S. B.; PAL, D. Free radicals, natural antioxidants, and their reaction mechanisms. **RSC Adv.**, v. 5, n. 35, p. 27986–28006, 2015.

NORDBERG, J.; ARNÉR, E. S. J. Reactive oxygen species, antioxidants, and the mammalian thioredoxin system<sup>1</sup> <sup>1</sup>This review is based on the licentiate thesis “Thioredoxin reductase—interactions with the redox active compounds 1-chloro-2,4-

dinitrobenzene and lipoic acid” by Jonas Nordberg,. **Free Radical Biology and Medicine**, v. 31, n. 11, p. 1287–1312, 2001.

OREN, M.; ROTTER, V. Mutant p53 gain-of-function in cancer. **Cold Spring Harbor perspectives in biology**, v. 2, n. 2, p. a001107, 2010.

PACHER, P.; BECKMAN, J. S.; LIAUDET, L. Nitric Oxide and Peroxynitrite in Health and Disease. **Physiological Reviews**, v. 87, n. 1, p. 315–424, 2007.

PAEK, A. L. et al. Cell-to-Cell Variation in p53 Dynamics Leads to Fractional Killing. **Cell**, v. 165, n. 3, p. 631–642, 2016.

PARK, H.-A. et al. Glutathione disulfide induces neural cell death via a 12-lipoxygenase pathway. **Cell death and differentiation**, v. 16, n. 8, p. 1167–1179, 17 ago. 2009a.

PARK, I. et al. Isoliquiritigenin induces G2 and M phase arrest by inducing DNA damage and by inhibiting the metaphase/anaphase transition. **Cancer Letters**, v. 277, n. 2, p. 174–181, 2009b.

PATTERSON, S.; WYLLIE, S. Nitro drugs for the treatment of trypanosomatid diseases: Past, present, and future prospects. **Trends in Parasitology**, v. 30, n. 6, p. 289–298, 2014.

PAUMI, C. M. et al. Role of multidrug resistance protein 1 (MRP1) and glutathione S-transferase A1-1 in alkylating agent resistance. Kinetics of glutathione conjugate formation and efflux govern differential cellular sensitivity to chlorambucil versus melphalan toxicity. **Journal of Biological Chemistry**, v. 276, n. 11, p. 7952–7956, 2001.

PERJÉSI, P. et al. (E)-2-Benzylidenebenzocyclanones: Part VII. Investigation of the conjugation reaction of two cytotoxic cyclic chalcone analogues with glutathione: An HPLC-MS study. **Monatshefte fur Chemie**, v. 143, n. 8, p. 1107–1114, 2012.

PREMKUMAR, D. R. et al. ABT-737 Synergizes with Bortezomib to Induce Apoptosis, Mediated by Bid Cleavage, Bax Activation, and Mitochondrial Dysfunction in an Akt-Dependent Context in Malignant Human Glioma Cell Lines. **Journal of Pharmacology and Experimental Therapeutics**, v. 341, n. 3, p. 859–872, 2012.

RAPPA, G. et al. Evidence That the Multidrug Resistance Protein ( MRP ) Functions as a Co-Transporter of Glutathione and Natural Product Toxins Advances in Brief Evidence That the Multidrug Resistance Protein ( MRP ) Functions as a Co-Transporter of Glutathione and Natura. **Cancer Research**, n. 9, p. 5232–5237, 1997.

RIXE, O.; FOJO, T. Is cell death a critical end point for anticancer therapies or is cytostasis sufficient? **Clinical Cancer Research**, v. 13, n. 24, p. 7280–7287, 2007.

ROSIN, D. L.; OKUSA, M. D. Dangers Within: DAMP Responses to Damage and Cell Death in Kidney Disease. **Journal of the American Society of Nephrology**, v. 22, n. 3, p. 416–425, 2011.

ROUNDHILL, E. A.; BURCHILL, S. A. Detection and characterisation of multi-drug resistance protein 1 (MRP-1) in human mitochondria. **British Journal of Cancer**, v. 106, n. 6, p. 1224–1233, 2012.

SAHIN, K. et al. Sensitization of cervical cancer cells to cisplatin by genistein: The role of NF  $\kappa$  B and Akt/mTOR signaling pathways. **Journal of Oncology**, v. 2012, 2012.

SCHAEFER, L. Complexity of danger: The diverse nature of damage-associated

molecular patterns. **Journal of Biological Chemistry**, v. 289, n. 51, p. 35237–35245, 2014.

SHENG, Y. et al. Superoxide dismutases and superoxide reductases. **Chemical Reviews**, v. 114, n. 7, p. 3854–3918, 2014.

SISA, M. et al. Photochemistry of Flavonoids. v. 15, p. 5196–5245, 2010.

SMITHERMAN, P. K. Role of Multidrug Resistance Protein 2 (MRP2, ABCC2) in Alkylating Agent Detoxification: MRP2 Potentiates Glutathione S-Transferase A1-1-Mediated Resistance to Chlorambucil Cytotoxicity. **Journal of Pharmacology and Experimental Therapeutics**, v. 308, n. 1, p. 260–267, 2003.

SRIVASTAVA, S. et al. Quercetin, a natural flavonoid interacts with DNA, arrests cell cycle and causes tumor regression by activating mitochondrial pathway of apoptosis. **Scientific Reports**, v. 6, n. April, p. 1–13, 2016.

STIBOROVÁ, M. et al. The influence of dicoumarol on the bioactivation of the carcinogen aristolochic acid I in rats. **Mutagenesis**, v. 29, n. 3, p. 189–200, 2014.

SYNTICHAKI, P.; TAVERNARAKIS, N. Death by necrosis. Uncontrollable catastrophe, or is there order behind the chaos? **EMBO Reports**, v. 3, n. 7, p. 604–609, 2002.

SZAREWSKI, A. HPV vaccination and cervical cancer. **Current Oncology Reports**, v. 14, n. 6, p. 559–567, 2012.

TANIDA, S. et al. Mechanisms of cisplatin-induced apoptosis and of cisplatin sensitivity: Potential of BIN1 to act as a potent predictor of cisplatin sensitivity in gastric cancer treatment. **International Journal of Surgical Oncology**, v. 2012, 2012.

TAYLOR, R. C.; CULLEN, S. P.; MARTIN, S. J. Apoptosis: Controlled demolition at the cellular level. **Nature Reviews Molecular Cell Biology**, v. 9, n. 3, p. 231–241, 2008.

TEWARI, K. S. et al. Bevacizumab for advanced cervical cancer: final overall survival and adverse event analysis of a randomised, controlled, open-label, phase 3 trial (Gynecologic Oncology Group 240). **The Lancet**, v. 390, n. 10103, p. 1654–1663, 2017.

THOMAS, M.; PIM, D.; BANKS, L. The role of the E6-p53 interaction in the molecular pathogenesis of HPV. p. 7690–7700, 1999.

TOYODA, Y. et al. MRP class of human ATP binding cassette (ABC) transporters: Historical background and new research directions. **Xenobiotica**, v. 38, n. 7–8, p. 833–862, 2008.

TURELLA, P. et al. Proapoptotic Activity of New Glutathione S -Transferase Inhibitors. n. 9, p. 3751–3762, 2005.

VALKO, M. et al. Free radicals and antioxidants in normal physiological functions and human disease. v. 39, p. 44–84, 2007.

VANDEN BERGHE, T. et al. Determination of apoptotic and necrotic cell death in vitro and in vivo. **Methods**, v. 61, n. 2, p. 117–129, 2013.

WANG, T. et al. Biodegradable Self-Assembled Nanoparticles of Galactose-Containing Amphiphilic Triblock Copolymers for Targeted Delivery of Paclitaxel to HepG2 Cells. **Macromolecular Bioscience**, v. 16, n. 5, p. 774–783, 2016.

WANG, T. et al. Necroptosis in cancer: An angel or a demon? **Tumor Biology**, v. 39, n. 6, 2017.

WANG, Y. et al. Hesperidin inhibits HeLa cell proliferation through apoptosis mediated by endoplasmic reticulum stress pathways and cell cycle arrest. **BMC Cancer**, v. 15, n. 1, p. 1–11, 2015.

WANG, Z. et al. The mitochondrial phosphatase PGAM5 functions at the convergence point of multiple necrotic death pathways. **Cell**, v. 148, n. 1–2, p. 228–243, 2012.

WHO. **Comprehensive Cervical Cancer Control**. 2014

WILLIAMS, A. B.; SCHUMACHER, B. p53 in the DNA damage repair process. **Cold Spring Harbor perspectives in medicine**, v. 6, n. 5, p. 10.1101/cshperspect.a026070 a026070, 2016.

WINTER, E. et al. In vitro and in vivo effects of free and chalcones-loaded nanoemulsions: Insights and challenges in targeted cancer Chemotherapies. **International Journal of Environmental Research and Public Health**, v. 11, n. 10, p. 10016–10035, 2014.

WONG, D. Y. Q.; LIM, J. H.; ANG, W. H. Induction of targeted necrosis with HER2-targeted platinum (iv) anticancer prodrugs. **Chem. Sci.**, v. 6, n. 5, p. 3051–3056, 2015.

YANG, L. et al. The Chalcone 2'-hydroxy-4',5'-dimethoxychalcone Activates Death Receptor 5 Pathway and Leads to Apoptosis in Human Nonsmall Cell Lung Cancer Cells. **Iubmb Life**, v. 65, n. 6, p. 533–543, 2013.

YANG, X. et al. Continuous activation of Nrf2 and its target antioxidant enzymes leads to arsenite-induced malignant transformation of human bronchial epithelial cells. **Toxicology and Applied Pharmacology**, v. 289, n. 2, p. 231–239, 2015.

YHEE, J. Y. et al. Tumor-targeting transferrin nanoparticles for systemic polymerized siRNA delivery in tumor-bearing mice. **Bioconjugate Chemistry**, v. 24, n. 11, p. 1850–1860, 2013.

YUAN, S. et al. The holo-apoptosome: Activation of procaspase-9 and interactions with caspase-3. **Structure**, v. 19, n. 8, p. 1084–1096, 2011.

ZHANG, B. et al. Synthesis of xanthohumol analogues and discovery of potent thioredoxin reductase inhibitor as potential anticancer agent. **Journal of Medicinal Chemistry**, v. 58, n. 4, p. 1795–1805, 2015a.

ZHANG, D. D. et al. Keap1 Is a Redox-Regulated Substrate Adaptor Protein for a Cul3-Dependent Ubiquitin Ligase Complex Keap1 Is a Redox-Regulated Substrate Adaptor Protein for a Cul3-Dependent Ubiquitin Ligase Complex. **American Society of Microbiology**, v. 24, n. 24, p. 10941–10953, 2004.

ZHANG, Y.-K. et al. Multidrug Resistance Proteins (MRPs) and Cancer Therapy. **The AAPS Journal**, v. 17, n. 4, p. 802–812, 2015b.

ZHENG, Z.-M.; BAKER, C. C. Papillomavirus genome struture, expression, and post-transcriptional regulation. **Frontiers in bioscience : a journal and virtual library**, v. 11, p. 2286–2302, 2006.

ZHOU, P. et al. **Flavokawain B, the hepatotoxic constituent from kava root, induces GSH-sensitive oxidative stress through modulation of IKK/NF-kappaB and MAPK signaling pathways.**FASEB Journal, 2010.

ZITKA, O. et al. Redox status expressed as GSH:GSSG ratio as a marker for oxidative stress in paediatric tumour patients. **Oncology Letters**, v. 4, n. 6, p. 1247–1253, 2012.